Use Authorization

In presenting this dissertation in partial fulfillment of the requirements for an advanced degree at Idaho State University, I agree that the Library shall make it freely available for inspection. I further state that permission to download and/or print my dissertation for scholarly purposes may be granted by the Dean of the Graduate School, Dean of my academic division, or by the University Librarian. It is understood that any copying or publication of this dissertation for financial gain shall not be allowed without my written permission.

Signature _____

Deepesh Poudel

Date _____

SYSTEMIC AND WOUND BEHAVIOR OF ^{238}Pu(IV) CITRATE IN NONHUMAN PRIMATES

By

Deepesh Poudel

A dissertation

submitted in partial fulfillment

of the requirements for the degree of

Doctor of Philosophy in Nuclear Science and Engineering

Idaho State University

May 2016

To the Graduate Faculty:

The members of the committee appointed to examine the dissertation of Deepesh Poudel find it satisfactory and recommended that it be accepted.

Dr. Richard R. Brey
Major Advisor

Dr. Thomas F. Gesell
Committee Member

Dr. Raymond A. Guilmette
Committee Member

Dr. Jason T. Harris
Committee Member

Dr. Chikashi Sato
Graduate Faculty Representative

ACKNOWLEDGEMENTS

It is my great pleasure to acknowledge the people who in one way or another contributed and extended their valuable assistance in the preparation and completion of this dissertation. I would not have been able to finish the thesis without the guidance of my committee members, help from my friends, and support from my family and wife.

I would like to express my utmost gratitude to my major advisor Dr. Richard Brey for his sincere and unfailing support throughout my dissertation and throughout my years in Idaho State University. His knowledge, patience and encouragement were instrumental to the completion of this study. I would also like to thank Dr. Jason Harris and Dr. Thomas Gesell for accepting the invitation to serve on my dissertation committee as my co-advisors and supporting me in this research. Special thanks also goes to Dr. Raymond Guilmette for providing us with the nonhuman primates' data and for adding his valuable experiences from several years of his research in internal dosimetry. My sincere thanks goes to Dr. Chikashi Sato for serving as a Graduate Faculty Representative on my committee. I would also like to express my thanks to Dr. Alan Birchall of the Health Protection Agency, United Kingdom for providing us with the software used in this study.

The work in graduate school would have overwhelmed me had it not been for all of the support I received along the way from my parents. I am forever indebted to the sacrifice my wife made while I completed graduate school and for her patience and unwavering love. I thank my brother-in-law Dr. Bhoj Gautam for setting the bar for high standards. I also thank my sisters for their constant support and encouragement. I am also thankful for the support I received from my parents-in-law and my brother-in-law.

TABLE OF CONTENTS

LIST OF FIGURES

LIST OF TABLES

LIST OF ABBREVIATIONS AND ACRONYMS

%ID	Percentage of injected dosage
BEIR	Committee on Biological Effects of Ionizing Radiation
BIPM	International Bureau of weights and Measures
Bq	Becquerel
CIS	Colloidal and Intermediate States
CM	Cortical marrow
CS	Cortical surface
CV	Cortical volume
df	Degrees of freedom
DOE	United States Department of Energy
DTPA	Diethylenetriaminepentaacetic acid
IDEAS	General Guidelines for the Estimation of Committed Dose from Incorporation Monitoring Data
FIA	Fraction of injected activity
GI	Gastrointestinal
GSD	Geometric Standard Deviation
IAEA	International Atomic Energy Agency
IARC	International Agency for Research on Cancer
ICRP	International Commission on Radiological Protection
im	Intramuscular(ly)
IMBA	Integrated Modules for Bioassay Analysis
IPP	IMBA Professional Plus
IRF	Intake Retention Fraction

iv	Intravenous(ly)
keV	Kiloelectronvolt
LBL	Lawrence Berkeley National Laboratory
MeV	Megaelectronvolt
N	Normal
NCRP	National Council on Radiation Protection and Measurements
NHPs	Nonhuman Primates
NUREG	Nuclear Regulatory Guide
PABS	Particles, Aggregates and Bound States
Pu	Plutonium
sc	Subcutaneous(ly)
SF	Scattering Factor
TM	Trabecular marrow
TPA	Trapped Particles and Aggregates
TS	Trabecular surface
TV	Trabecular volume
UA	Uncertainty Analyzer
UBC	Urinary bladder contents
ULI	Upper large intestine
USNRC	United States Nuclear Regulatory Commission
USTUR	United States Transuranium and Uranium Registries

ABSTRACT

Despite the presence of a relatively large amount of human data available on the metabolism of plutonium, the experimental animal data is still important in constructing and parameterizing the biokinetic models. Recognizing this importance, the biokinetic data obtained from studies done by P.W. Durbin in nonhuman primates (NHPs) were evaluated against the ICRP 67 systemic model and the two human models developed thereafter. The default transfer rates recommended for adult humans in these models predict the urinary excretion in NHP to a certain extent. However, they were unable to describe the fecal excretion rates several days post intake and the activities in skeleton and liver tissues at the time of death. Recognizing these inconsistencies as the result of metabolic and physiological differences between the humans and the NHPs, a biokinetic model for nonhuman primates was developed by adopting the basic model structure and adapting the transfer rates described for metabolism of plutonium in adult humans. Significant changes were necessary to explain the shorter retention of plutonium in liver and skeleton tissues of the NHPs, the differences in liver to bone partitioning ratios, and the significantly higher excretion of plutonium in feces compared to that of humans.

Our work also evaluated the efficacy of the NCRP 156 wound model. The predictions of the wound model described in NCRP Report No. 156 coupled with the systemic model described in ICRP 67 were compared with the actual urinary excretion data and wound retention data from nonhuman primates injected intramuscularly or subcutaneously with ^{238}Pu(IV) citrate. Our results indicated that the early behavior of ^{238}Pu(IV) citrate in wounds can be adequately described by the default retention parameters for moderately retained radionuclides suggested by the report. The urinary excretion rates

after 200 days post intake could not be described well by the parameters of any of the default wound models because of the differences in the systemic handling of plutonium by humans compared to nonhuman primates.

Chapter 1 :
Introduction

1.1. Statement of the Problem

Radioactive materials can enter the body through various pathways, including inhalation, ingestion, injection, wounds or transdermal absorption. The knowledge of the behavior of radioactive materials within the body and the time-dependent distribution of radioactive materials in various organs is a necessary requisite to determine the intake, organ-level absorbed dose, and also to determine the need for medical intervention. The biokinetic models are formulated based on this knowledge of the retention, distribution and clearance of a radionuclide following an intake (Khursheed et al. 1996, Doerfel et al. 2006 and 2012, Castellani et al. 2013).

Given the large number of radionuclides to which humans can be exposed, and the limited amount of element-specific human biokinetic data available, it is important to recognize the role that results of innumerable experimental animal studies have played in constructing and parameterizing the biokinetic models needed for human internal dosimetry. Additionally, the large majority of information on health effects from internally deposited radionuclides has come from animal studies. Thus, historically, consensus scientific committees have utilized the available experimental animal data to supplement and bridge these knowledge gaps in biokinetics, dosimetry and health effects in people (e.g., in reports by ICRP (1972, 1986, 1995, 2001), NCRP (1991, 1993, 1998, 2001, 2006), BEIR (1988) and IARC 2001)).

Plutonium has been used in military and civilian activities since its discovery in 1941. Thus, the metabolism and translocation of plutonium has been a subject of constant investigations, modifications, and improvements. There is a relatively large amount of human data available on plutonium – mainly from accidental and occupational exposure cases, but also from a small number of human experimental studies (for example, Langham et al. 1980., Talbot et al. 1993 and 1997, Ham and Harrison 2000, Etherington et al. 2003, Hodgson et al. 2003). These data have been used to construct biokinetic models for Pu in man. Nevertheless, the quantity of human data is limited and the quality uncertain due to such factors as the use of terminally ill patients, unknown intake quantities, the physicochemical form of the Pu involved in accidental exposures, and the small number of subjects. The current biokinetic models are heavily influenced by the plutonium metabolism studies conducted on mammals like rats (e.g., Durbin et al. 1972, Talbot et al. 1990), dogs (e.g., Lloyd et al. 1978, Polig et al. 2000), rabbits (e.g., Rosenthal et al. 1972), and monkeys (e.g., Durbin et al. 1985).

The advantages of using experimental studies for biokinetics investigations include: (1) the animals can be exposed to higher activities of radioactive materials than humans as needed, (2) the exposure scenario, intake, and the physicochemistry of the contaminants are well known, and (3) the experimental situations are more controlled than when considering accidental exposure of humans. This study evaluates the biokinetic data obtained from studies done by Dr. P.W. Durbin in nonhuman primates (NHPs) in the 1960s and 1970s (Durbin and Jeung 1990a and b, described in Chapter 3) with the objectives described in section 1.2.

1.2. Objectives of this Study

1.2.1. Systemic Behavior of ^{238}Pu(IV) Citrate in NHPs

The first report of ICRP on permissible doses, ICRP 2 (ICRP 1959), defined the maximum permissible burden for isotopes of plutonium for bone, liver, kidneys and the total body. The report assigned 80% of absorbed Pu to bone, 15% to liver, and 2% to kidneys primarily based on the studies of Pu metabolism on rats. It also defined the biological half-lives in skeleton and liver as 200 years and 85 years respectively, based on the data from Langham studies (Langham et al. 1980). As more and more data on the metabolism of Pu on rats, mice, dogs and pigs from injection studies as well as studies on humans became available, the understanding of the systemic behavior of plutonium gradually evolved, and the recommendations changed (ICRP 19 (ICRP 1972), ICRP 48 (ICRP 1986), ICRP 30 (ICRP 1979), ICRP 56 (ICRP 1990)).

The most recent and updated consensus systemic model for plutonium used for dosimetry purposes is given in ICRP 67 (ICRP 1993a). The structure of the model was adopted from an age-specific model developed for americium (Leggett 1992), and is represented by a compartmental structure with blood as a central compartment that is connected to several tissues or organs each of which are represented by one or more compartments. The translocation of activity from one compartment to another is assumed to follow first order kinetics, and the transfer rates between the compartments are given for different age groups (Chapter 2).

The ICRP 67 model for plutonium includes a pathway from intermediate soft tissues (ST1) to the urinary bladder that lacks physiological justification (ICRP 1993a,

Luciani 2002, Luciani and Polig 2000, Leggett et al. 2005, Konzen et al. 2016). Moreover, the model also under-predicts the blood and fecal bioassays for intermediate periods (Konzen et al. 2015). As more data became available after the publication of ICRP 67, researchers (Luciani and Polig 2002, Legett et al. 2005) have focused on correcting the shortcomings of the ICRP 67 model (Chapter 2).

The current study evaluates the Pu biokinetic data obtained from the NHP studies by applying these data to existing reference human models (ICRP 1993; Luciani and Polig 2000; Leggett et al. 2005). The intakes obtained from the maximum likelihood analysis of urinary, fecal and blood data are compared to the actual known intakes administered to the animals. In addition, the activities predicted in liver and skeleton using the human reference models are compared with the actual measured activities in these organs at the time of sacrifice. Such comparative studies help identify pathways that are physiologically similar or distinct between the NHPs and humans for the translocation of plutonium (Chapter 4).

Our objective was also to describe the biokinetics of plutonium in the NHPs by adopting the basic model structure and adapting the transfer rates described for adult humans (Chapter 6). This is accomplished by understanding the physiological similarities and differences between the humans and the NHPs based on the results of comparison studies (Chapter 4) and early biokinetic studies in animals.

1.2.2. Wound Behavior of ^{238}Pu (IV) Citrate in NHPs

The NCRP 156 wound model (NCRP 2006), the first consensus biokinetic model to describe the behavior of radioactive materials in wound, was heavily based on animal data. The authors of the report acknowledge this limitation and recommended that the

model be validated using human cases (Guilmette et al. 2007). More than 2,100 wounds contaminated with radioactive materials have been reported in the scientific literature (NCRP 2006), however a majority of these wound cases are confounded by other forms of intake such as inhalation or multiple wounds, or have been treated medically by chelation or excision. The intake scenarios and the actual intake are not clearly known thus exacerbating the difficulty of modeling wound biokinetics. These disadvantages can be addressed to an extent when data from animal studies, such as the Durbin NHP studies, are used to evaluate and validate the wound model.

The intramuscular injections are thought to simulate deep wounds. Radionuclide retention in contaminated muscle and subcutaneous tissues are thought to be similar (NCRP 2006). One of the objectives of our study was to use the urinary excretion data from intramuscularly and subcutaneously injected animals to evaluate the applicability of the NCRP 156 wound model's parameters (Chapter 5).

Chapter 2 :
Literature Review

2.1. Internal Dosimetry Concepts

2.1.1. Assessment of Internal Doses

Radioactive materials enter the human body through different pathways: ingestion, inhalation, injection, absorption via wounds, and through the skin. Inhalation is a common pathway of intake in occupational scenarios, and is particularly important for workers involved in nuclear fuel production or reprocessing (Watts 1975). Ingestion is a typical pathway for the general population due to consumption of contaminated food and water, and it is also an important pathway for workers when contaminated hands are used when handling food (i.e., with poor hygienic practices). Intake via wound is also a common pathway of intake – more than 2,100 wounds contaminated with radioactive materials have been reported in the literature (NCRP 2006). Injection is a pathway of increasing significance because of administration of radiopharmaceuticals for diagnostic and therapeutic purposes. Although intact skin is a good barrier against the entry of most radionuclides, some radioactive materials such as tritiated water and iodine can be transferred to the blood through the skin (IAEA 1999).

Internal dosimetry is a technique to assess the doses to humans who are routinely or potentially exposed to radiation through intakes of radioactive materials via any of the pathways mentioned above. Such assessments constitute an integral part of most radiation protection programs, and help provide timely control of the hazardous conditions to which workers may be exposed. Assessment of internal dose is also important to show compliance

with standards and regulations. Internal dosimetry may provide information on whether large intakes have occurred and this may help to make decisions if medical intervention is necessary (Potter 2004).

Assessment of internal doses may be prospective or retrospective (Etherington et al. 2006). Prospective dose assessment is an estimation of the intake and prediction of dose based on the information available about a particular exposure scenario. Retrospective dose assessment is an estimation of intake and dose based on the amount of radioactive material present in the body or bioassay samples.

In vivo measurements of activity (e.g., thyroid, lungs, whole-body) provides a quick and convenient estimate of activity in the body, but are feasible only for those radionuclides (e.g., ^{131}I, ^{137}Cs, ^{60}Co) that can be detected from outside the body. When considering radionuclides that have no or just low-energy x-ray or gamma-ray emissions, excreta monitoring may be the only viable measurement technique. Although urine is most commonly used, fecal analysis may be useful in cases of relatively insoluble materials. Nose-blowing or nasal smears may be useful in certain cases to help identify possible inhalation events. Blood is rarely used for monitoring purposes, but can be useful in cases of suspected high intakes (Doerfel et al. 2012). Although the type of bioassay measurement largely depends on the major route of excretion associated with the radioactive material, factors such as the ease of collection, analysis and interpretation must also be taken into account (IAEA 1999).

2.1.2. Biokinetic Models in Internal Dosimetry

Interpretation of the monitoring data in terms of intake and/or internal dose requires knowledge of the behavior of radioactive materials within the human body and the time-dependent distribution of radioactive material in various organs of the body (Doerfel et al. 2012, Khursheed et al. 1996). Such knowledge is obtained from biokinetic models. Biokinetic models may be metabolic models that are used to describe the translocation of radioactive material inside the body, or dosimetric models that are based on the radiological characteristics of the radionuclide and the organs or tissues where deposition occurs (IAEA 2003). These models are based on extensive animal and/or human studies that have, in some cases, been carried out for decades.

The metabolic models are mathematical descriptions of the time-dependent distribution and excretion of substance after being incorporated into the body (Leggett and Eckerman 1994). Such models describe the translocation of radioactive material and help dosimetrists understand the patterns of deposition, retention and excretion of radioactive materials in humans. These models depend on the mode of intake, the physico-chemical molecular form of the ligand to which the radionuclide the radionuclide is bound, and the type of element. The models are described using compartments, transfer routes and excretion routes. The compartments represent the tissues, including fluids and organs where the material is expected to spend a finite amount of time after intake. The transfer routes among the compartments indicate the translocation of radioactive material between those tissues or organs, and are described with a set of transfer rates in units of per time (IAEA 2003).

The dosimetric models address the distribution of radioactive materials within tissues or organs where significant deposition may occur. Such models address the effectiveness or quality of the different types and energy of radiation, as well as the radiosensitivity of deposition site tissue or organs. These weighting factors are respectively called radiation weighting factor (W_R) and tissue weighting factor (W_T). The dosimetric models also take into account the contribution to adjacent target organs from source organs (IAEA 2003).

The International Commission on Radiological Protection (ICRP) and National Council on Radiation Protection and Measurements (NCRP) have developed and recommended various biokinetic models to assist in assessment of intake and doses from bioassay and monitoring data. Such biokinetic models are either generic or pre-systemic models which represent the behavior of various radionuclides after entering the human body via an intake pathway, or systemic models which describe the translocation of radioactive material after the direct uptake into the blood. The biokinetic models are revised as necessary when new data and information are available.

The ICRP Publication 66, *Human Respiratory Tract Model for Radiological Protection* (1994) describes the biokinetics of inhaled radioactive materials. This document represents a significant revision of the model used in ICRP Publication 30, *Limits on Intakes of Radionuclides by Workers* (ICRP 1979). Unlike the ICRP 30 approach which provided methods to exclusively calculate the average dose to the lungs, ICRP 66 considers specific tissues of the respiratory tract and takes into account the differences in radiosensitivity of various tissues within the respiratory tract (ICRP 1979, 1994). The ICRP 66 methodology provides a means to determine the deposition of inhaled particles for all

regions of the respiratory tract as a function of particle size, breathing parameters, and workload (ICRP 1994).

The gut model described in ICRP 30 (1979) describes the biokinetics of radioactive material intake that occur by ingestion (direct ingestion or transfer from the respiratory tract). This model has been replaced by the ICRP Publication 100, *Human Alimentary Tract Model for Radiological Protection* (2006) which describes the biokinetics of radionuclides taken into the system via ingestion (direct ingestion or transfer from the respiratory tract). This model, which replaces the ICRP 30 model of the gastrointestinal tract (1979), includes all alimentary tract organs including the oral cavity, esophagus, stomach, small intestine, right colon, left colon and rectosigmoid (ICRP 2006).

The NCRP has, in collaboration with the ICRP, developed a biokinetic model for exposure to radioactive materials *via* contaminated wounds (NCRP 2006). This model was largely based on experimental animal data due to the lack of human data. The human data that were available were often confounded by medical intervention such as tissue excision or DTPA administration. This model can be used to calculate doses to the wound site, as well as doses to organs and tissues when coupled with a systemic biokinetic model. A detailed description of the wound model is provided in section 2.4.

Unlike the ingestion, inhalation or wound pathways, no general model exists to describe the entry of radioactive materials through the skin. This is because of the large variability of situations that may occur: differences in the chemical forms of compounds, differences in the location of contamination in the skin, differences in the physiological state of the skin, etc. (Doerfel et al. 2012).

Despite the mode of intake, a certain fraction of the intake enters the blood. This fraction is referred to as uptake. The fate of the radionuclides after entering the blood depends on several factors. Some radionuclides distribute throughout the body (e.g., ^{3}H, ^{24}Na, ^{42}K, ^{137}Cs); some selectively deposit in a particular tissue or a number of tissues (e.g., ^{131}I in thyroid, ^{90}Sr in bone, ^{239}Pu and ^{241}Am in bone and liver); and some follow the pathway of similar elements (e.g., ^{90}Sr and ^{226}Ra behave similarly to Ca, ^{137}Cs and ^{86}Rb behave similarly to K) (Doerfel et al. 2012). The systemic biokinetic models have been published in several ICRP Publications including publication 56 (1990), 67 (1992), 69 (1995a), 71 (1995b), and 78 (1997). Detailed discussions of ICRP 67 systemic models for plutonium and americium are provided in sections 2.2.3 and 2.3.2 respectively.

2.2. Properties of Plutonium

Plutonium in an important element from the health physics point of view. Occupational exposure primarily consists of exposures to nuclear workers associated with weapons development and electric energy generation, most importantly those involved with handling and processing spent fuel. Measurable amounts of plutonium have also been found in foods and in human tissues due to fallout from nuclear weapon tests (ICRP 1979).

2.2.1. Physical and Chemical Properties of Plutonium

Plutonium, atomic number 94, is a transuranic radioactive chemical element with the symbol Pu. It is a silvery-white metal with a density of 19.7 g cm^{-3} at 25 $^{\circ}C$. The melting and boiling point of the metal are 639.5 $^{\circ}C$ and 3,235 $^{\circ}C$ respectively (Taylor 1973).

Currently, 20 isotopes of plutonium, ranging from mass numbers 228 to 247, have been identified. The radioactive properties of the most common isotopes, those with mass numbers from 238 to 244, are described in Table 2.1 (ICRP 1983).

Table 2.1. Properties of isotopes of plutonium

Isotope	Half-time	Decay mode[c]	Energy (MeV)	Yield (%)
^{238}Pu[a]	87.74 y	Alpha	5.499	71.6
		Alpha	5.456	28.3
^{239}Pu[a]	2.41×10^4 y	Alpha	5.157	73.8
		Alpha	5.144	15.2
		Alpha	5.105	10.7
^{240}Pu[a]	6.56×10^3 y	Alpha	5.168	73.4
		Alpha	5.124	26.5
^{241}Pu	14.35 y	Beta	0.02[b]	100
		Alpha	4.897	2.04×10^{-3}
^{242}Pu[a]	3.73×10^5 y	Alpha	4.984	100
^{243}Pu	4.956 h	Beta	5.823[b]	100
^{244}Pu[a]	8.08×10^7 y	Alpha	4.666	100

[a]also undergoes spontaneous fission
[b]maximum beta energy
[c]most important, i.e., high yield decay modes

The availability of the isotopes of plutonium in nature depends on the half-time of the radionuclide. Three isotopes of plutonium have so far been identified in nature, specifically in the concentrated uranium ores – ^{239}Pu, ^{240}Pu, and ^{244}Pu. The first one is produced in nature by the neutron capture of ^{238}U; the latter two occur in nature in smaller amounts. When ^{239}Pu captures a neutron, ^{240}Pu is formed approximately one-fourth of the time. ^{244}Pu found in nature is cosmogenic in its origin (Hoffman et al. 1971).

Two of these twenty isotopes, ^{238}Pu and ^{239}Pu, are significant from a commercial and military point of view. The former was the first isotope of plutonium produced in substantial quantities. It was produced by bombarding uranium with deuterons at the University of California in 1941 (Seaborg 1946):

$$^{238}_{92}U\ (d,2n)\ ^{238}_{93}Np \xrightarrow{\beta^-} ^{238}_{94}Pu \tag{2.1}$$

^{238}Pu makes up a limited fraction of the reactor-bred plutonium, and hence it is difficult to separate from other isotopes of plutonium. Pure ^{238}Pu, to be used in thermoelectric generators, is produced by short-term irradiation of ^{241}Am targets with a high thermal neutron flux (Jones 2005). Pure ^{238}Pu can also be produced by irradiation of ^{237}Np:

$$^{237}_{93}Np\,(n,\gamma)\ ^{238}_{93}Np \xrightarrow{\beta^-} ^{238}_{94}Pu \tag{2.2}$$

^{239}Pu can be produced by neutron capture of ^{238}U in nuclear reactors (equation 2.3). Plutonium thus produced contains certain higher mass isotopes of plutonium. The generation of ^{240}Pu and ^{241}Pu in reactor fuel is expected, and it builds up over time.

$$^{238}_{92}U(n,\gamma)^{239}_{92}U \xrightarrow{\beta^-} ^{239}_{92}Np \xrightarrow{\beta^-} ^{239}_{94}Pu \tag{2.3}$$

Plutonium is capable of exhibiting oxidation states from three to seven. It oxidizes very quickly in the presence of moist air forming a powdery surface coating composed mainly of plutonium dioxide. Plutonium in such coated form is pyrophoric and can ignite spontaneously in a non-inert environment. Plutonium dioxide is in particulate form and can be easily inhaled thus representing dose hazards. In mammalian fluids such as blood, lung fluids, tissue liquids, bile and urine, plutonium predominantly exists in its fourth oxidation

state, Pu(IV), mostly because most ligands stabilize the Pu(IV) state (ICRP 1972 and 1986, Durbin 1975).

Plutonium ions are capable of forming various compounds. The compounds potentially important for radiation protection includes oxides, chlorides, oxychlorides, carbonate, nitrate, nitride and oxalate. The oxidized forms of plutonium are considered to be the most important from radiological protection point of view. However, organic complexes such as citrate, phytate, lactate and proteins are also important (ICRP 1986).

2.2.2. Biochemistry of Plutonium

The biological behavior of plutonium is heavily influenced by the physico-chemical form in which the element enters the body (ICRP 1986). Because of its high ionic charge, plutonium has a strong tendency to hydrolyze (ICRP 1972 and 1986, Durbin 1975, Taylor 1988). The hydrolysis of plutonium depends on several factors including the concentration of plutonium in the solution, the acidity, the temperature, and the presence of other ions. Polymers or particles start to form at pH values greater than 2, but in absence of stabilizing ligands, the polymeric products can be formed in pH values as low as 0.5 (ICRP 1986).

At physiological pH levels, plutonium does not exist predominantly as simple ions, rather, it forms complexes with endogenous biochemical ligands. It has been reported that plutonium binds with transferrin in a way similar to that of iron (Fe(III)); such binding forms the predominant transport protein in the plasma (ICRP 1972 and 1986; Jensen et al. 2012). Plutonium has also been reported to bind with other proteins such as ferritin, bone sialoprotein and salivary proteins, as wells as non-protein ligands such as citrate and lactate (Chipperfield and Taylor 1970, ICRP 1986).

The metabolism of plutonium depends on the chemistry, particle size, density and solubility of the material (ICRP 1972 and 1986). The effect of the chemistry of inhaled plutonium can be illustrated by the differences in metabolism of plutonium nitrate vs. plutonium oxide. The former has an initial blood absorption of 10% with little long-term lymph node retention compared to the latter, which has an initial absorption of 0.1% and significant long-term retention (ICRP 1972). The differences in retention of monomeric and polymeric forms of plutonium and the effect of the chemical form of plutonium in absorption from the wounds are discussed in sections 2.3.1.2 and 2.4.2 respectively.

2.3. Metabolism of Plutonium

2.3.1. Historical Studies on Distribution and Retention of Plutonium

The metabolism of plutonium has been a subject of constant investigation. The data for such investigations come from various animal and human studies. Sections 2.3.1.2 and 2.3.1.2 discuss various studies on humans and animals within the last several decades. These studies have contributed to our knowledge of the biokinetics of plutonium, leading to improvement of our understanding and modification of biokinetic models.

2.3.1.1. Human Studies

The information on metabolism of plutonium in humans was primarily derived from several studies including experimental injection studies, studies on occupationally exposed individuals, and studies performed on persons exposed to worldwide fallout of plutonium from nuclear weapon tests.

One of the most important non-animal data sets is a study on the distribution, retention and excretion of intravenously injected plutonium citrate in human volunteers

(Langham et al. 1980). The study involved intravenous injection of trace quantities of plutonium citrate solution in twelve human volunteers, most of whom were older than 45 years and suffered chronic disorders such that survival beyond ten years was unlikely. The Langham et al. (1980) study reported four additional cases from studies performed at Chicago and Berkeley. Incremental blood, daily urine and composited 4-day fecal samples were collected from the volunteers following injection. Based on these data, Langham et al. came up with mathematical expressions to describe urinary and fecal excretions as functions of time. The study calculated the biological half-time of plutonium in humans as 118 years, with values ranging from 84 to 175 years.

Durbin (1971, 1972) reviewed and critically analyzed the data discussed above supplemented with two additional cases performed at Berkeley, in addition to several animal studies (discussed in Section 2.2.2.2). Durbin emphasized the data from the cases without liver or kidney abnormalities, and concluded that the retention of plutonium in bone and liver 15 years after intake is roughly equal. Further, she calculated the average soft-tissue release half-time to be less than 480 days and the bone turnover for the whole skeleton to be roughly 5% per year (1971).

Talbot et al. (1993, 1997) studied the distribution and excretion of ^{237}Pu(IV) citrate in six male and six female volunteers. Talbot et al. (1997) compared the biokinetics of plutonium in these subjects with the predictions of the ICRP 67 (ICRP 1993) systemic plutonium model and found that the model fails to explain the variation of plutonium levels in blood (the central compartment), thus raising questions as to whether the model is valid in many other respects. The authors (Talbot et al. 1997) also suggested possible sex-related differences in the balance of metabolites in the circulation.

Ham and Harrison (2000) studied the gastrointestinal absorption and urinary excretion of ^{244}Pu(IV) citrate in five healthy adult males in a two stage study – ingestion of 10^{14} atoms of ^{244}Pu followed by the intravenous injection of 2×10^{12} atoms six months later. The study measured urinary excretion for the following 7 to 9 days and subsequently at intervals over periods up to 5 to 6 years. They determined that the fractional absorption of Pu from the gastrointestinal tract was consistent with the value reported by ICRP. The authors also determined that the urinary excretion results measured were in general agreement with model predictions, the greatest differences being on the first day after injection and at the latest measurement times (5 to 6 years post intake).

The data on occupational exposures to plutonium form another major source of information on plutonium metabolism. One of the biggest source of occupational exposure data is the data from workers at Mayak Production association, a plutonium production facility in Russia. Workers at the Mayak plant were exposed to relatively large internal radiation intakes particularly in the early years of its operation (Vasilenko et al. 2007). Several studies on the biokinetics and dosimetry of plutonium have focused on the Mayak data. One of the major works on the systemic model of plutonium was by Leggett et al. (2005), which focused on modifications of the ICRP 67 (ICRP 1993) systemic model for plutonium to reflect recently developed data and improve dose estimates for Mayak workers. The improved biokinetic model has been discussed in details in section 2.2.3.2.

Another large source of the data on plutonium comes from the United States Transuranium and Uranium Registries (USTUR). The USTUR is the registry of almost 500 volunteers who worked at Department of Energy (DOE) sites and received measurable internal doses from plutonium and/or uranium and other transuranic elements. Access to

records such as employment, occupational exposure and medical histories, along with an autopsy report and the results of radiochemical analyses of the radionuclide content of major body organs enable the registry to maintain a unique collection of data, which have been used in the development, validation, or update of several biokinetic models (James and Brooks 2007).

Extensive data are available on fall-out plutonium distribution in members of general public. Several studies on the distribution of fallout plutonium in human tissues have been published (for example, Fox et al. 1980, Mussalo 1981, Bunzl and Kracke 1983). The difficulty with the fallout studies is high variability among the subjects. Several adjustments need to be made to account for outliers, and time and age trends present in the data. The data from the fallout plutonium distribution studies can be used as baseline levels to evaluate possible future changes in the plutonium deposition (Bunzl and Kracke 1983).

There is a relatively large amount of human data available on metabolism of plutonium (compared to that on other radionuclides), mainly from published accidental occupational exposure cases but also from a small number of human experimental studies discussed above. These data have been used to construct biokinetic models for plutonium in humans. Nevertheless, the quantity of human data is limited and the quality uncertain due to such factors as the use of terminally ill patients, unknown intake quantities and physicochemical form of plutonium exposure material, and small number of subjects. Thus, data from controlled animal experiments are still important to construct and parametrize the biokinetic models needed for human internal dosimetry.

2.3.1.2. Animal Studies

The large majority of information on health effects from internally deposited radioactive materials has come from animal studies. Historically, consensus scientific committees have used the available experimental animal data to supplement and bridge the knowledge gaps in biokinetics, dosimetry and health effects in people [e.g., in reports by ICRP (1972, 1986, 1995, 2001), NCRP (1991, 1993, 1998, 2001, 2006), BEIR (1988), and IARC (2001)]. Discussion on the understanding of the biokinetic models is therefore incomplete without the discussion of the role of innumerable experimental animal studies described in the literature. The current understanding of plutonium distribution is heavily influenced by the plutonium metabolism studies conducted on mammals like rats (e.g., Taylor 1962, Durbin et al. 1972, Stanley et al. 1982, Sontag 1991, Talbot et al. 1990), mice (e.g., Bhattacharyya et al. 1989, Austin and Lord 2000, Ellender et al. 1995), dogs (e.g., Lloyd et al. 1978, Smith et al. 1982, Stanley et al. 1982, Polig 1989, Polig et al. 1998 and 2000), rabbits (e.g., Rosenthal et al. 1972), baboons (e.g., Priest et al. 1992, Bhattacharyya et al. 1989, Larsen et al. 1983) and monkeys (e.g., Stanley et al. 1982, Durbin et al. 1985). The metabolism of plutonium can be affected by the activity of plutonium injected into the animals. Early experimental studies conducted using high activity concentrations may have produced results different than what would be anticipated at levels experienced by humans in typical occupational environment. Arnold and Jee (1962) injected dogs with Pu(IV) citrate with dosage levels ranging from 0.016 to 2.7 uCi/kg of body weight and reported that the skeletal deposition and kinetics were dependent on the amount of dosage administered. Similarly, Lloyd et al. (1984) reported that the retention of injected ^{241}Am in the liver was dependent on the dosage level, and came up with a retention equation for

different dosage levels. Polig et al. (2000) realized the effect of the dosage levels, and hence used the data from animals injected only with the dosage levels believed not to cause any acute toxic effects when developing the biokinetic and dosimetric model of plutonium in the dog.

Comparative studies of the metabolism of different physical and chemical forms of plutonium have also been conducted in laboratory animals. These studies have shown that the uptake of polymeric plutonium by reticuloendothelial tissues is greater than that of monomeric plutonium in the first week (Schubert et al. 1961, Markley et al. 1964). As an example, 7 to 14% of the principally monomeric plutonium compared to 70% of polymeric plutonium was deposited in the liver of rabbits in the first week. Similarly, 27 to 51% of monomeric plutonium was deposited in the skeleton compared to 23 to 38% of polymeric plutonium during the first week after injection (Taylor et al. 1969, Belyayev et al. 1963). Considering periods of longer duration post intake, it was observed that monomeric plutonium was lost at a greater rate from the liver than the polymeric plutonium (Rosenthal et al. 1972). Baxter et al. (1973) reported that monomeric plutonium cleared less rapidly from the blood compared to polymeric plutonium. Monomeric plutonium was deposited homogeneously in the liver, whereas polymeric plutonium was deposited near the sinusoidal cells at the center of the liver lobe (Baxter et al. 1973). Occupational intakes are mostly due to the monomeric forms of plutonium, and hence caution should be used when extrapolating animal data obtained from injection of polymeric plutonium.

Leggett (2003) indicated that the extrapolation of data from laboratory animals to man is particularly uncertain for the liver due to differences among species in handling different elements. Investigators have demonstrated shorter retention half-lives of

plutonium and americium in nonhuman primates such as macaques (Durbin et al. 1985) and baboons (Guilmette et al. 1980). ICRP 19 (1972) adopted 40 years as the half-life of plutonium in the liver based on an assumption that the retention half-time in various species was directly proportional to the body weight. However, this assumption is not valid for all the animals since longer-half-times have been reported for small animals like hamsters and grasshopper mice (Leggett 2003). Research has indicated that the liver kinetics in beagles are similar to those of humans. Therefore, ICRP Publications 56 and 67 (ICRP 1989, 1993) primarily used the beagle data to describe the liver kinetics in human.

These observations indicate that the application of experimental animal data to describe metabolism in humans provides mixed results due to several factors including the differences in physiology between the animals and humans, differences in the chemistry of the contaminant, concentration, and the activity of intake used in experimental animals compared to that in occupational exposure scenarios. Animal studies provide useful insight to the understanding of biokinetics in human, but they should be extrapolated with caution.

2.3.2. Systemic Biokinetic Models of Plutonium

2.3.2.1. Early ICRP Models

Most of the early biokinetic models (prior to ICRP 56) on plutonium were basically simple mathematical expressions which addressed only the initial distribution and net rate of decline of radioactive materials in a few organs. The complex metabolic models (for example, ICRP 1993, 1997) were not available until relatively recently because of several reasons including the lack of computing abilities and lack of enough data to justify use of more complex models. Complex models like those used today were also not necessary

because the intention for early models was only to predict long-term activities in various organs (Leggett et al. 1994).

ICRP 2 (ICRP 1959), the first report of ICRP on permissible doses, defined the maximum permissible burden for isotopes of plutonium for bone, liver, kidneys and the total body. ICRP 2 assigned 80% of absorbed Pu to bone, 15% to liver, and 2% to kidneys primarily based on investigations on rats. The biological half-times were defined to be 200 years for bone and roughly 85 years for the liver and kidneys based on the data by Langham et al. (1980).

The recommendations of ICRP 2 were modified and revised as more data became available. ICRP reviewed the metabolic data available until 1971 which primarily included animal studies on rats, mice, dogs and pigs, as well as the data from the Langham study, and published report 19 (ICRP 1972) on the behavior of plutonium along with other actinides. The report assumed that 45% of plutonium deposited on bone surfaces, 45% in the liver, and 10% directly went to excretion. This assumption was carried over in ICRP 30 (ICRP 1988), which assigned the half-lives of 40 years and 100 years in liver and skeleton respectively.

ICRP 19 was superseded by ICRP Publication 48 (ICRP 1986) to account for the data that became available after the publication of ICRP 19. Based heavily on the autopsy data from occupationally and environmentally exposed persons, ICRP 48 suggested that although the average deposition of plutonium is most likely to be 50% in skeleton and 30% in liver, the variability between the cases infer that 45% each for both liver and bone is an adequate assumption for radiation protection purposes. Further, the report recommended

the half-lives of 20 years and 50 years in liver and skeleton respectively, both significantly shorter than the recommendations of ICRP 30. ICRP 54 (1988) adapted the urinary and fecal excretion functions from Durbin's (1972) analyses of healthy human subjects supplemented with animal data.

Because the primary purpose of the ICRP 30 models was to serve as a basis for calculating the long-term doses to various tissues, the models did not consider the excretion and other physiological behavior patterns. As such, the models could not be used to interpret bioassay measurements. Moreover, ICRP 30 was overly-simplified especially when models for bone were considered (ICRP 1979, Leggett 1985), and thus the need for a physiologically based model arose.

The systemic model for plutonium by Leggett (1985) was one of the most comprehensive physiological models that were developed early. Instead of simplification of model and the calculations, Leggett focused on actual physiological processes. To do so, he developed a multi-compartmental model—the skeleton was divided into cortical and trabecular volume, surfaces and marrow; and the liver was divided into hepatocytes and reticuloendothelial cells. The structure also contained compartments for soft tissues and urinary tract components. The transfer rates for various compartments were suggested for different age groups (Leggett 1985).

The interest of researchers and that of the consensus committees grew in development of age-specific biokinetic models grew as the regulatory agencies required estimates of risk encountered by all members of the general public in addition to occupational cohorts. A physiological modeling approach was considered to be appropriate

because of the lack of age-specific data. Such a framework provided distribution, translocation and excretion pathways thus allowing development of age-specific models to represent changes in physiology with the changes in the age (Leggett et al. 1994). The physiological approach was useful when trying to account for the differences due to bone restructuring and remodeling, as well as recycling of plutonium among various tissues (ICRP 1990). ICRP 56 (ICRP 1989) recommended age-specific dose coefficients for various organs using the available data and compartmental approach. The ICRP 56 model was later revised in ICRP 67 (ICRP 1993).

2.3.2.2. ICRP 67 Systemic Model for Plutonium

ICRP 67 (ICRP 1993) represents the most recent and updated systemic model for plutonium used for dosimetry purposes. The model was an extension of the ICRP 56 model (ICRP 1989), and it accounts for the updated information on the long-term distribution of Pu in workers. The model also addresses the concept of equivalent dose introduced in ICRP publication 60 (ICRP 1991). ICRP Publication 68 (ICRP 1994) uses the ICRP 67 systemic model to calculate the dose coefficients for plutonium intake by workers, and ICRP Publication 78 (ICRP 1997) uses the model for interpretation of bioassay measurements.

As discussed in Poudel (2012), the general structure of the model described in ICRP 67 is an adaptation of an age-specific model developed for americium by Leggett (1992). Blood forms the central compartment of the model, and this is connected to several tissues and organs including soft-tissues, skeleton, liver, kidneys, and the urinary bladder each of which are represented by one or more compartments (Fig. 2.1). The model treats blood as a uniformly mixed pool (ICRP 1993).

Three compartments are used to describe the biokinetics of plutonium in soft-tissues: the ST0 compartment which represents the rapid-turnover tissues, the ST1 compartment which represents the intermediate-term retention tissues, and the ST2 which represents the tenacious retention tissues. The ST0 compartment, which includes extracellular fluids, represents a fast exchange (hours or days) between the soft-tissues and the blood. The ST1 compartment describes the retention of up to two years, and the ST2 compartment describes the retention over several years. The ST1 and ST2 compartments represent "massive soft tissues" like muscle, skin, subcutaneous fat and other tissues not included in the model.

The kinetics of plutonium in skeleton is explained by the division of the skeleton into cortical and trabecular compartments, each of which is further divided into bone surfaces, bone volumes, and bone marrow. The activity is transferred to the skeleton from the blood via the bone surface. The process of bone formation transfers the activity from bone surface to bone volume; and that of bone resorption transfers the activity from bone surface and bone volume to bone marrow. The activity is removed from the bone marrow into the blood from where it is re-distributed.

The liver is divided into two compartments in order to better represent the long-term retention of plutonium. One compartment (liver 1) loses a portion of activity in the liver to the gastrointestinal (GI) tract – via biliary secretion – over a period of a year. A fraction of the activity in liver 1 is also transferred to the other compartment: liver 2. The liver 2 compartment, which can be physiologically associated with the reticulo-endothelial system (Luciani 2002), retains plutonium for many years. Activity leaving liver 2 enters the blood.

In the ICRP 67 model of kidneys, the urinary path is treated differently from the other kidney tissues. The urinary path compartment describes the pathway through which the plutonium reaches the urinary bladder, whereas the "other kidney tissues" compartment exchanges the plutonium activity with the blood. The inclusion of the urinary bladder as a listed organ for tissue-weighting factors in ICRP 60 (ICRP 1991) required that urinary bladder be explicitly included in the urinary excretion pathway (ICRP 1993). The total activity in the urinary bladder is contributed from two other pathways as well: the direct transfer of activity from blood, and transfer from the ST1 compartment. The transfer from ST1 to the urinary bladder has no physiological significance, but was introduced for mathematical convenience to fit the long-term empirical data.

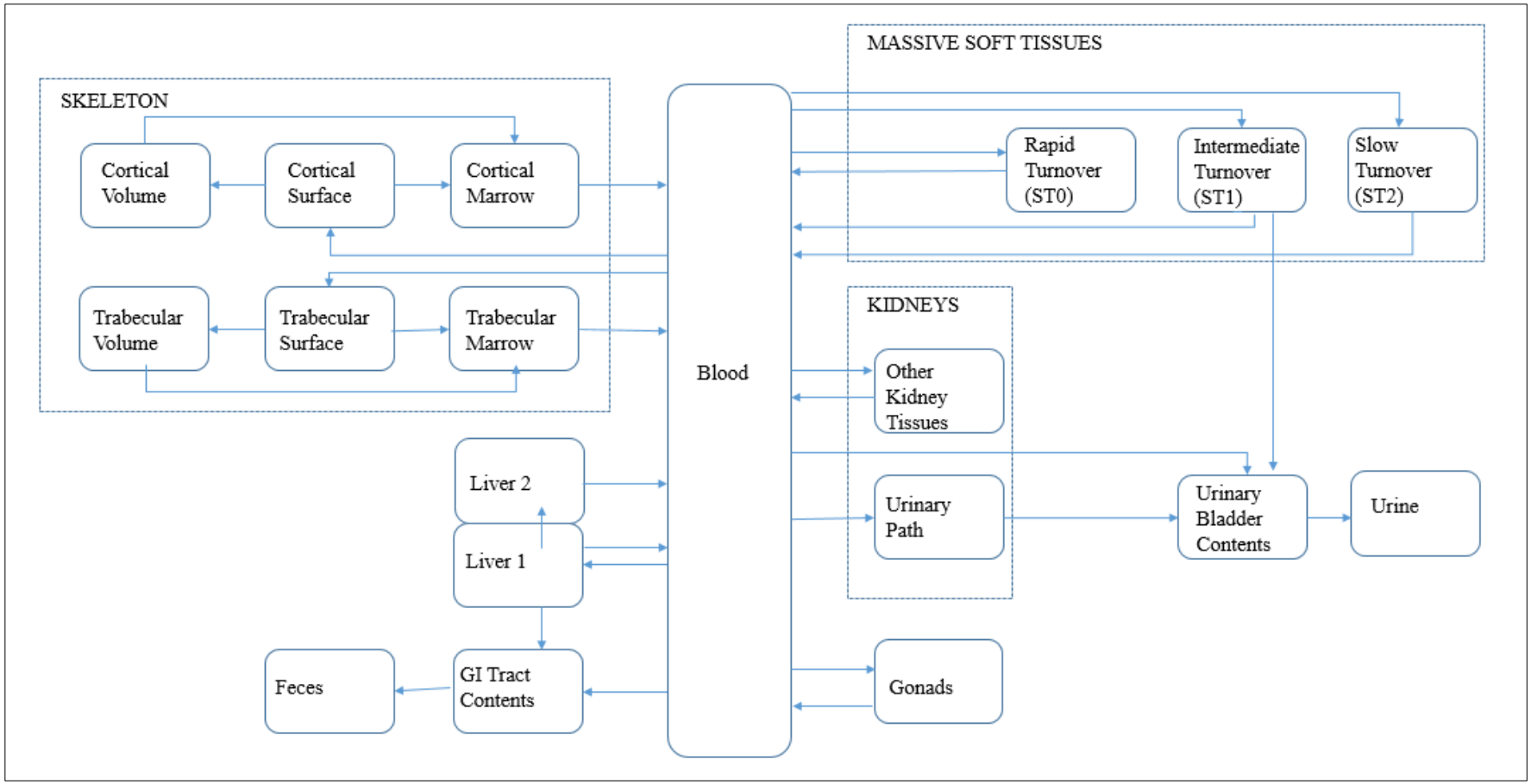

Fig. 2.1. Diagram of the ICRP 67 biokinetic model for plutonium (ICRP 1993)

Activity reaches the GI tract through two pathways: from the liver 1 compartment to the small intestine via absorption, and direct transfer from blood to the upper large intestine via absorption. Activity is removed from the GI tract by fecal excretion.

The translocation of activity from one compartment to another in such a compartmental model is assumed to follow first order kinetics. Parameter values for a pair of compartments are expressed as fractional flows per unit time and are referred to as transfer rates. Most of the transfer rates are calculated from deposition fractions and removal half-times. Deposition fractions provide a simple way of describing the initial distribution of activity transferred from blood to various compartments. Removal half-times refer to the biological half-time if there were no recycling to the compartments (ICRP 1993).

Table 2.2. ICRP 67 transfer rates for adult human (ICRP 1993)

Pathway	Transfer rate (day^{-1})
blood to liver 1	0.1941
blood to cortical surface	0.1294
blood to trabecular surface	0.1941
blood to urinary bladder content	0.0129
blood to kidney (urinary path)	0.00647
blood to other kidney tissue	0.00323
blood to ULI contents	0.0129
blood to testes	0.00023
blood to ovaries	0.000071
blood to ST0	0.2773
blood to ST1	0.0806
blood to ST2	0.0129
ST0 to blood	0.693
kidneys (urinary path) to bladder	0.01386
other kidney tissue to blood	0.00139
ST1 to blood	0.000475
ST1 to urinary bladder contents	0.000475
ST2 to blood	0.000019
trabecular surface to volume	0.000247
trabecular surface to marrow	0.000493
cortical surface to volume	0.0000411
cortical surface to marrow	0.0000821
trabecular volume to marrow	0.000493
cortical volume to marrow	0.0000821
cortical marrow to blood	0.0076
trabecular marrow to blood	0.0076
liver 1 to liver 2	0.00177
liver 1 to small intestine	0.000133
liver 2 to blood	0.000211
gonads to blood	0.00019

The ICRP 67 plutonium model can be used to obtain information on the metabolism of plutonium in both male and female subjects. The model recommends the same transfer rates for all compartments except the gonads irrespective of the gender. The

transfer rates are given for different age groups: 3 months, 1, 5, 10 and 15 year old subjects and adults. The transfer rates recommended for adults are given in Table 2.2.

2.3.2.3. Revisions of the ICRP 67 Systemic Model for Plutonium

The ICRP 67 model is a physiologically based model except for the flow of activity from ST1 to the urinary bladder. This pathway, which was introduced to account for an apparent increase in urinary clearance of plutonium with time, provides mathematical convenience but lacks physiological justification (ICRP 1993, Luciani 2002, Luciani and Polig 2000, Leggett et al. 2005). Moreover, the pathway dominates the transfer of activity from blood and urinary path by up to a factor of five roughly after 100 days post intake (Luciani 2000).

As more data became available after the publication of ICRP 67, researchers have focused on correcting the shortcomings of the ICRP 67 model. Some of the important revisions of the model includes the revisions by Luciani and Polig (2002) and Leggett et al. (2005). These models are discussed in detail.

Luciani's Revision of ICRP 67 Model

Luciani and Polig (2000) revised the ICRP 67 model in order to remove the unphysiological assumption of the model (i.e., transfer of activity from ST1 to urinary bladder), and to correct the model for its inadequacy in predicting the urinary excretion rates at long times after intake. The modifications were carried out on the basis of the available data and empirical expression for plutonium excretion after injection. The primary changes to the model include: removal of the pathway from ST1 to UBC, and use of time-dependent bone turnover rates.

The model was used to predict urinary excretion and checked with the available data from occupationally exposed individuals. A consistently better agreement was obtained with Luciani's model than with the ICRP 67 model parameters. Moreover, the model correctly estimated the skeleton-liver partitioning as observed in some autopsy studies. Finally, the use of the time-dependent skeletal transfer rates allowed for the explanation of increase of plutonium activity in urine over time. The model is given in Fig. 2.2Fig. 2.2. Luciani's optimized model for systemic behavior of plutonium (Luciani and Polig 2000) and the transfer rates are given in Table 2.3 (Luciani and Polig 2000).

Leggett's Revision of ICRP 67 Model

Leggett (2005) revised the ICRP 67 model to reflect the information developed since its publication, to remove biologically unrealistic features of the model, and to resolve several discrepancies between model predictions and the observed data, particularly the partitioning between the liver and the skeleton. Major sources of data for this revision included the data from the intravenous injection of plutonium in volunteers, as well as the autopsy and excretion data from the Mayak workers (Leggett 2003).

The model proposed by Leggett (2005) is shown in Fig. 2.3. One of the major changes in the model included the splitting up of blood into two compartments: blood 1 and blood 2 in agreement with an assumption that the recycled plutonium has higher urinary clearance (roughly three times) than the original input to blood (Leggett 2003). Similarly, a liver 0 compartment is added to the model of liver to represent a rapid turnover compartment. The skeletal model proposed by Leggett is different from the one described in ICRP 67 in that the bone volumes receives activity directly from the blood as well as from the bone surface in ICRP 67. Finally, the pathway from ST1 to the urinary bladder

was removed. The transfer rates suggested for a typical healthy adult are given in Table 2.4.

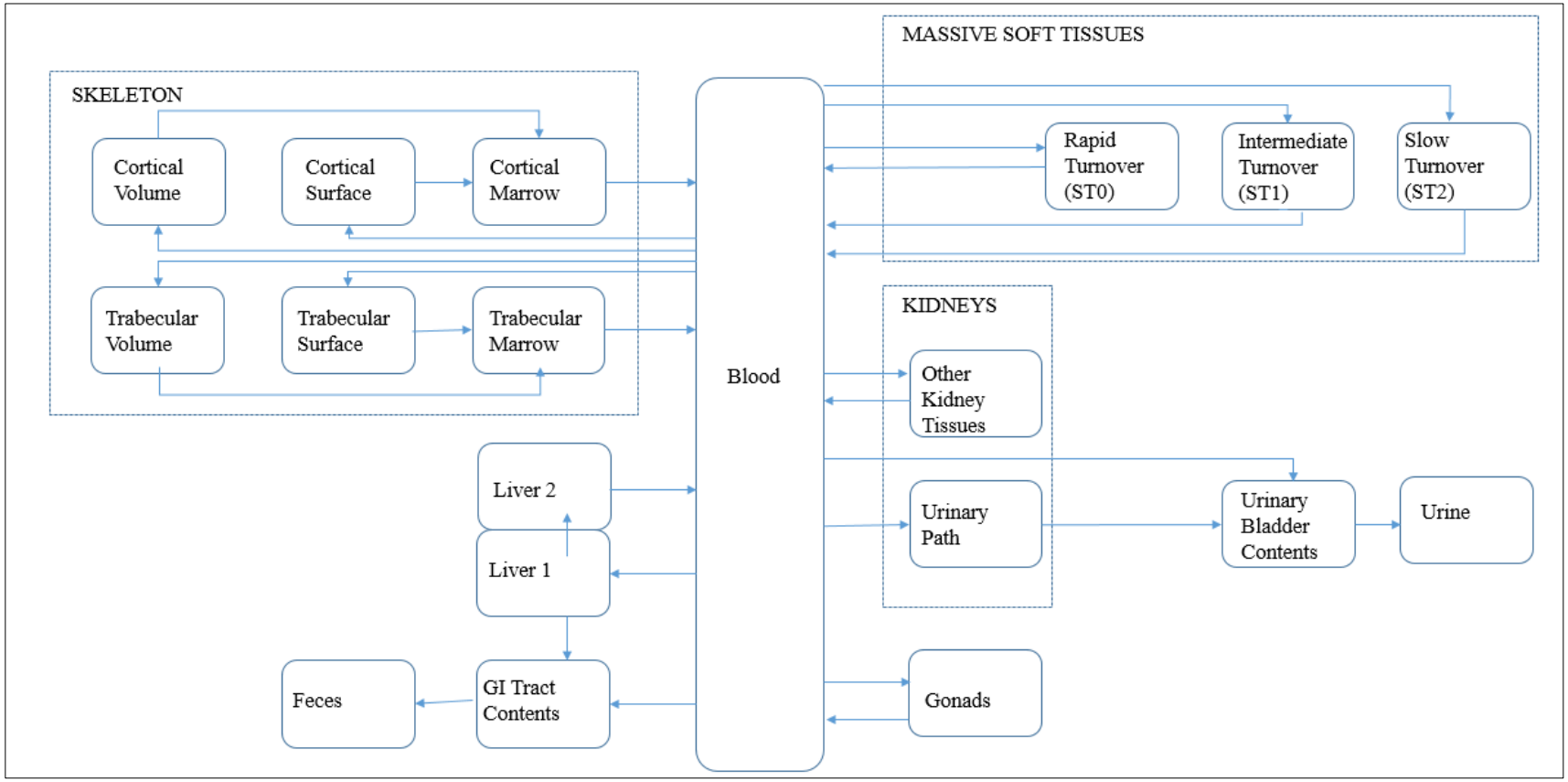

Fig. 2.2. Luciani's optimized model for systemic behavior of plutonium (Luciani and Polig 2000)

Table 2.3. Transfer rates of the Luciani's optimized model for systemic behavior of plutonium (Luciani and Polig 2000)

Pathway	**Transfer rate (day^{-1})**
blood to liver 1	0.12
blood to cortical surface	0.0952
blood to trabecular surface	0.226
blood to cortical volume	0.00448
blood to trabecular volume	0.0716
blood to urinary bladder content	0.00946
blood to kidney (urinary path)	0.00992
blood to other kidney tissue	0.00323
blood to ULI contents	0.008
blood to testes	0.00023
blood to ST0	0.2773
blood to ST1	0.0806
blood to ST2	0.0129
ST0 to blood	0.139
kidneys (urinary path) to bladder	0.0102
other kidney tissue to blood	0.00139
ST1 to blood	0.00095
ST2 to blood	0.000019
trabecular surface to marrow	0.00159[a]
cortical surface to marrow	0.000156[a]
trabecular volume to marrow	0.00159[a]
cortical volume to marrow	0.0000822[a]
cortical marrow to blood	0.0076
trabecular marrow to blood	0.0076
liver 1 to liver 2	0.01
liver 1 to small intestine	0.0004
liver 2 to blood	0.0004
gonads to blood	0.00019

[a]Values up to 35 years age. Double values at 60 y and linear interpolation between 35 and 60 y are assumed.

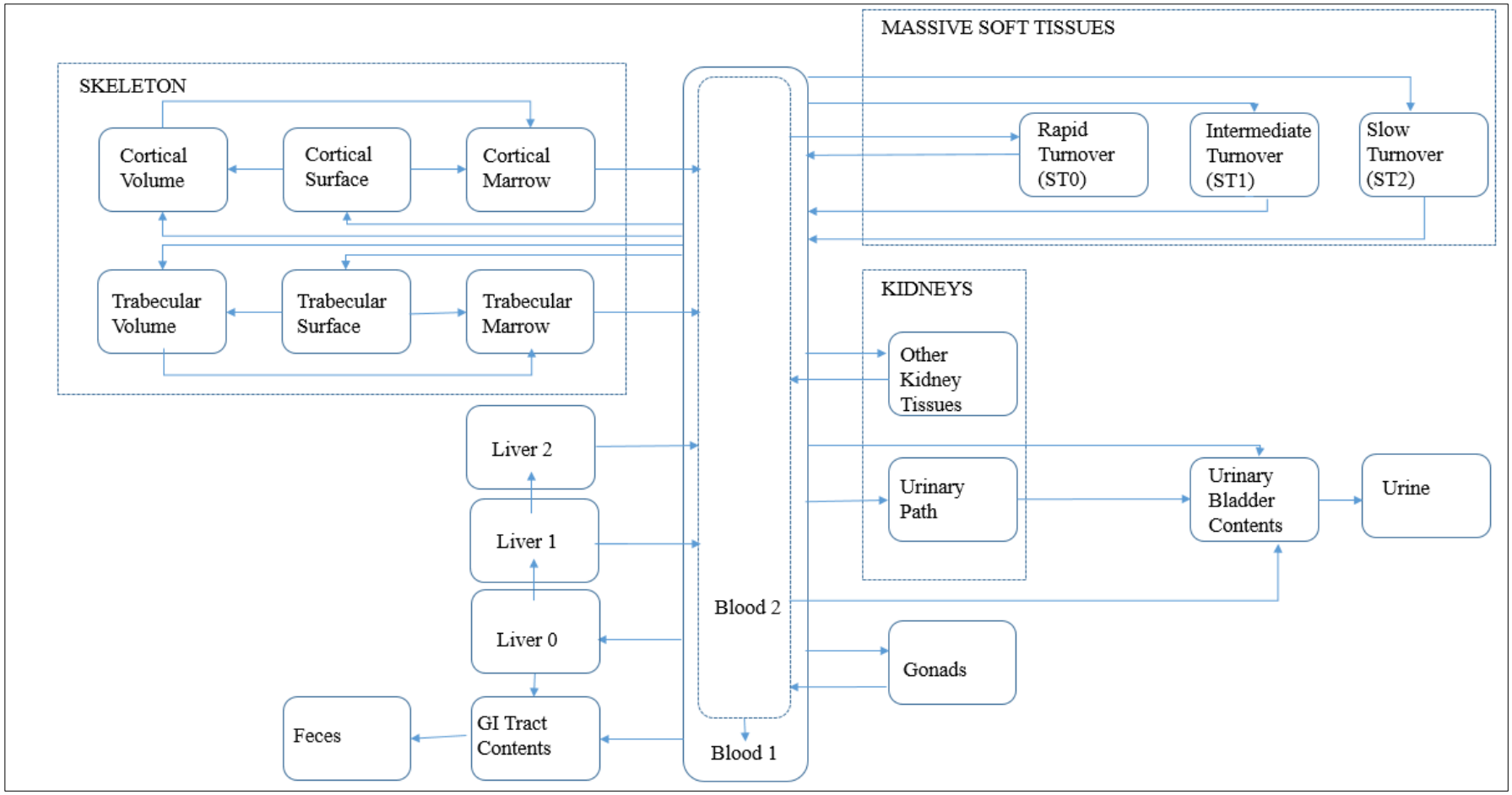

Fig. 2.3. Structure of the model proposed by Leggett et al. (2005)

Table 2.4. Parameter values recommended by Leggett et al. (2005) for a typical healthy adult

Pathway	Transfer rate (day^{-1})
blood 1 to liver 0	0.462
blood 1 to cortical surface	0.08778
blood 1 to trabecular surface	0.12474
blood 1 to cortical volume	0.00462
blood 1 to trabecular volume	0.01386
blood 1 to urinary bladder content	0.0154
blood 1 to kidney (urinary path / renal tubules)	0.0077
blood 1 to other kidney tissue	0.000385
blood 1 to ULI contents	0.01155
blood 1 to testes	0.00027
blood 1 to ovaries	0.000085
blood 1 to ST1	0.018511
blood 1 to ST2	0.0231
ST0 to blood 1	0.099
blood 2 to urinary bladder contents	3.5
blood 2 to blood 1	67.55
blood 2 to ST0	28.95
kidneys (urinary path / renal tubules) to urinary bladder contents	0.017329
other kidney tissue to blood 2	0.000127
ST1 to blood 2	0.001386
ST2 to blood 2	0.000127
trabecular surface to marrow	0.000493
cortical surface to marrow	0.000082
trabecular volume to marrow	0.000493
cortical volume to marrow	0.000082
cortical marrow to blood 2	0.0076
trabecular marrow to blood 2	0.0076
liver 0 to liver 1	0.045286
liver 1 to blood 2	0.00152
liver 1 to liver 2	0.00038
liver 0 to small intestine	0.000924
liver 2 to blood 2	0.000127
gonads to blood 2	0.00038

Note: The initial input to blood by absorption or injection is assumed to distribute rapidly between Blood 1 (70%) and ST0 (30%).

2.4. NCRP 156 Wound Model

The NCRP, in collaboration with the ICRP, developed a biokinetic and dosimetric model for exposure to radioactive materials from contaminated wounds. This report (NCRP Report 156, NCRP 2006) is a relatively recent addition to the current family of biokinetic models developed for various types of intakes. The wound model, created using a mechanistic framework of chemical and biological principles, can be used to calculate the doses to the wound site from the wound intake of radioactive material. In addition, it can also be coupled with a systemic biokinetic model to predict the urinary and fecal excretion rates for bioassay interpretation, and to calculate the committed doses to organs and tissues (Doerfel et al. 2012).

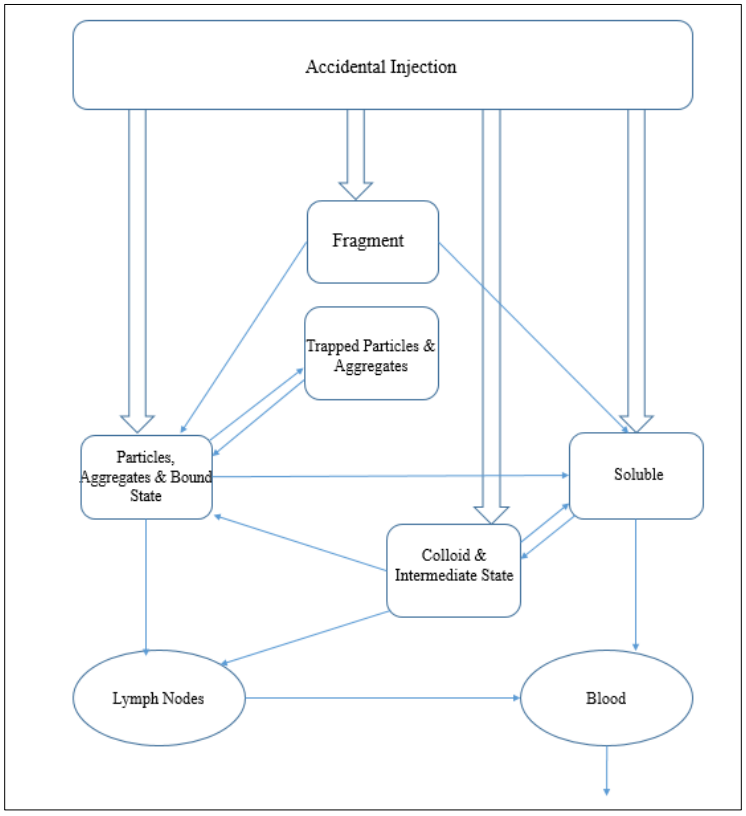

Fig. 2.4. Generic NCRP 156 compartment wound model of the biokinetics of radioactive materials deposited in a wound (NCRP 2006)

The generic NCRP 156 wound model is given in Fig. 2.4. The model consists of five compartments: Soluble; Colloidal and Intermediate States (CIS); Particles, Aggregates and Bound States (PABS); Trapped Particles and Aggregates (TPA) and Fragments, which conceived in order to describe the behavior of both soluble and insoluble radioactive materials regardless of the initial physical and chemical state. The radioactive materials may be contained in the compartments in their original states, or may undergo changes and move from one compartment to another (NCRP 2006, Doerfel et al. 2012).

Table 2.5. NCRP 156 designation for various soluble radioactive materials (NCRP 2006)

Retention Class	**Radionuclides**
Weak	$^{131}I^-$, $^{71}GeO_3^{2-}$, $^{74}AsCl_5^{2-}$, $^{124}SbO^{3-}$, $^{75}SeO_4^{2-}$, $^{95,96}TcCl_6^{2-}$, $^{191}WO_4^{2-}$, $^{86}Rb^+$, $^{137}Cs^+$, $^{45}Ca^{2+}$, $^{90}Sr^{2+}$, $^{140}Ba^{2+}$, $^{64}Cu^{2+}$, and $^{230}UO_2^{2+}$
Moderate	$^{110}Ag^+$, $^{223}Ra^{2+}$, $^{48}VO_3^-$, $^{105}RhCl_6^{3-}$, $^{127m}TeO_4^{2-}$, $^{191,193}PtCl_4^{2-}$, and $^{188}OsO_5^{2-}$
Strong	^{106}Ru ($RuCl_5^{2-}$), $^{7}Be^{2+}$, $^{51}Cr^{3+,}$ $^{67}Ga^{3+}$, $^{88}Y^{3+}$, $^{95}Nb^{2+}$, $^{114m}In^{3+}$, $^{140}La^{3+}$, $^{143}Ce^{3+}$, $^{143}Pr^{3+}$, $^{147}Nd^{3+}$, $^{147}Pm^{3+}$, $^{154,155}Eu^{3+}$, $^{160}Tb^{3+}$, $^{170}Tm^{3+}$, $^{227}Ac^{3+}$, $^{241}Am^{3+}$, $^{242,244}Cm^{3+}$, $^{210}Po^{4+}$, $^{238}Pu^{4+}$, and ≤ 3.2 μg of $^{239}Pu4+$
Avid	$^{46}Sc^{3+}$, $^{95}Zr^{4+}$, $^{113}Sn^{4+}$, $^{233}Pa^{5+}$, and $^{228,234}Th^{4+}$

The category “soluble” is further divided into retention classes of weak, moderate, strong and avid categories depending on their solubility. NCRP 156 classifies several anions and cations into one of these classes of “soluble” radionuclides (Table 2.5). Materials introduced into the wound initially in a soluble form enter the soluble compartment. A fraction of this activity would be absorbed into the blood compartment, and the remaining activity enters the CIS compartment. The transfer of radionuclides to the CIS compartment is governed by the tendency of the aqueous solution chemistry of the

radioactive material. The tendency of the radioactive material to hydrolyze eventually determines the retention of the material at the wound site. A fraction of the activity in the CIS compartment will be transformed into bound states in the PABS compartment. Material in CIS and PABS compartments solubilize and transfer back into the soluble compartments, albeit very slowly. A fraction of the activity in the CIS and PABS compartment is transferred to the lymph nodes, which represents long-term retention in the wound (NCRP 2006).

Particulate radionuclides, based on their physical properties and retention pattern, have been grouped into three main categories: colloid, particle and fragment. Colloids are formed as hydrolysis products, and have particulate properties. Fragments and particulates are solids, which include pure materials such as plutonium metal or oxides, mixtures such as mixed oxides or metal alloys, or solid materials contaminated on their surface with soluble radionuclides. The particle category represents material whose individual physical sizes are ≤ 20 μm. This upper limit of 20 μm represents the size of particles that can be phagocytized by tissue macrophages or can be moved to the lymph nodes. The fragment category comprises larger particles and fragments whose size or quantity cause a foreign body tissue reaction. The particulate materials have much longer retention in the wound compared to soluble materials primarily due to the insolubility of the materials and the foreign-body encapsulation phenomenon (NCRP 2006, Castellani et al. 2003).

First-order kinetics are used to describe the transfer of material from one compartment to another. The transfer rates between the compartments for various pathways for various types of materials are given in Table 2.6 (NCRP 2006).

Table 2.6. NCRP 156 default transfer rates for various wound types (NCRP 2006)

Pathway	Transfer rate (day^{-1})						
	Radionuclides initially in solution				Colloids[a]	Particles[a]	Fragments[a]
	Weak	Moderate	Strong	Avid			
Soluble to blood	45	45	0.67	7	0.5	100	
Soluble to CIS	20	30	0.6	30	2.5		
CIS to soluble	2.8	0.4	2.4×10^{-2}	0.03	2.5×10^{-2}		
CIS to PABS	0.25	6.5×10^{-2}	1.0×10^{-2}	10	5×10^{-2}		
CIS to lymph nodes	2×10^{-5}	2×10^{-5}	2×10^{-5}	2×10^{-5}	2×10^{-3}		
PABS to soluble	8×10^{-2}	2×10^{-2}	1.2×10^{-3}	0.005	1.5×10^{-3}	2×10^{-4}	0.0
PABS to lymph nodes	2×10^{-5}	2×10^{-5}	2×10^{-5}	2×10^{-5}	4×10^{-4}	3.6×10^{-3}	0.004
PABS to TPA						4×10^{-2}	0.7
TPA to PABS						3.6×10^{-3}	5×10^{-4}
Lymph nodes to blood					3×10^{-2}	6×10^{-4}	3×10^{-2}
Fragment to soluble							0.0
Fragment to PABS							8×10^{-3}

[a]Colloids, Particles or Fragments deposit into the CIS, PABS and fragment compartments respectively.

The retention in the wound can also be expressed as a sum of two to three exponential functions in the form of:

$$R(t) = \sum_i a_i e^{-\lambda_i t} \tag{2.4}$$

The default parameters for this equation to describe the retention of various categories of radionuclides in wounds are given in Table 2.7 (NCRP 2006). These parameters, however, are accurate for cases in which significant transfer of radionuclides to the lymph nodes does not occur, for example, the radionuclides belonging to one of the four categories of "soluble" materials (Table 2.5). In cases where such transfer occurs, for example the particulate material, these parameters will overestimate the absorption to the blood and hence the urinary excretion rate (NCRP 2006).

Table 2.7. Default parameters for equations describing the retention of various categories of radionuclides in wounds (NCRP 2006)

	Wound retention equation parameters					
Category	**A_1 (%)**	**λ_1 (d^{-1})**	**A_2 (%)**	**λ_2 (d^{-1})**	**A_3 (%)**	**λ_3 (d^{-1})**
Weak	55	55	40	6	5.0	0.1
Moderate	55	55	35	0.5	10	0.02
Strong	50	1.0	30	0.03	20	0.001
Avid	19	37	81	0.001		
Colloid	15	3.0	8	0.055	77	7×10^{-4}
Particle	5	0.05	95	4×10^{-4}		
Fragment	0.5	0.009	99.5	6.5×10^{-6}		

The transfer of activity away from both wound site and lymph nodes is required to combine the NCRP wound model with a systemic model. The coefficients of the exponential function to describe the wound and lymph node retention are different from the ones given in Table 2.7

Chapter 3 :
Data and Measurements

The majority of the information on this chapter comes from Durbin and Jeung (1990a, 1990b) unless otherwise indicated, and has also been summarized elsewhere (Poudel 2012, Poudel et al. 2016a, 2016b, 2016c).

3.1. Motivation

During the early 1970s, there was a general concurrence that the data available on plutonium metabolism in man were incomplete and unsatisfactory for the development of biokinetic and dosimetric models (Durbin 1972). To supplement the scarce data on plutonium metabolism in humans, experimental data from laboratory animals, specifically those that are phylogenetically closely related to human, were deemed to be a priority. The primary motivation behind such an undertaking was to enhance the understanding of the relationship between plutonium excretion and body deposition, and consequently improve the predictability of the urinalysis methods. Moreover, the behavior of plutonium in bones was also not clearly understood (Durbin and Jeung 1990a).

3.2. Animals

In these studies, three different species of the genus *Macaca*—Rhesus (*M. mulatta*), Cynomolgus (*M. fascicularis*), and Stumptail (*M. arctoides*)—were used (Table 3.1). A mixed population of both genders and different species were used because of the difficulties in obtaining an adequate number of adults of a single gender and species. Combining the data from the various species for this study was considered appropriate because of the well-known genetic similarity among the three species and their capability

to interbreed. The laboratory records, purchasing records, dentition and skeletal roentgenograms were used to determine the chronologic age of the animals. Animal care and use were accomplished using the standards at LBNL at the time of the studies.

3.3. Injections

The use of ^{238}Pu instead of ^{239}Pu in the Durbin experiments permitted smaller injection because of the higher specific radioactivity of ^{238}Pu. Moreover, the 17-keV x-rays of the ^{238}Pu progeny facilitated easy and accurate measurement of activity over a wide range of plutonium concentrations.

The Pu solution was prepared by dissolving a $^{238}PuO_2$ source in concentrated HNO_3. It was then reduced with SO_2, dried and then oxidized to the tetravalent oxidation state using concentrated HNO_3 and diluted in 0.08M citric acid-sodium citrate buffer. The final radioactivity of the stock solution was 8.4×10^7 Bq L^{-1}, and its pH 4. This solution was stored in a frozen state. Previous studies had demonstrated that plutonium citrate stored for 3 months at 6°C was not subjected to disproportionation and colloid formation. No biological or radiochemical evidence of colloid formation was observed during the storage. Prior to injection, the stock solution was thawed, filtered and loaded into disposable syringes for injection.

The solutions were then injected into the animals intravenously, intramuscularly or subcutaneously (Table 3.1). The intravenous injections were made into the superficial veins of the calf and ankle; intramuscular injections were made into the thickest part of the thigh.

Table 3.1. Injection Data

Case[a]	Mode[b]	Age	Weight	Amount (kBq)	Dosage (kBq/kg)	Days from injection to death	Case[a]	Mode[b]	Age	Weight	Amount (kBq)	Dosage (kBq/kg)	Days from injection to death
C89M	iv	8	6.2	259	41.8	7	C77F[c]	im	>11	4	172.05	43.29	0.083
C109F	iv	6	3.5	77	22.1	7	C108F[c]	im	>6.3	4	148	37	0.83
R119F	iv	3.8	4	49.6	12.4	7	C103F[c]	im	3.2	2	78.81	39.22	0.85
R121M	iv	4	4.6	44.4	9.76	7	S114F	im	>8	11.4	143.56	12.58	7
R101F	iv	>10	6.2	83.3	13.3	8	C145M	im	8	5.79	77.7	13.32	7
R120M	iv	4	3.9	55.5	14.2	8	C131F	im	>6.4	4.88	54.02	11.1	56
R122F	iv	4	4.5	51.1	11.4	8	R186M	im	~18	7.71	99.16	12.95	103
R192M	iv	14	11	122	11.1	8	C106M	im	>8	7.3	92.5	12.58	106
R100F	iv	>11	6.8	80.7	11.9	67	C166M	im	>8	7.3	129.5	17.76	106
C79F	iv	>11	3	51.1	17.3	106	C80F	im	>13	5.22	60.31	11.47	1100
C107M	iv	6.7	5.8	66.2	11.3	173	C95F	sc	>10.5	4	296	74	8
C111F	iv	>8	3.2	37	11.5	173							
R99F	iv	14.5	7.4	89.5	12.1	370							
C105M	iv	6	8	82.9	10.4	552							
S116F	iv	>5	8	102	12.7	559							
C94F	iv	9	7.4	72.9	9.85	587							
R102F	iv	8.5	4.7	63.3	13.5	1099							

[a] C = Cynomolgous, R = Rhesus, S = Stumptail; M = male, F = female

[b] iv = intravenous, im = intramuscular, sc = subcutaneous

[c] No urine data on these cases were available, because they were sacrificed less than one day post-injection

3.4. Sample Collection, Preparation and Measurements

3.4.1. Excreta Samples

As part of the experiment, urine and feces were collected from the animals, which were housed in metabolism cages, at frequent intervals from the day of injection to death. The collection frequency was daily or every other day for the first two weeks and twice weekly thereafter. If for any reason, the excreta samples were lost or a collection was skipped, the values for missing plutonium were calculated using the following equation:

$$\text{Pu in missing interval} = 0.5\left[\%\text{ID d}^{-1}(\text{week preceding gap}) + \%\text{ID d}^{-1}(\text{week after gap})\right] \times \text{Number of days skipped} \quad (3.1)$$

where, %ID is the percentage of injected dosage.

3.4.2. Blood and Plasma Samples

Small amounts of blood were taken from the leg veins of the animals to better understand the retention and clearance of plutonium from plasma.

To calculate the concentration of plutonium in plasma volume, the densities of whole blood and plasma (1.058 g-mL^{-1} and 1.027 g-mL^{-1} respectively) were assumed to be the same as for ICRP 23 reference man (ICRP 1974). Total Pu in plasma volume was calculated by Durbin and Jeung (1990a, 1990b) using the findings of Gregersen et al. (1959) who measured the red cell and plasma volumes of rhesus monkeys of both sexes: plasma (mL) = 36.4 mL kg^{-1}; whole body hematocrit = 0.56.

For plasma samples,

$$\text{Plasma Pu (\%ID)} = \frac{36.4\ \text{ml/kg x Body Mass (kg)} \times \%\text{ID in sample} \times 1.027\ \text{g/ml}}{\text{Mass of sample (g)}} \tag{3.2}$$

For whole blood samples,

$$\text{Plasma Pu (\%ID)} = \frac{36.4\ \text{ml/kg x Body Mass (kg)} \times \%\text{ID in sample} \times 1.058\ \text{g/ml}}{\text{Mass of sample (g)} \times (1 - 0.44)} \tag{3.3}$$

Although equations (1) and (2) were derived based on the analysis of rhesus monkeys weighing 3 to 7 kg (Gregersen et al. 1959), it was assumed that the results can be extended to monkeys weighing more than 7 kg.

3.4.3. Autopsy

The animals were dissected after an overdose of Sernylan and Diabutal, or Ketelar and Diabutal. The animals' abdomen was opened and all blood was withdrawn. Throacic and abdominal organs were removed altogether and placed in beakers for drying and ashing. The contents of the GI tract were added to the last fecal collection. The skeleton was separated from the body, and the organs and the bones were weighed.

3.4.4. Sample Preparation and Counting

The excreta samples were dried at 200ºC; the tissues and bones at 100ºC. The dried samples were ashed in a furnace at 600ºC as long as necessary to reduce them to a grey ash. The dry ash was then digested with concentrated nitric acid to produce a carbon-free-

salt. The plasma and blood samples were ashed in a small furnace by raising the temperature of the furnace to a range between 450 to 500ºC over the period of several hours. The ash, when cooled, was dissolved in 6N nitric acid and thereafter transferred into volumetric flasks.

Ashed sampled of blood, plasma, small tissues, small bones, and aliquots of large soft tissues of low Pu content were counted using alpha counting. The samples were dissolved in 6N nitric acid, and the entire solution and rinses or an appropriate aliquot of the solution was placed in a glass planchet. The samples were dried on a hot plate to expel volatile nitrates. The planchets were reweighed to calculate the sample mass, and corrections were made for self-absorption.

The 17-keV L x-rays of the ^{234}U were used to determine the Pu content in the livers from animals killed within a year of injection, bones of more than 4-g ash weight, and biological samples assumed to contain more than 0.05% of the injected activity. The ashed samples were dissolved in nitric acid, the solution and its rinse were then transferred into one or more 60-ml or 125-ml plastic bottles. The samples were counted in a dual-crystal scintillation detection system (12.5 cm in diameter and 3-mm thick NaI(Tl) crystals). For excreta collected after 2 weeks, samples were chemically processed to remove the sodium and potassium salts thus increasing the count rate by decreasing self-absorption and introducing less error into the calculation of true dry weight of the samples. The background blanks were prepared from known composition of KCl solution and the urine or feces of uninjected monkeys of the same body size were used as backgrounds.

Because the alpha activity of late blood and plasma samples was too low after eight weeks post-injection, plutonium was isolated from these samples by ion exchange and then plated on metal discs. The activity was measured by counting for sufficiently longer periods of time.

3.4.5. Mass Balance

Since it was not possible to achieve a 100% material recovery because of the combination of the incomplete collection of excreta, and errors in measurement of injected activity, measurement of the amount injected and systematic errors in radioanalysis of the samples, all collection data for each case was normalized to 100% recovery by Dr. Durbin. The normalization factor was computed using equation 3:

$$\text{Normalization factor} = 100\%\,[\%\text{ of injected activity in tissues, bones, excreta} - (\%\text{ of injected activity in blood samples})] \quad (3.4)$$

The normalization factor thus computed was applied to all samples – tissues, bones, excreta.

Chapter 4 :
Comparison of the Biokinetic Data with the Predictions of ICRP 67 and Other Plutonium Systemic Models

4.1. Objective

Despite the presence of relatively large amounts of human data available on the metabolism of plutonium, the experimental biokinetic data obtained from the NHPs (discussed in Chapter 3) is still important in constructing and parametrizing biokinetic models. The objective of this study was to determine the efficacy of the ICRP 67 systemic model for plutonium (ICRP 1993) along with two human models developed thereafter (Luciani and Polig 2000, Leggett et al. 2005) in predicting the urinary and fecal excretion rates, retention in blood, as well as retention in liver and skeleton at the time of death. Such comparative studies also help identify pathways that are physiologically similar or distinct between the NHPs and humans for the translocation of plutonium.

4.2. Data Analysis

4.2.1. Methods for Analysis of Bioassay Data

Proper interpretation of bioassay measurements is necessary for the estimation of intake and the dose experienced by the workers and the public. A simple general approach to estimate the intake (I) from a direct or indirect bioassay measurement is given as (IAEA 2004):

$$I = \frac{M(t)}{m(t)} \tag{4.1}$$

where, *M(t)* is the measured body content, body region content or excretion rate at time *t*, and *m(t)* is the fraction of unit intake retained in the whole body or in body organs (intake retention fraction (IRF)) or the amount excreted in a time period from the body at time *t* (intake excretion fraction). The information on intake retention or excretion fractions are obtained from the biokinetic models. As an example, NUREG/CR-4884 (USNRC 1987) contains a list of IRFs for different radionuclides and for different modes of intakes. This method of making a point estimate is useful when only a single bioassay measurement is available.

Because of the inherent uncertainty in estimating the intake from a single bioassay measurement, more than one bioassay measurements is frequently taken. NUREG/CR-4884 suggests the use of the least squares method to estimate the intake when data from several bioassay measurements is available. Such method minimizes the sum of the squares of the deviations *S* of the observed measurements from the model predictions.

$$S = \sum_i \left[M_i - I\ m(t_i)\right]^2 \tag{4.2}$$

The best estimate of intake *I* is given as (USNRC 1987, IAEA 2004):

$$I = \frac{\sum_i M_i m(t_i)}{\sum_i m(t_i)^2} \tag{4.3}$$

where, $m(t_i)$ is the intake retention fraction associated with the *i*th measurement and M_i is the value of the *i*th measurement.

Several other statistical methods can be used to obtain the best estimate of intake from multiple bioassay measurements. Information on the uncertainty of measurements and knowledge on the confidence of each point in a data set can be used to assign weighting factors. Such weighting of the data-point or a data-set to obtain a better estimate of the intake is often referred to as a weighted least squares fit method (Skrable et al. 1988, IAEA 2004). Using the weighted least squares fitting method, the best estimate of intake I is given as:

$$I = \frac{\sum_i \left[M_i m(t_i) w_i\right]}{\sum_i [m(t_i)]^2 w_i} \tag{4.4}$$

where w_i is the weighting factor based on either the information on the error associated with each measurement or on the subjective assessment of confidence in each data point or data set. This method minimizes the sum S where,

$$S = \sum_i \left[M_i - I\ m(t_i)\right]^2 w_i \tag{4.5}$$

One widely accepted statistical fitting method, which was also used for this study, is the maximum likelihood method (IAEA 2004, Doerfel et al. 2006, 2012). This method is commonly used for estimating the parameter(s) of a statistical model from a sample data set (Cam 1990). The weighted and unweighted least squares fit can be considered special cases of the maximum likelihood method.

The maximum likelihood method is useful in internal dosimetry when making estimates of intake *I* from a set of multiple bioassay measurements. This method minimizes the value of chi-square, which is given as:

$$\chi^2 = \frac{\sum_i \left[M_i - I\ m(t_i)\right]^2}{{\sigma_i}^2} \tag{4.6}$$

where σ_i is the standard deviation of M_i. The best estimate of intake *I* is then given as:

$$I = \frac{\left\{\sum_{i=1}^{n}\left[M_i m(t_i)/{\sigma_i}^2\right]\right\}}{\left\{\sum_{i=1}^{n}\left[m^2(t_i)/{\sigma_i}^2\right]\right\}} \tag{4.7}$$

The knowledge of the standard deviation, σ_i , for each measurement is needed to use the maximum likelihood analysis. A detailed mathematical description of the maximum likelihood method follows the discussion on the uncertainties of bioassay measurements.

4.2.2. Uncertainties in Bioassay Measurements

Each bioassay measurement is associated with certain errors and uncertainties. The components of such uncertainty in a measurement can be divided into Type A and Type B uncertainties depending on whether the uncertainties are based on statistical means or non-statistical means (BIPM et al. 2010). The Type A and Type B errors, in some instances, can be considered as random and systemic effects respectively (Cox and Harris 2004). In the case of measurement of activity (*in vivo* or *in vitro*), Type A uncertainties arise from the stochastic nature of the radioactive decay and thus can be described by Poisson

distribution (Hurtgen and Cossonnett. 2003, Castellani et al. 2013). The Type B errors are results of measurement and sampling techniques. The most common sources of Type B uncertainties with *in vitro* bioassay measurements are due to the variations in sample volume or weight, chemical yield, electronic stability, contamination of sample and impurities, source positioning for counting, counting efficiency, counting time, and background measurements (Skrable et al. 1994, Hurtgen and Cossonnett 2003, Castellani et al. 2013). Similarly, Type B uncertainties with *in vivo* measurements may be the results of counting geometry errors, positioning or movement of the individual, differences between phantom and individual or organ, electronic instability, variations in background radiation, external contamination of the person, uncertainties in calibration source, etc. (Castellani et al. 2013).

The assessment of these uncertainties is critical to the proper estimation of intake, as such assessment enables the calculation of chi-square statistics and goodness of fit parameters which are used to compare the consistency of models with the data (Doerfel et al. 2006, 2012). Moreover, proper assessment of uncertainties in the measurement data is critical because uncertainties have a strong influence on the estimation of intake (and hence the dose) when using the maximum likelihood method (Skrable et al. 2002).

The General Guidelines for the Estimation of Committed Dose from Incorporation of Monitoring Data (IDEAS guidelines) (Doerfel et al. 2006, 2012, Castellani et al. 2013), established to bring consistency in evaluations for internal dosimetry, suggested that the uncertainties in the bioassay measurements can be described in terms of a log-normal distribution, and the scattering factor (*SF*) is defined as its geometric standard deviation. The guidelines recommend using scattering factors as analogous to the geometric standard

deviation. If SF_A and SF_B are the scattering factors corresponding to the counting and "other" uncertainties respectively, the total scattering factor, *SF*, is then,

$$SF = \exp\sqrt{[\ln(SF_A)]^2 + [\ln(SF_B)]^2} \tag{4.8}$$

An analysis of several example cases indicated that the SF_A has little influence on the overall *SF* calculation (i.e., SF_B dominates the calculation of *SF*), and hence the IDEAS guidelines adopted the SF_B as the overall *SF* in the bioassay measurements (Doerfel et al. 2006, 2012; Castellani et al. 2013).

The guidelines suggest the log-normal scattering factors of 1.1 for true 24-hour urine samples, and 2 to 4 for 24-hour fecal samples. The guidelines recommend a scattering factor of 1.3 to 1.8 for simulated 24-hour urine samples as such samples do not truly reflect the urine excreted during 24 hours. The guidelines, based on judgement and experience, recommend use of average scattering factors of 1.6 for urine samples and 3 for fecal bioassay samples.

Blood samples are generally not used for intake calculation, and thus the distribution of errors in measurements of blood is not as well-known as those for urine samples. However, the scattering factor *SF* can be calculated by calculating the geometric standard deviation (GSD) of the data (M_i) around the trend (i.e., the predicted quantities, p_i):

$$SF = e^{\sigma} \tag{4.9}$$

$$\text{where, } \sigma^2 = \frac{\sum_{i=1}^{n}[\ln(M_i) - \ln(p_i)]^2}{n - z} \tag{4.10}$$

where, n is the number of samples, and z is the number of parameters used to determine the trend of the data (two for each exponential term) (Marsh et al. 2007). The scattering factor of 2.1 for blood samples calculated by Konzen (2015) and Konzen et al. (2016) using the equations 4.9 and 4.10 above was used in our analysis. The summary of the scattering factors used for our analysis is presented in Table 4.1.

Table 4.1. Scattering factors for various bioassay data used in this analysis

Bioassay data type	Scattering factor used	Source
Urine	1.6	IDEAS Guidelines (Doerfel et al. 2006, 2012; Castellani et al. 2013)
Feces	3	"
Blood	2.1	Konzen 2015, Konzen et al. 2016, based on Marsh et al. 2007

4.2.3. The Likelihood Function and the Maximum Likelihood Analysis Method

The likelihood function, $L_i(I)$, is the central statistical quantity of the maximum likelihood analysis method, and is defined by (Castellani et al. 2013):

$$L_i(I) = P(M_i \mid I) \tag{4.11}$$

where, $P(M_i \mid I)\, dM_i$ is the probability of observing measurement value M_i in the interval between M_i *and* $M_i + dM_i$ given that the true value of the intake is I. When there are n

independent measurements, the likelihood function is the product of the individual likelihood functions, i.e.,

$$L(I) = \prod_{i=1}^{n} L_i(I) \tag{4.12}$$

If $P(M_i \mid I)$ is given by a lognormal distribution (Castellani et al. 2013),

$$L_i(I) = \frac{1}{M_i \ln(SF_i)\sqrt{2\pi}} \exp\left[- \frac{\left[\ln(M_i) - \ln(I\ m(t_i))\right]^2}{2\left[\ln(SF_i)\right]^2} \right] \tag{4.13}$$

where, SF_i is the scattering factor described in section 4.2.3. If the likelihood functions for all individual measurements are represented by lognormal distributions given in equation (4.13) above and none of the measurements are less than the detection limit, the combined likelihood function can be obtained using equation (4.13) and (4.12) above (Castellani et al. 2013):

$$L(I) = \prod_{i=1}^{n} \left[\frac{1}{M_i \ln(SF_i)\sqrt{2\pi}} \exp\left[- \frac{\left[\ln(M_i) - \ln(I\ m(t_i))\right]^2}{2\left[\ln(SF_i)\right]^2} \right] \right] \tag{4.14}$$

$$\text{or, } L(I) = constant \times \exp\left[- \frac{\chi^2(I)}{2} \right] \tag{4.15}$$

$$\text{where, } constant = \prod_{i=1}^{n} \frac{1}{\sqrt{2\pi} M_i \ln(SF_i)} \tag{4.16}$$

$$\text{and, } \chi^2(I) = \sum_{i=1}^{n} \frac{\left[\ln(M_i) - \ln(I\ m(t_i))\right]^2}{\left[\ln(SF_i)\right]^2} \tag{4.17}$$

The likelihood function is maximum when $\chi^2(I)$ is a minimum. Differentiating with respect to ln(*I*), setting it equal to zero, and rearranging for *I* gives (Castellani et al. 2013):

$$\ln(I) = \frac{\sum_{i=1}^{n} \frac{\ln(I_i)}{[\ln(SF_i)]^2}}{\sum_{i=1}^{n} \frac{1}{[\ln(SF_i)]^2}} \tag{4.18}$$

where, I_i is the intake calculated from the *i*th measurement, and is given as, $I_i = M_i / m(t_i)$.

When data sets from different monitoring techniques (for example urine, fecal and blood measurements) are available, equation (4.18) can be extended to estimate the intake using maximum likelihood analysis (Castellani et al. 2013):

$$\ln(I) = \frac{\frac{\sum_{i=1}^{n_u} \ln(I_i)}{(\ln(SF_u))^2} + \frac{\sum_{i=1}^{n_f} \ln(I_j)}{(\ln(SF_f))^2} + \frac{\sum_{i=1}^{n_b} \ln(I_k)}{(\ln(SF_b))^2}}{\frac{n_u}{(\ln(SF_u))^2} + \frac{n_f}{(\ln(SF_f))^2} + \frac{n_b}{(\ln(SF_b))^2}} \tag{4.19}$$

where, I_i, I_j and I_k refer to the individual intake estimates from the urine, fecal and blood data respectively, SF_u , SF_f and SF_b are the scattering factors for urine, feces and blood data respectively, and n_u, n_f and n_b are the number of urine, feces and blood measurements available.

4.2.4. Integrated Modules for Bioassay Analysis

To evaluate the biokinetic predictions of different models used to analyze the NHP data, a suite of internal dosimetry software programs called the Integrated Modules for

Bioassay Analysis (IMBA) Professional Plus (Fig. 4.1**)** was used. A special academic version of this software which provides greater research flexibility was provided by the developer, the Radiation Protection Division of Health Protection Agency (HPA, currently Public Health England), UK, as part of this research collaboration. The suite can be used to calculate intake and doses from a set of bioassay measurements as well as to calculate bioassay values and doses from a known intake. Various modules of the software solve the currently recommended biokinetic and dosimetric models in order to estimate intake and dose based on the available data. In addition to the recommended models, the software provides sufficient flexibility to employ user-defined sets of model parameters (Birchall et al. 2007). This feature was, for example, employed to create the Luciani and Leggett models in IMBA.

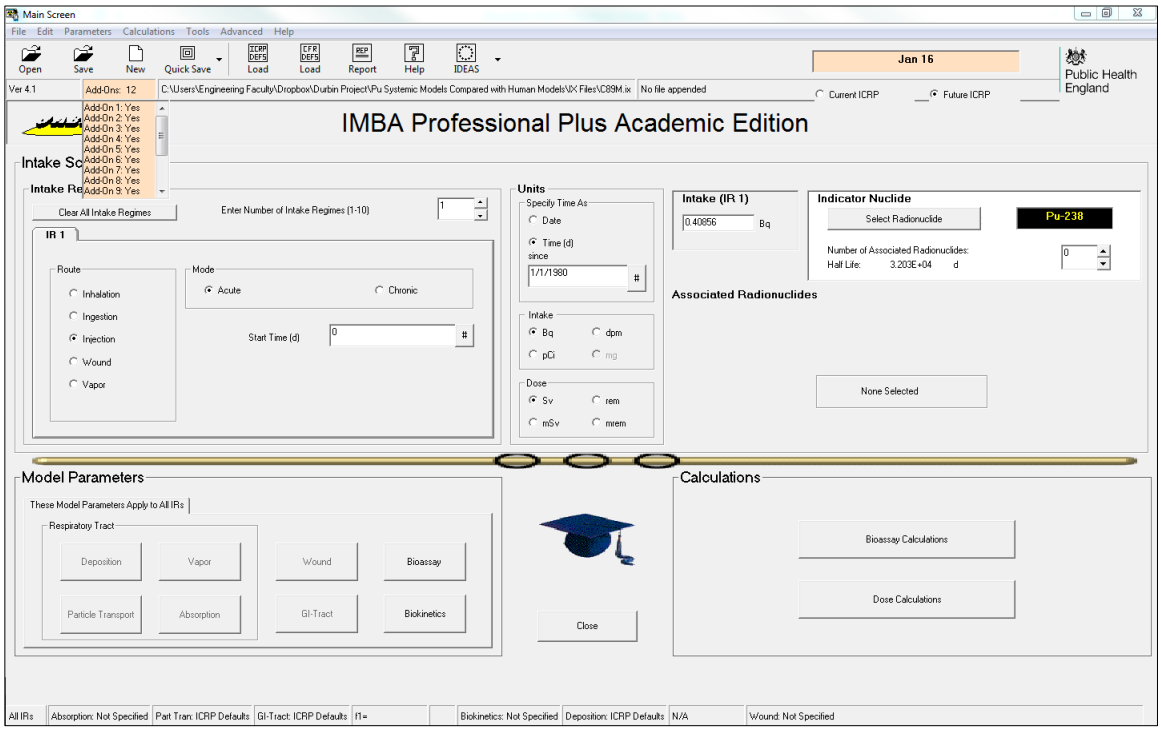

Fig. 4.1. Home Screen of IMBA Professional Plus Academic Edition

The software uses the maximum likelihood method to make estimates of intake *I* from a set of multiple bioassay measurements $m_i(t_i)$. The best intake *I* is calculated such that the product of *I* and *f(t)*, where *f(t)* represents an excretion or retention function, best fits the data (James 2005). The intakes predicted using the maximum likelihood analysis of the bioassay measurements were compared with the known intake to evaluate the efficacy of the models.

The software can also be used "in reverse" to calculate the activities in organs at various times after the intake. This feature was used to compare the actual measured activities in the liver and skeleton tissues of the animals with what would be predicted using the three reference models given the known intake.

4.3. Results of Comparison Analysis

The bioassay measurements and the activities in the skeleton and liver tissues measured at death were plotted against the biokinetic predictions of the three different models (Fig. 4.2, Fig. 4.3, and Fig. 4.4). Our initial impressions, based on these plots, were that the reference human models satisfactorily predicted the urinary excretion rates, activities in blood, and activities in liver at early times post intake. Results of the detailed analysis of the urinary, fecal and blood data using the maximum likelihood method follows.

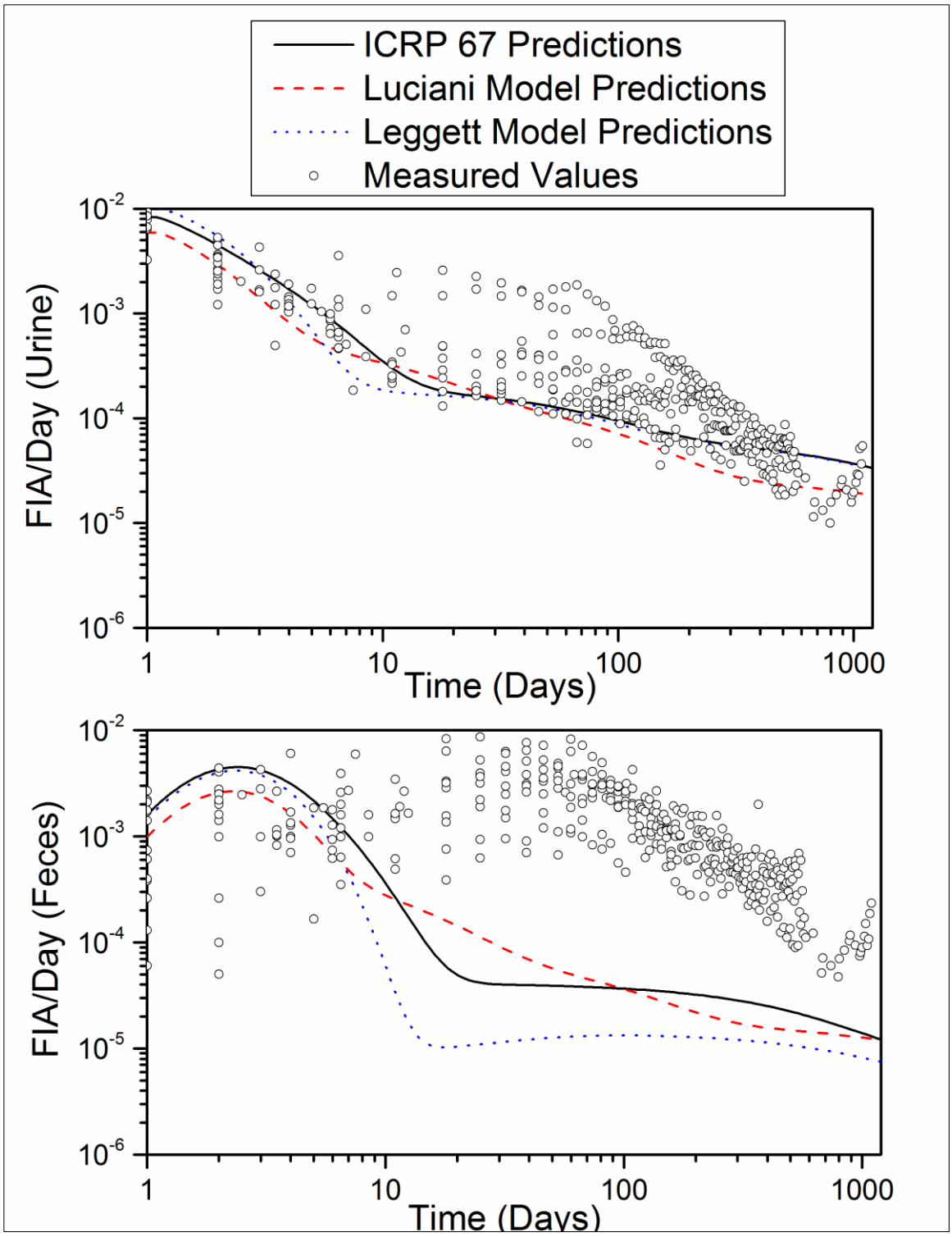

Fig. 4.2. Urinary excretion [fraction of injected activity (FIA) per day], fecal excretion (FIA/day) data from the NHPS compared with the predictions of the reference models

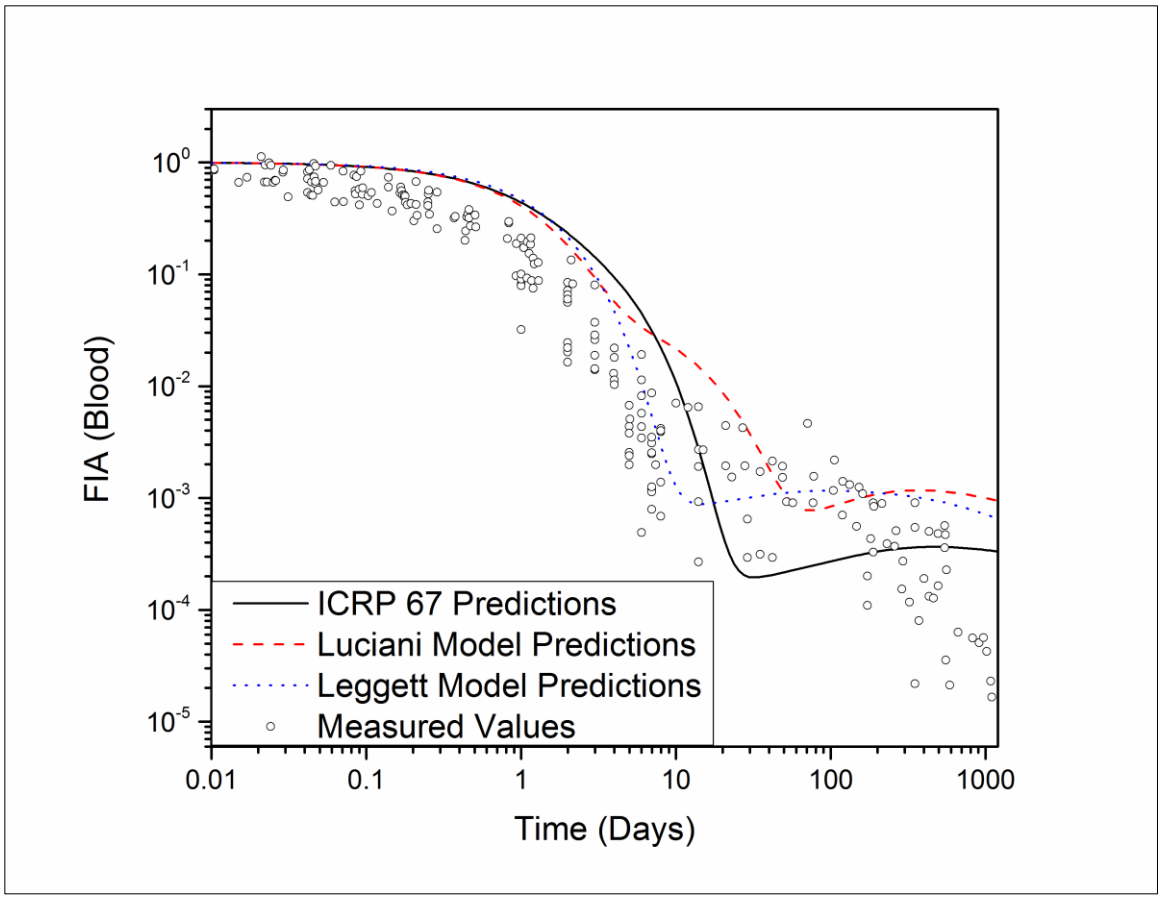

Fig. 4.3. Retention in blood (FIA) in NHPs compared with the predictions of reference models

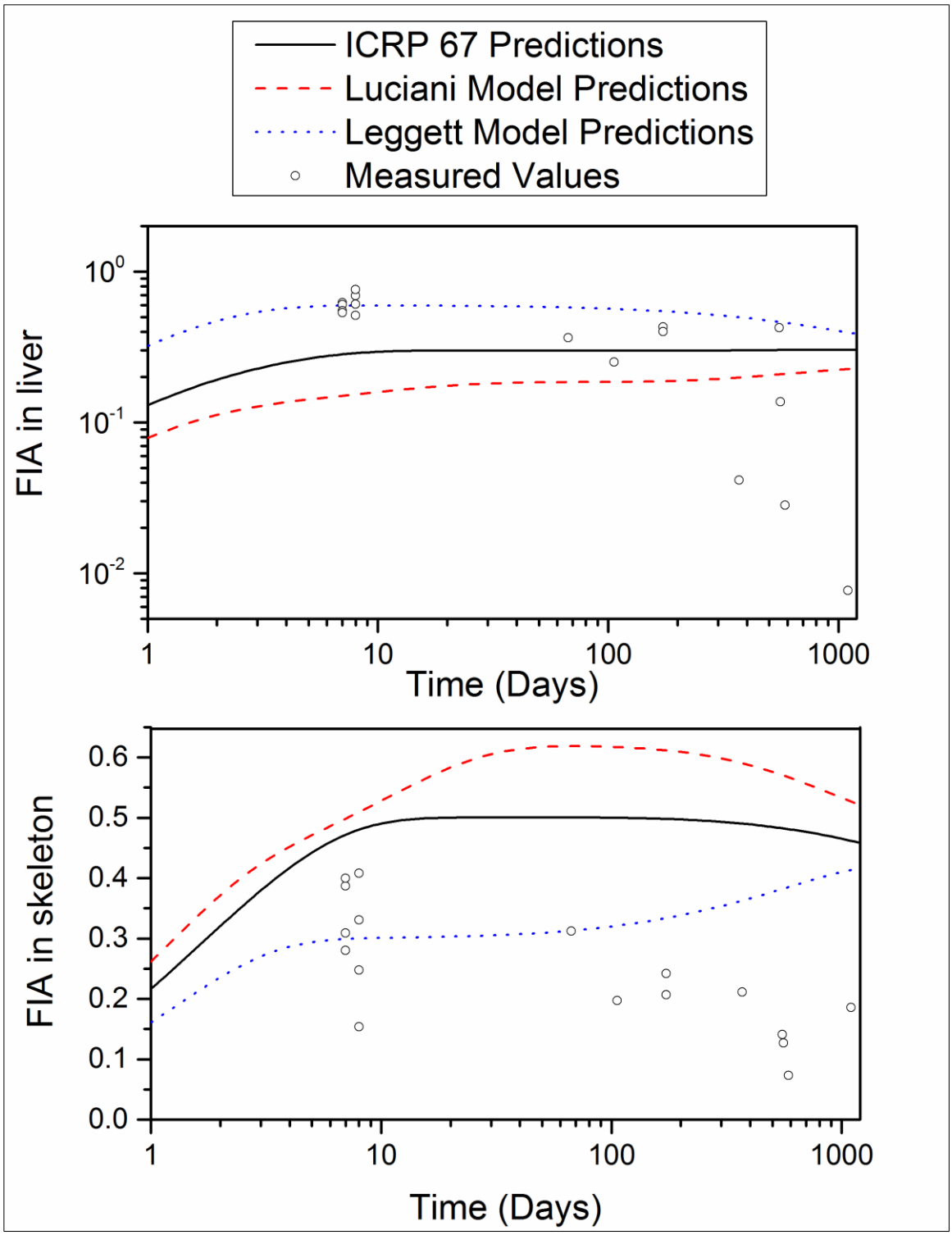

Fig. 4.4. Activities in liver and skeleton tissues (FIA) measured in NHPs compared with the predictions of reference models

4.3.1. Results of Maximum Likelihood Analysis of Urinary, Fecal, and Blood Data

Maximum likelihood analysis of urinary excretion data was conducted using the ICRP 67, Luciani and Leggett models (Table 4.2). Considering 17 cases, acceptable fits ($p > 0.05$) were obtained for 13, 14 and 15 cases using the Leggett model, ICRP 67 model and Luciani model respectively. Unacceptable fits were obtained for cases sacrificed after 560 days post injection using all three models. The ratios of intake predicted using the maximum likelihood analysis of urine data to the actual intake ranged from 0.68 to 2.25 with an average of 1.28 ± 0.52[1] using the ICRP 67 model, 1.12 to 3.69 with an average of 1.95 ± 0.79 using the Luciani model, and 0.80 to 2.49 with an average of 1.42 ± 0.54 using the Leggett model (Fig. 4.5). This suggests that the urinary excretion in macaques is predicted reasonably well by the reference models for humans.

The intakes predicted using the maximum likelihood analysis of the fecal data were from four times less than the actual intake to 29 times more than the actual intake using the ICRP 67 model (Table 4.3). The predicted intakes varied from 0.45 to 33 times the actual intake using Luciani model and 0.31 to 77 times the actual intake using the Leggett model (Fig. 4.6). Using the ICRP 67 model, the average ratio of intakes for the cases sacrificed seven and eight days post injection is 0.55, whereas that for the cases sacrificed 67 to 1,099 days post injection is 19.0. After the first week, the measured fecal excretion exceeds the prediction curves by increasing amounts (Fig. 4.2), and accounts for the large overestimates of intake. These inconsistencies in the predictions of intake from fecal bioassay of NHP

[1] All errors are reported as 1 standard deviation.

point out the important physiological differences between the macaques and humans, as will be discussed later.

Similar analyses were also done for the blood data for each case. Although the use of blood Pu levels for dose assessment or intake predictions has little to no value, as blood samples are rarely taken in cases of radioactive material exposure, it can still be useful for interspecies model comparison. The ratios of activity predicted using the blood measurements to the actual activity ranged from 0.13 to 1.38 with an average of 0.50 ± 0.29 using the ICRP 67 model. The ratios ranged from 0.14 to 0.71 with an average of 0.36 ± 0.14 using the Luciani model, and 0.24 to 1.51 with an average of 0.51 ± 0.28 using the Leggett model. The maximum likelihood analysis of the blood data using ICRP 67 model does not adequately fit the data in ten of the seventeen cases (Table 4.4). In all three models, there is recycling of activity between blood and the liver, the skeleton and the alimentary canal. The difficulties in predicting the intake accurately using the blood data can be explained by the differences between humans and NHPs in the translocation of activities in liver, skeleton and the alimentary canal, as discussed later.

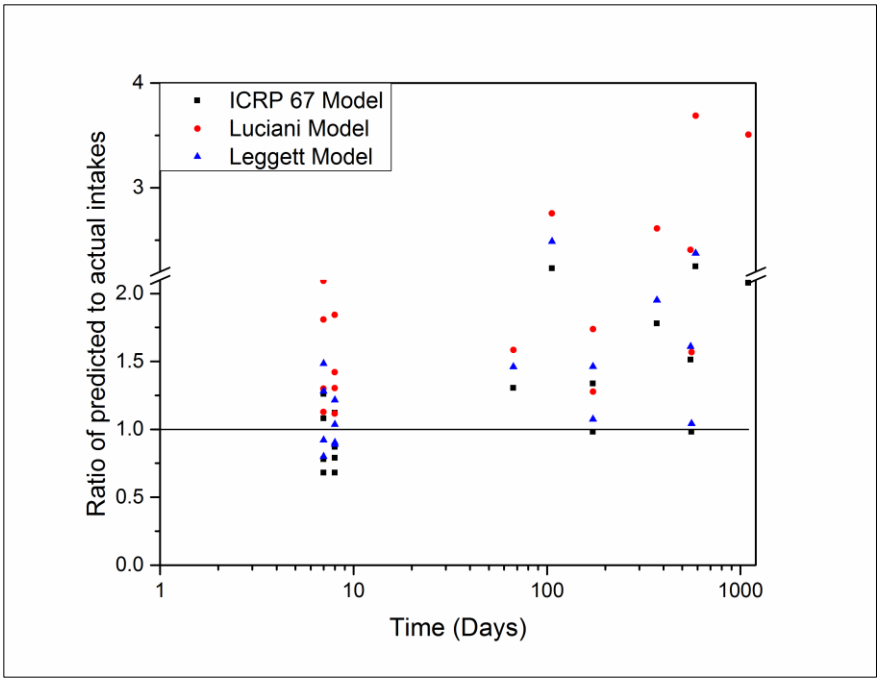

Fig. 4.5. Ratios of intakes predicted using the maximum likelihood analysis of urine data using various reference models to actual intake

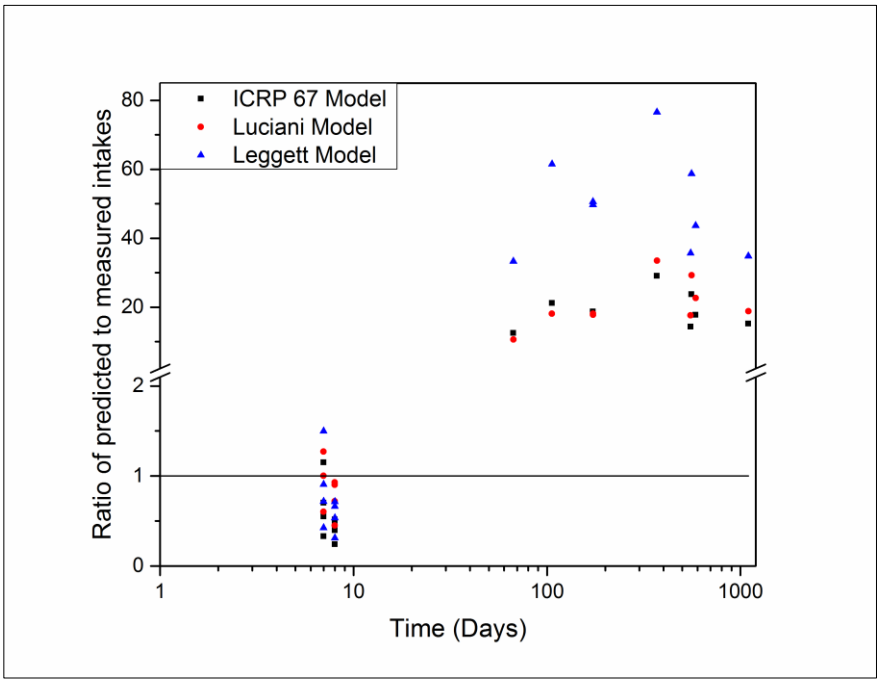

Fig. 4.6. Ratios of intakes predicted using maximum likelihood analysis of fecal data using various reference models to actual intake

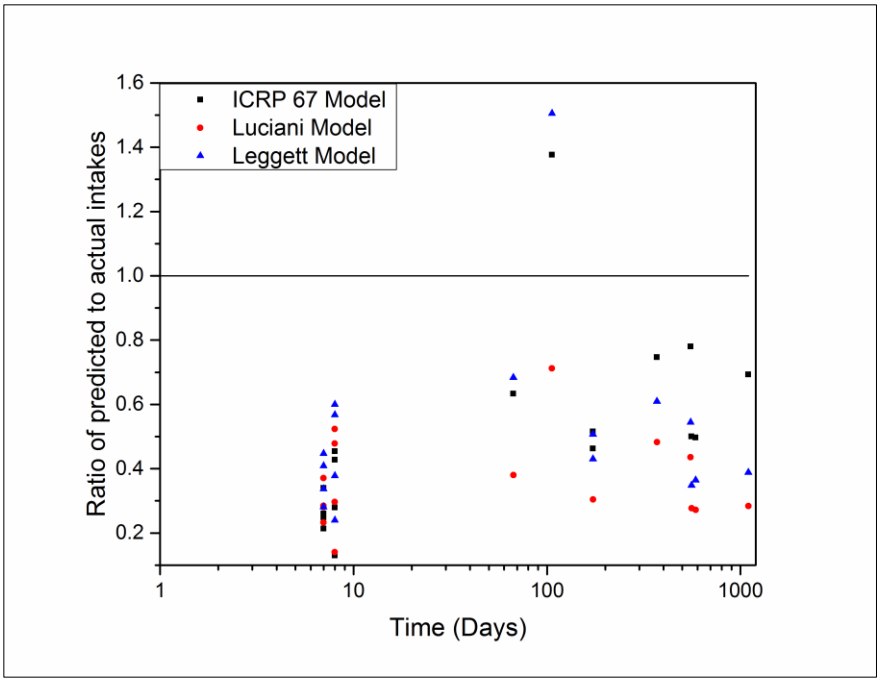

Fig. 4.7. Ratios of intakes predicted using the maximum likelihood analysis of blood data using various reference models to actual intake

Table 4.2. Maximum likelihood analysis of urine data using different human models

Case	Days from injection to death	ICRP 67 Model		Luciani Model		Leggett Model	
		P/M[a]	p-value[b]	P/M[a]	p-value[b]	P/M[a]	p-value[b]
C89M	7	1.08	**1.93 x 10 $^{-1}$**	1.81	**4.09 x 10 $^{-1}$**	1.28	**2.09 x 10 $^{-1}$**
C109F	7	1.26	**9.78 x 10 $^{-1}$**	2.09	**9.59 x 10 $^{-1}$**	1.48	**3.44 x 10 $^{-1}$**
R119F	7	0.78	**3.17 x 10 $^{-1}$**	1.30	**4.33 x 10 $^{-1}$**	0.92	**1.24 x 10 $^{-1}$**
R121M	7	0.68	**2.34 x 10 $^{-1}$**	1.13	**3.23 x 10 $^{-1}$**	0.80	**9.88 x 10 $^{-2}$**
R101F	8	1.12	**9.43 x 10 $^{-1}$**	1.84	**9.06 x 10 $^{-1}$**	1.22	**3.56 x 10 $^{-1}$**
R120M	8	0.68	**2.71 x 10 $^{-1}$**	1.12	**1.69 x 10 $^{-1}$**	0.89	**3.63 x 10 $^{-1}$**
R122F	8	0.87	**1.54 x 10 $^{-1}$**	1.42	**2.33 x 10 $^{-1}$**	1.04	7.84 x 10 $^{-3}$
R192M	8	0.79	**2.15 x 10 $^{-1}$**	1.30	**3.98 x 10 $^{-1}$**	0.90	**2.47 x 10 $^{-1}$**
R100F	67	1.30	1.54 x 10 $^{-2}$	1.59	**1.33 x 10 $^{-1}$**	1.46	1.58 x 10 $^{-2}$
C79F	106	2.23	**8.45 x 10 $^{-1}$**	2.76	**9.62 x 10 $^{-1}$**	2.49	**4.07 x 10 $^{-1}$**
C107M	173	1.34	**4.11 x 10 $^{-1}$**	1.74	**1.83 x 10 $^{-1}$**	1.46	**2.66 x 10 $^{-1}$**
C111F	173	0.98	**9.99 x 10 $^{-1}$**	1.28	**9.20 x 10 $^{-1}$**	1.07	**9.87 x 10 $^{-1}$**
R99F	370	1.78	**4.60 x 10 $^{-1}$**	2.61	**4.33 x 10 $^{-1}$**	1.95	**5.10 x 10 $^{-1}$**
C105M	552	1.51	**9.82 x 10 $^{-1}$**	2.41	**6.57 x 10 $^{-1}$**	1.61	**9.24 x 10 $^{-1}$**
S116F	559	0.98	**9.47 x 10 $^{-1}$**	1.57	**9.98 x 10 $^{-1}$**	1.04	**8.67 x 10 $^{-1}$**
C94F	587	2.25	2.53 x 10 $^{-52}$	3.69	2.30 x 10 $^{-29}$	2.37	1.42 x 10 $^{-58}$
R102F	1099	2.08	5.49 x 10 $^{-41}$	3.51	1.65 x 10 $^{-23}$	2.17	1.31 x 10 $^{-44}$
Average		1.28		1.95		1.42	
Median		1.12		1.74		1.28	

[a] The ratio of intake predicted using maximum likelihood analysis to the actual intake

[b] p-value > 0.05 indicates adequate fits (indicated in bold).

Table 4.3. Maximum likelihood analysis of fecal data using different human models**.**

Case	Days from injection to death	ICRP 67 Model		Luciani Model		Leggett Model	
		P/M[a]	p-value[b]	P/M[a]	p-value[b]	P/M[a]	p-value[b]
C89M	7	0.33	**7.67 x 10 $^{-1}$**	0.60	**6.54 x 10 $^{-1}$**	0.42	**5.54 x 10 $^{-1}$**
C109F	7	1.15	**4.80 x 10 $^{-1}$**	2.10	**3.74 x 10 $^{-1}$**	1.50	**2.75 x 10 $^{-1}$**
R119F	7	0.55	**9.42 x 10 $^{-1}$**	1.00	**8.86 x 10 $^{-1}$**	0.72	**7.61 x 10 $^{-1}$**
R121M	7	0.70	**6.07 x 10 $^{-1}$**	1.27	**5.76 x 10 $^{-1}$**	0.91	**4.34 x 10 $^{-1}$**
R101F	8	0.24	3.25 x 10 $^{-3}$	0.45	2.07 x 10 $^{-3}$	0.31	1.50 x 10 $^{-3}$
R120M	8	0.49	3.04 x 10 $^{-2}$	0.90	2.01 x 10 $^{-2}$	0.71	7.34 x 10 $^{-3}$
R122F	8	0.40	**1.17 x 10 $^{-1}$**	0.72	**8.05 x 10 $^{-2}$**	0.53	**3.49 x 10 $^{-2}$**
R192M	8	0.51	**5.79 x 10 $^{-2}$**	0.93	4.73 x 10 $^{-2}$	0.66	3.52 x 10 $^{-2}$
R100F	67	12.49	6.57 x 10 $^{-11}$	10.61	3.44 x 10 $^{-6}$	33.32	3.78 x 10 $^{-6}$
C79F	106	21.15	1.38 x 10 $^{-17}$	18.10	6.49 x 10 $^{-12}$	61.47	0.00
C107M	173	18.73	4.28 x 10 $^{-5}$	18.14	6.05 x 10 $^{-4}$	50.54	1.31 x 10 $^{-7}$
C111F	173	18.41	5.11 x 10 $^{-7}$	17.83	3.07 x 10 $^{-4}$	49.68	2.22 x 10 $^{-11}$
R99F	370	29.08	1.88 x 10 $^{-4}$	33.49	2.00 x 10 $^{-2}$	76.52	1.40 x 10 $^{-7}$
C105M	552	14.36	**6.39 x 10 $^{-1}$**	17.67	**8.31 x 10 $^{-1}$**	35.66	**1.51 x 10 $^{-1}$**
S116F	559	23.71	**7.81 x 10 $^{-2}$**	29.26	**6.78 x 10 $^{-1}$**	58.66	3.69 x 10 $^{-4}$
C94F	587	17.73	3.11 x 10 $^{-3}$	22.69	**2.27 x 10 $^{-1}$**	43.63	8.50 x 10 $^{-7}$
R102F	1099	15.20	**7.34 x 10 $^{-1}$**	18.80	**9.70 x 10 $^{-1}$**	34.78	4.39 x 10 $^{-2}$
Average		10.31		11.45		26.47	
Median		12.49		10.61		33.32	

[a] The ratio of intake predicted using maximum likelihood analysis to the actual intake

[b] p-value > 0.05 indicates adequate fits (indicated in bold).

Table 4.4. Maximum likelihood analysis of blood data using different human models

Case	Days from injection to death	ICRP 67 Model		Luciani Model		Leggett Model	
		P/M[a]	p-value[b]	P/M[a]	p-value[b]	P/M[a]	p-value[b]
C89M	7	0.25	**1.790 x 10 $^{-1}$**	0.28	**3.740 x 10 $^{-1}$**	0.41	**9.960 x 10 $^{-1}$**
C109F	7	0.34	**4.540 x 10 $^{-1}$**	0.37	**6.640 x 10 $^{-1}$**	0.45	**9.880 x 10 $^{-1}$**
R119F	7	0.21	1.120 x 10 $^{-2}$	0.23	3.940 x 10 $^{-2}$	0.28	**3.040 x 10 $^{-1}$**
R121M	7	0.26	6.160 x 10 $^{-3}$	0.28	2.580 x 10 $^{-2}$	0.34	**4.360 x 10 $^{-1}$**
R101F	8	0.45	**6.110 x 10 $^{-1}$**	0.52	**8.760 x 10 $^{-1}$**	0.57	**8.590 x 10 $^{-1}$**
R120M	8	0.13	**3.130 x 10 $^{-1}$**	0.14	4.270 x 10 $^{-3}$	0.24	**1.900 x 10 $^{-1}$**
R122F	8	0.28	**1.270 x 10 $^{-1}$**	0.30	**2.090 x 10 $^{-1}$**	0.38	**7.580 x 10 $^{-1}$**
R192M	8	0.43	**4.360 x 10 $^{-1}$**	0.48	**6.840 x 10 $^{-1}$**	0.60	**8.880 x 10 $^{-1}$**
R100F	67	0.63	2.420 x 10 $^{-4}$	0.38	**3.830 x 10 $^{-1}$**	0.68	**4.080 x 10 $^{-1}$**
C79F	106	1.38	6.000 x 10 $^{-4}$	0.71	**9.900 x 10 $^{-1}$**	1.51	**7.190 x 10 $^{-2}$**
C107M	173	0.52	**5.080 x 10 $^{-1}$**	0.30	**1.320 x 10 $^{-1}$**	0.51	**9.320 x 10 $^{-1}$**
C111F	173	0.46	1.210 x 10 $^{-2}$	0.30	3.470 x 10 $^{-3}$	0.43	**5.640 x 10 $^{-1}$**
R99F	370	0.75	2.440 x 10 $^{-4}$	0.48	2.600 x 10 $^{-2}$	0.61	2.060 x 10 $^{-3}$
C105M	552	0.78	4.960 x 10 $^{-5}$	0.44	**9.970 x 10 $^{-2}$**	0.54	**9.730 x 10 $^{-1}$**
S116F	559	0.50	3.950 x 10 $^{-4}$	0.28	2.820 x 10 $^{-2}$	0.35	**5.410 x 10 $^{-1}$**
C94F	587	0.50	8.780 x 10 $^{-10}$	0.27	5.730 x 10 $^{-5}$	0.36	4.340 x 10 $^{-6}$
R102F	1099	0.69	2.140 x 10 $^{-12}$	0.28	3.360 x 10 $^{-8}$	0.39	8.230 x 10 $^{-8}$
Average		0.50		0.36		0.51	
Median		0.46		0.30		0.43	

[a] The ratio of intake predicted using maximum likelihood analysis to the actual intake

[b] p-value > 0.05 indicates adequate fits (indicated in bold).

4.3.2. Predictions of Activities in Liver and Skeleton

Plutonium activities in the skeleton of NHPs were also predicted using the reference human models, and compared to the actual activities measured at the time of death of the NHP. The activities predicted in the skeleton using the ICRP 67 model was 1.18 to 6.55 times the actual activity measured in the NHP's skeleton. The ratios ranged from 1.25 to 7.71 using the Luciani model, and 0.74 to 5.24 using the Leggett model. If those cases that were sacrificed after 173 days post injection were excluded, the average ratio was 1.82 ± 0.61, 2.06 ± 0.71, and 1.17 ± 0.40 using the ICRP 67, Luciani and Leggett models respectively. It is important to note that model predictions tend to increasingly overestimate as time post intake increases. This is possibly because of skeletal remodeling, during which most of the Pu initially deposited in the skeletal surface is removed by osteoclastic activity (Lloyd et al. 1997). Because the life expectancy of NHPs used in this study was 25 to 31 years[2], which is significantly shorter than that of humans, the measured activity deposited in the skeleton tissues is less than that predicted by the human reference models. Most of the Pu removed from the bone surfaces during the remodeling ends up in excreta, principally the feces (Durbin et al. 1983). This is one of the reasons the fecal excretion rates in the NHP are much higher than the predictions by the reference models (Fig. 4.2).

[2] Primate Info Net. National Primate Research Center, University of Wisconsin-Madison. pin.primate.wisc.edu

Table 4.5. Ratios of predicted to measured activities in liver and skeleton at death using different models

Case	Days from injection to death	ICRP 67 Model		Luciani Model		Leggett Model	
		Liver	Skeleton	Liver	Skeleton	Liver	Skeleton
C89M	7	0.45	1.53	0.24	1.61	0.95	0.97
C109F	7	0.47	1.69	0.25	1.78	0.98	1.07
R119F	7	0.52	1.22	0.27	1.29	1.08	0.77
R121M	7	0.53	1.18	0.28	1.25	1.11	0.75
R101F	8	0.56	1.18	0.30	1.25	1.17	0.74
R120M	8	0.42	1.94	0.22	2.05	0.86	1.21
R122F	8	0.47	1.45	0.25	1.54	0.98	0.91
R192M	8	0.38	3.12	0.20	3.31	0.78	1.95
R100F	67	0.82	1.60	0.51	1.98	1.58	1.00
C79F	106	1.19	2.54	0.74	3.13	2.25	1.63
C107M	173	0.69	2.41	0.44	2.95	1.27	1.61
C111F	173	0.75	2.06	0.47	2.53	1.37	1.38
R99F	370	7.24	2.32	4.78	2.80	12.02	1.72
C105M	552	0.71	3.42	0.49	4.05	1.09	2.71
S116F	559	2.20	3.80	1.52	4.49	3.38	3.01
C94F	587	10.71	6.55	7.44	7.71	16.25	5.24
R102F	1099	39.37	2.48	29.41	2.83	51.23	2.22
Average		3.97		2.81		5.79	
Median		0.69		0.44		1.17	

The ratios of predicted to measured activity for the liver using the ICRP 67 and Luciani models were generally less than one for those animals sacrificed at or less than 173 days (Table 4.5). Using Leggett's model, the average ratio for cases sacrificed at or less than 67 days was 1.20 ± 0.39. The predicted activity in liver was more than 7 times larger than the measured activity for the case sacrificed at 370 days post injection. Considering animals sacrificed after 552 days post injection, the ratio tended to be large, ranging from 2.20 for animals sacrificed at 559 days to about 40 for an animal sacrificed at 1,099 days.

Analysis of the data using the Luciani and Leggett models yielded similar results (Table 4.5).

The discrepancies in predictions of activities in liver and skeleton can be explained by the differences in biokinetics between humans and NHPs. Plutonium entering the blood undergoes nearly time-constant partition (for the period of concern) in the ratios of 3:5 and 3:10 between the liver and bone according to the ICRP 67 model and Luciani model respectively. However, the analysis of our data showed that the early partitioning is closer to 2:1 between the liver and bone, which seemed to be more in agreement with the Leggett model's predictions (Fig. 4.8).

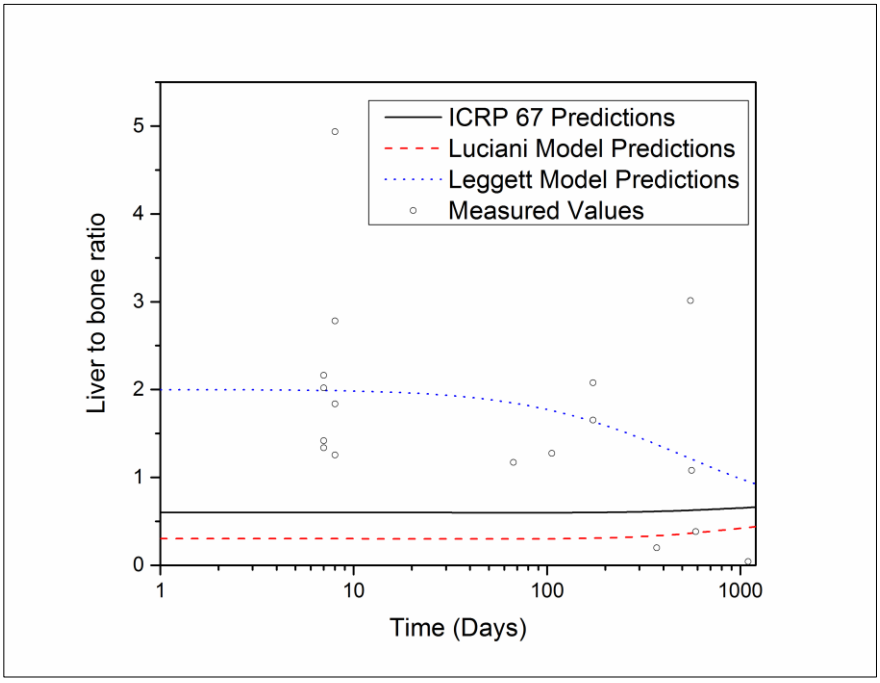

Fig. 4.8. Ratios of activities in liver and skeleton at various times post-intake compared with the model predictions

4.3.3. Discussions of Similarities and Discrepancies

The overprediction of Pu in the liver at longer times after injection suggests that the retention half-time of Pu in the liver of NHP is significantly less than that modeled for humans. The initial uptake of activity in liver of non-human primates in the given data-set was 64%, which decreases with a half-life of approximately 170 days compared to 30% initial uptake and a half-life of 30 years in humans as predicted by the ICRP 67 model. Durbin et al. (1985) described Pu retention in the liver with a 180-d half time, whereas Guilmette (personal communication) refit their data and obtained a 230-d half time and an initial uptake of 54% of injected activity. It has also been shown that the retention half time of ^{241}Am in baboons was short, i.e., 28 d (Guilmette et al. 1980), lending support to the hypothesis that the retention of actinides in NHP is not nearly as tenacious as it is in humans. Because the amount of Pu in feces is driven principally by the biliary secretion of Pu, this also explains why the fecal excretion rates in macaques at longer times post-injection are much higher than what are predicted by the reference human models.

It is important to note that Luciani's model uses time dependent skeletal transfer rates (Luciani and Polig 2000, Luciani 2002). However, because of the inherent complexity associated with setting up time-dependent transfer rates in IMBA, the transfer rates suggested by Luciani for adults up to 35 years of age were used. All animals, with the exception of R1119F, R121M, R120M and R122F, were adult (> 5 years old) animals. The adolescent animals were killed 7 to 8 days post injection resulting in the lack of enough data to investigate the effects of age and aging on plutonium metabolism. The possibility of existence of sub-groups in the sample population based on their age is acknowledged. It is also acknowledged that no attempt was made to scale the life expectancy differences

between the humans and NHPs because of the associated uncertainties in doing so. Nevertheless, our analyses pointed out the similarities and differences between the physiology of humans and NHPs in regards to handling of Pu. As such, significant changes to the pathways involving liver and skeleton may be necessary when attempting to scale the NHP biokinetic model to humans or vice versa.

4.4. Conclusions

The default transfer rates recommended for adult humans in the ICRP 67, Luciani and Leggett models predict the urinary excretion in NHP to a certain extent. However, these models were unable to describe the fecal excretion rates in monkeys several days post-intake. The plutonium activities in the skeleton and liver at the time of death were also not consistently predicted in the monkeys. These inconsistencies, however, are not inadequacies of the human models, but rather the result of metabolic and physiological differences between NHP and humans as demonstrated by early biokinetic studies.

NHP, especially macaques, are often used to develop biokinetic models for radioactive materials. Although most pathways between human and macaques are similar, our results indicate that notable differences between their handling of Pu, especially the pathways involving the liver and skeleton do exist. Thus, this must be taken into account when using NHP data to estimate the biokinetic behavior of Pu in humans.

Chapter 5 :
Analysis of Urinary and Wound Data from Simulated Wounds in NHPs

5.1. Objectives

Much if not all the data that contributed to the development of the NCRP Report No. 156 (NCRP 2006) was based on animal experiments. Although the authors of the report acknowledged that the wound model needs to be applied to human cases involving radioactive-contaminated wounds for further validation (Guilmette et al. 2007), several difficulties arise when undertaking such a study. One of these challenges is the difficulty in finding wound cases that are not confounded by treatments like chelation and excision, or other forms of intakes such as inhalation or multiple wounds. Further, the major problem with most of the human cases is that the actual intake and intake scenarios are not clearly known. These disadvantages can be addressed to an extent when data from experimental animal studies are used as a new source of data for evaluating and validating the models.

The purpose of this study was to use urinary excretion data from NHPs injected intramuscularly or subcutaneously with plutonium to evaluate the applicability of the NCRP 156 wound model's default compartment-model transfer-rate parameters coupled with the ICRP 67 systemic model for Pu.

5.2. Biokinetic Model and Data Analysis

5.2.1. Data

Between 1973 and 1985, several animals of the genus *Macaca* – Rhesus *(M. mulatta)*, Cynomolgus *(M. fascicularis)* and Stumptail *(M. arctoides)* — were given one intramuscular or subcutaneous injection of ^{238}Pu(IV) at various dosages. As part of the

experiment, urine samples were collected from the animals at frequent intervals from the day of injection to death. A detailed description of the data collection and analysis methods was given in Chapter 3.

Intramuscular injections are thought to simulate deep puncture wounds and since radioactive material in contaminated muscle and subcutaneous tissues behave similarly (NCRP 2006), the measured urinary excretion data from these animals can be compared with the predictions of the NCRP 156 wound model coupled with the ICRP 67 systemic model.

5.2.2. Biokinetic Models

The physiological behavior of radionuclide-contaminated wounds can be described using the NCRP 156 wound model (NCRP 2006). The report proposes a multi-compartmental biokinetic model comprised of five compartments that lead to systemic uptake into the blood or clearance into the lymph nodes. The compartments were conceived in order to account for various physicochemical forms and solution properties of the radionuclides entering the wound. Transfer among the compartments is described by first order kinetics, and the recommended values for clearance rates among the compartments are given in the report. A detailed description of the wound model was given in Chapter 3.

The wound model is linked together with the systemic model by the blood compartment, which serves as a final clearance compartment from the wound model, and a transfer compartment for the systemic model (Fig. 5.1). The currently recommended systemic model for plutonium is described in ICRP Publication 67 (ICRP 1993). The blood compartment in the systemic model, is connected to soft tissues, skeleton, liver, kidneys

and the urinary bladder each of which are represented by one or more compartments. Transfer between the compartments is characterized by first order kinetics; the default transfer rates for plutonium are given in ICRP Publication 67. A detailed description of the systemic model was also given in Chapter 3.

5.2.3. Data Analysis

As with the data from intravenously injected NHPs, the IMBA Professional Plus software suite was used for the analysis of the urinary excretion data. The software uses the maximum likelihood method (Chapter 4) to make estimates of intake from a set of multiple bioassay measurements. The default wound models for various categories were used in conjunction with the ICRP 67 biokinetic model to calculate the intake based on the available urine data. The IMBA code requires the uncertainty of each bioassay data point and the assumption of the type of the error that best describes that data. According to the IDEAS guidelines (Castellani et al. 2013), the overall uncertainty of an individual data point can be described by a log-normal distribution. These guidelines suggest a scattering factor (SF) (discussed in section 4.2.2) of 1.1 for true 24-hour urine, and 1.6 for simulated 24-hour urine samples. An SF of 1.6 was used based on these recommendations.

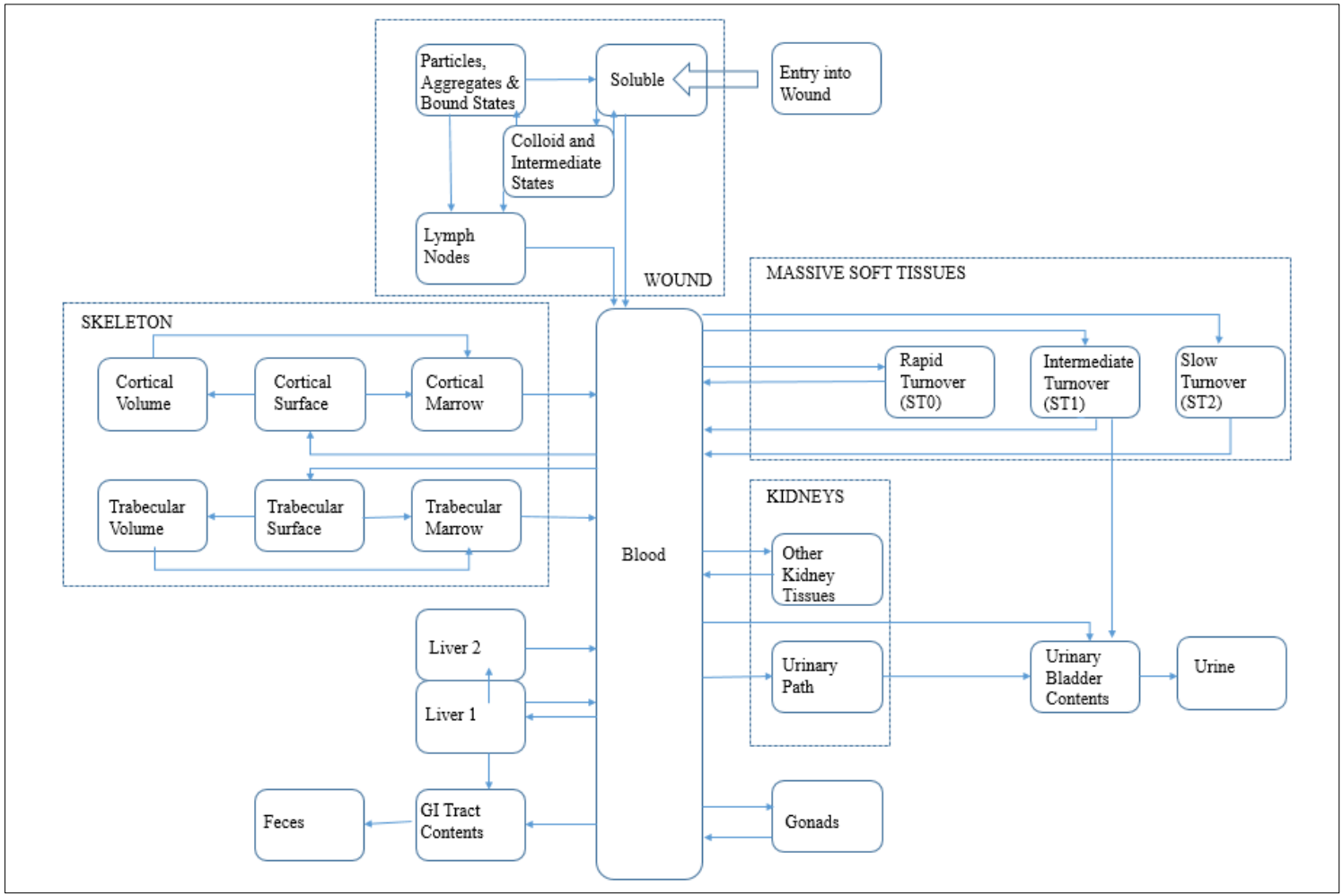

Fig. 5.1. The NCRP Report 156 wound model for soluble radionuclides combined with the ICRP 67 systemic model for plutonium

It must be noted that the Pu injected intramuscularly was as a citrate complex. Pu-citrate is considered to be chemically stable and quite soluble, and was used experimentally for that reason. NCRP Report No. 156 considers tetravalent plutonium-238 (^{238}Pu(IV)) as a strongly retained radionuclide within the NCRP 156 solubility structure. However, an analysis of the early blood plutonium data in the Durbin dataset indicated that the early blood biokinetics in NHPs exhibited "moderate" retention properties (Konzen et al. 2015). Therefore, the default NCRP 156 moderately and strongly retained parameters were tested for the NHPs injected with Pu-citrate. Since the actual intake was known for all animals in this set, inferences about whether or not the NCRP 156 wound model and ICRP 67 model fits the urine data were made based on comparison of the known intakes with the intakes calculated using the maximum likelihood analysis method, as well as the chi-square values and the p-values which indicate goodness of how well the models fit the data. The chi-square statistics (χ^2) which is calculated by IMBA as shown in equation 5.1 is a measure of the disparity between the values observed in the time series data and the predicted curve (Allen et al. 2016, James 2005):

$$\chi^2(I) = \sum_{i=1}^{n} \frac{\left[\ln(M_i) - \ln(I\ m(t_i))\right]^2}{\left[\ln(SF_i)\right]^2} \tag{5.1}$$

where, M_i is measured bioassay data, I is the calculated intake, $m(t_i)$ is the predicted value at time t_i, SF_i is the scattering factor for the bioassay data. The p-values less than the chosen level of significance (0.05 for our purposes) imply that the fit of the measured data is not adequate.

5.3. Result of the Maximum Likelihood Analysis of Urinary Data

The urinary excretion data from the NHPs were plotted against the predictions of different default wound models (Fig. 5.2). The results from the maximum likelihood analysis of the urinary excretion rates from several NHPs using default NCRP 156 wound models for moderately retained and strongly retained materials are included in Table 5.1. The urinary excretion data were fit well (p value > 0.05) by default parameters for NCRP 156 moderately and strongly retained radionuclides for all cases except case C80F, which was sacrificed 1,100 days post injection. When case C80F is excluded, the ratio of intakes predicted by the maximum likelihood analysis of the data using the moderately retained model to the actual intake administered was 1.10 ± 0.45. The ratio when using the strongly retained model was 1.47 ± 0.72. This showed that the early urinary excretion rates due to simulated contaminated wounds in NHPs were predicted better by the parameters for moderately retained category than that by those for strongly retained category. This was in agreement with the findings of Konzen et al. (2015). The maximum likelihood analyses of some representative cases using the parameters for moderately retained category are given in Fig. 5.3.

As seen in Fig. 5.2, the nature of ^{238}Pu(IV), especially after 200 days post intake, seems to fall in between the predictions obtained using the parameters for colloid and particle categories and those obtained using the parameters for different soluble categories. As such, urinary excretion rates from case C80F was also analyzed using colloid and particulate models. However, none of these default models seem to predict the urinary excretion rates well throughout the period of concern (Fig. 5.4).

The urinary excretion rates from intramuscularly and subcutaneously injected NHPs were plotted along with the default model predictions using the ICRP 67 systemic model and the moderately retained wound model (Fig. 5.5). After 200 days, the predictions from the ICRP 67 systemic model essentially overlap with those using the moderately retained wound model combined with the systemic model. As such, the urinary excretion rates after 200 days post intake are essentially driven by the systemic model itself. Moreover, plutonium within NHPs was found to clear more through liver-biliary-fecal pathway than predicted by the ICRP 67 systemic model for plutonium (Chapter 4, Poudel et al. 2016a). Hence the drop in the late urinary excretion rates can be attributed to the differences in the systemic model between NHPs and humans.

The retention at the injection sites of the NHPs were compared against the retention in the wound sites predicted by the default wound models (Fig. 5.6). The measured values were closer to the predictions made when using the parameters of the moderately retained wound model than those by any other default parameters. This was again in agreement with the results of the maximum likelihood analysis of urine data and the findings of Konzen et al. (2015).

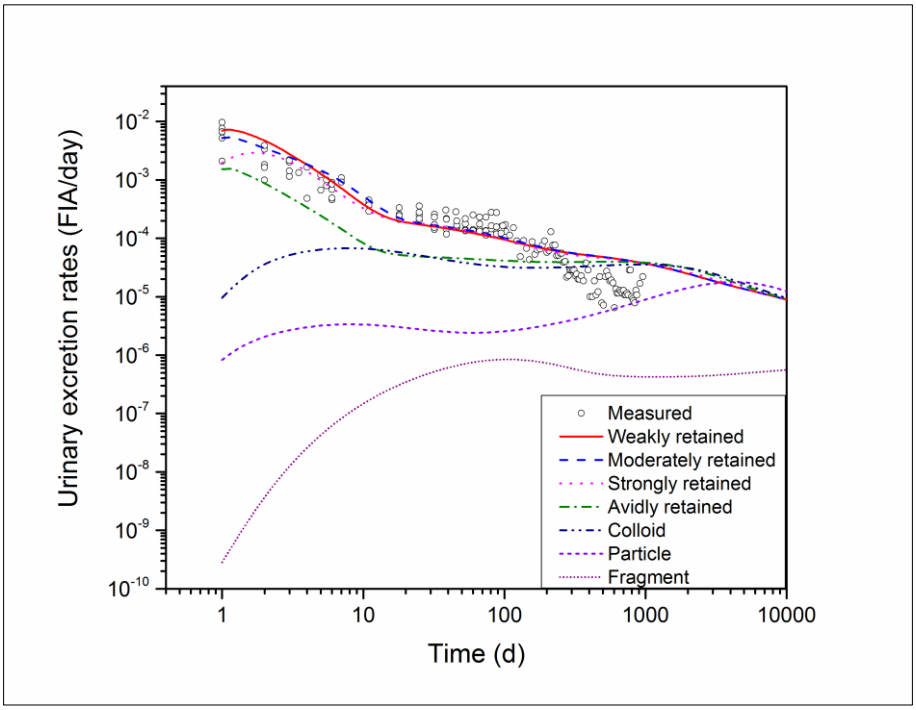

Fig. 5.2. Composited urinary excretion rates (FIA/day) from intramuscularly and subcutaneously injected animals compared with default wound models predictions

Table 5.1. Results of maximum likelihood analysis of urine data using NCRP 156 default parameters coupled with the ICRP 67 systemic model parameters

Case	Mode	df	Moderate		Strong	
			P/M[a]	p-values[b]	P/M[a]	p-values[b]
C145M	im	6	0.439	**0.372**	0.676	**0.117**
S114F	im	6	0.785	**0.809**	1.211	**0.166**
C95F	sc	4	1.880	**0.363**	2.969	**0.391**
C131F	im	9	1.254	**0.507**	1.563	**0.610**
R186M	im	16	1.239	**0.585**	1.452	**0.651**
C106M	im	17	1.087	**1.000**	1.260	**0.942**
C166M	im	17	1.004	**1.000**	1.164	**0.974**
C80F	im	90	0.559	2.13×10^{-8}	0.598	1.30×10^{-10}

[a] The ratio of intake predicted using maximum likelihood analysis (P) to the actual intake (M)

[b] p-values > 0.05 indicates adequate fits.

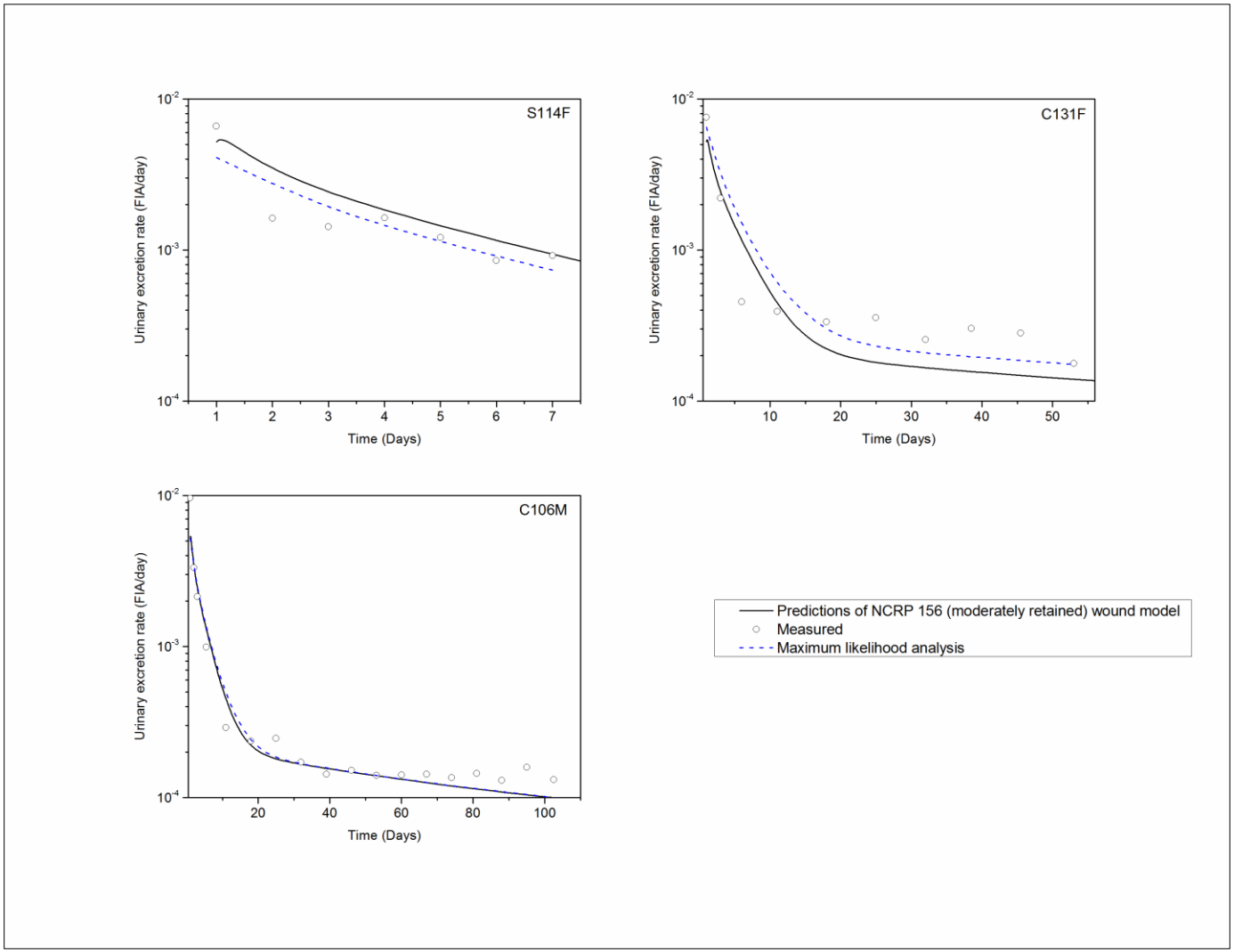

Fig. 5.3. Maximum likelihood analysis of urinary excretion data from representative cases S114F, C131F and C106M

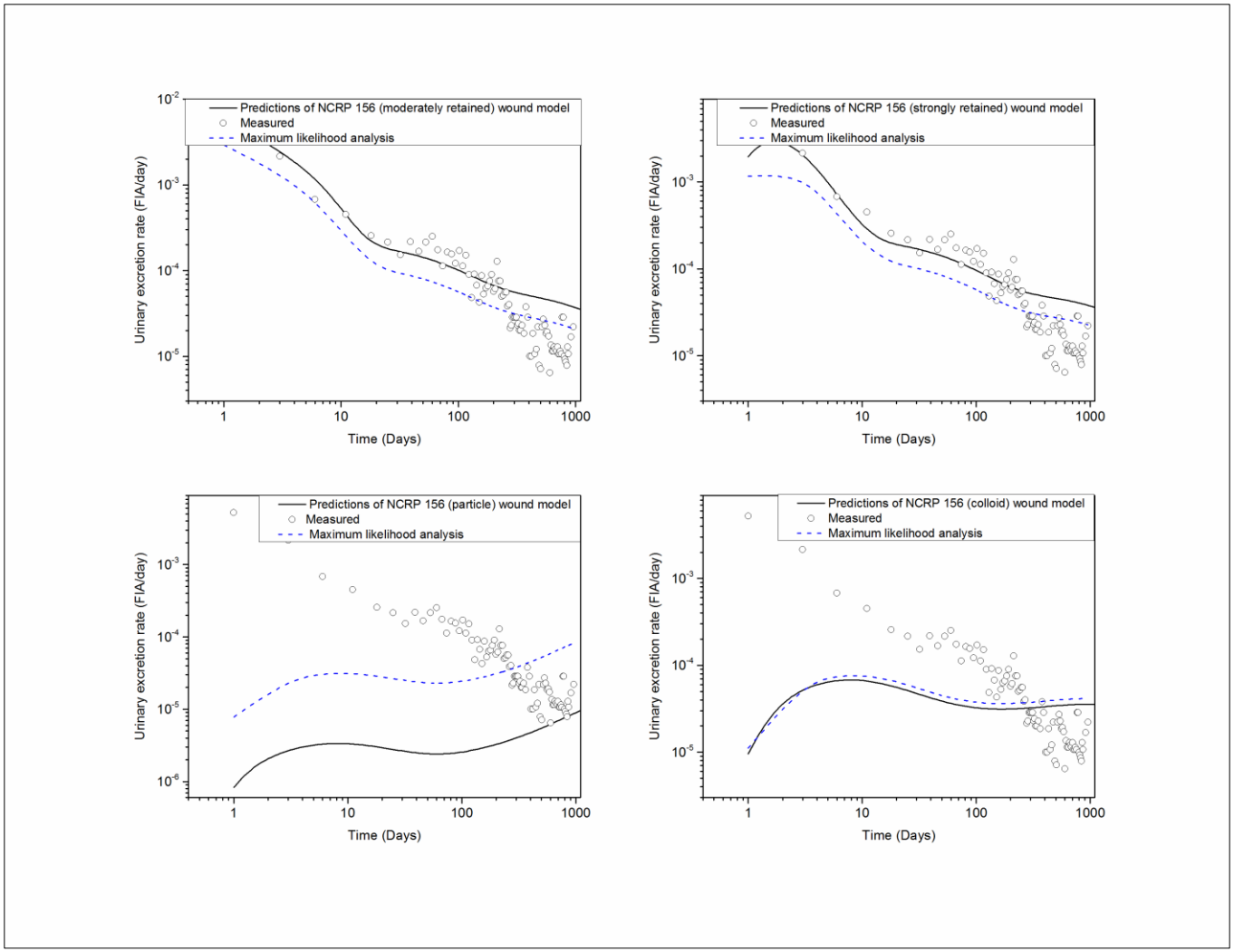

Fig. 5.4. Maximum likelihood analysis of urinary excretion data from case C80F using different wound models

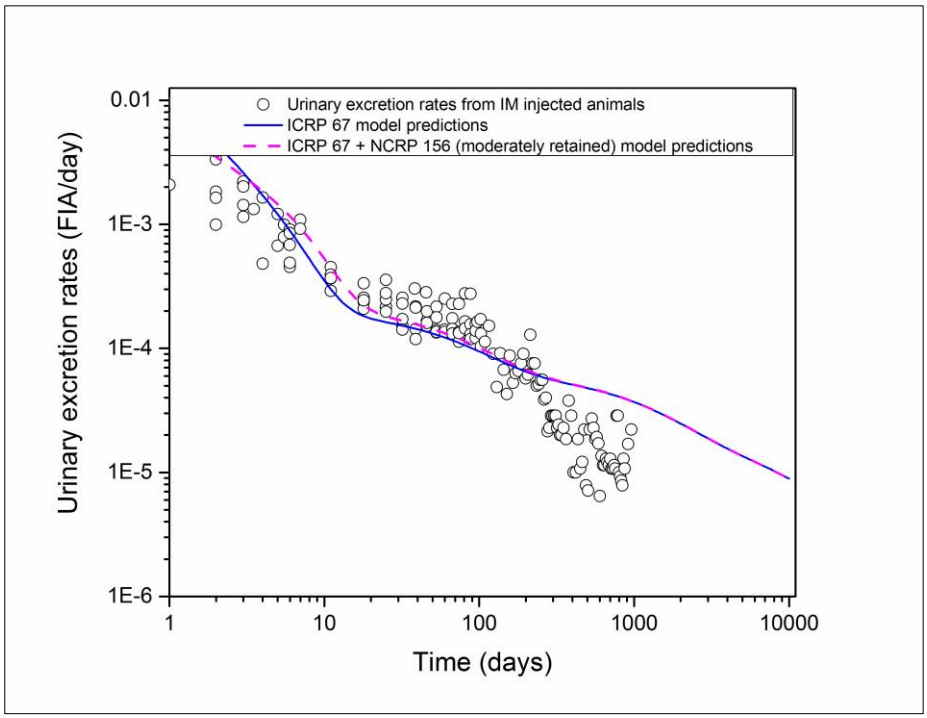

Fig. 5.5. Composited urinary excretion data from intramuscularly and subcutaneously injected animals compared with the predictions of ICRP 67 systemic model and ICRP 67 systemic model coupled with NCRP 156 (moderately retained) wound model

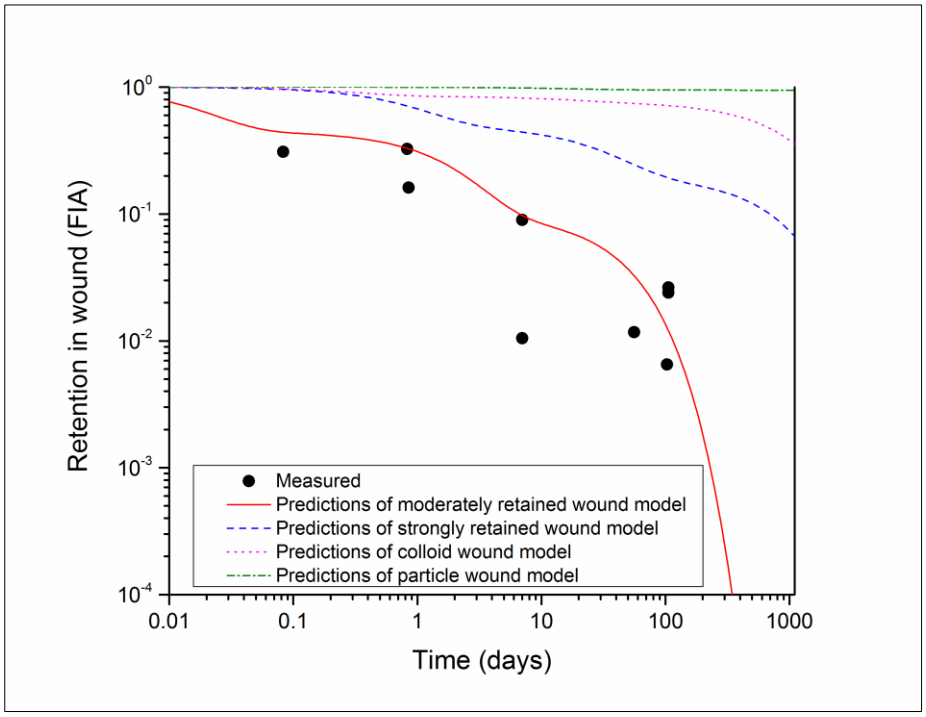

Fig. 5.6. Fraction of injected activity retained in the intramuscular sites compared with various model predictions

5.4. Conclusions

Our results demonstrated one of the important uses of the wound model – the model can be combined with the systemic model for the radioactive materials in question to aid in the interpretation of the urinary excretion data to assess intake. The results indicated that the default retention parameters for moderately retained radionuclides suggested by the NCRP 156 wound model were adequate to describe the early urinary excretion rates in NHPs, however, it was observed that the urinary excretion rates after 200 days post intake could not be described well because of the differences in the systemic handling of plutonium by monkeys and humans. It is important to note that most past occupational exposures were largely due to Pu-oxides or Pu-nitrates which may have a different physicochemistry than the Pu-citrate discussed in this paper.

Chapter 6 :
Systemic Biokinetics of Plutonium in Nonhuman Primates

6.1. Objectives

The International Commission on Radiological Protection (ICRP) adopted the current plutonium biokinetic model as described in ICRP 67 (ICRP 1993) based principally on human experimental data and investigation of accidental occupational exposures. Several modifications of this model (Luciani and Polig 2000; Leggett et al. 2005) have been suggested as new information on the biokinetics of plutonium in humans has been published. The ICRP 67 model along with its proposed revisions were reviewed in Chapter 2.

Poudel et al. (2016a) evaluated the biokinetic data obtained from experimental studies in nonhuman primates (NHPs) (Durbin and Jeung 1990a, 1990b) against the predictions of the human reference models (ICRP 1993, Luciani and Polig 2000, Leggett et al. 2005). It was found that the transfer rates defined in the human models were neither able to describe the fecal excretion rates several days post intake nor the activities in liver and skeleton tissues. This was attributed to the differences between the physiology of humans and NHPs in regard to the handling of plutonium especially by the liver and skeleton (Chapter 4, Poudel et al. 2016a).

The objective of this work is to describe the biokinetics of plutonium in NHPs by adapting the basic model structure the transfer rates described for adult humans.

6.2. Biokinetic Model

The structure of the biokinetic model for plutonium metabolism described in ICRP 67 (ICRP 1993) was adopted as a starting point. The ICRP 67 model is represented by a

compartmental structure with blood as a central compartment that is connected to soft-tissues, skeleton, liver, kidneys and the urinary bladder each of which are represented by one or more compartments. The model treats blood as a uniformly mixed pool. Certain structural modifications to the human model were made based on the understanding of the metabolism of Pu in monkeys or nonhuman primates in general. The liver and skeleton are the primary sites of plutonium deposition in humans.

The liver in the ICRP 67 model is divided into two compartments in order to better represent the long-term retention of plutonium. One compartment (liver 1) loses a portion of activity in the liver to the gastrointestinal (GI) tract over a period of a year. The other compartment (liver 2), which can be physiologically associated with the reticuloendothelial system (Luciani 2002), retains plutonium for many years. Since actinides are retained in the liver with much smaller half-times in the NHPs (Durbin et al. 1985, Guilmette et al. 1980, Poudel et al. 2016a), there is no need for a tenaciously retaining liver compartment to describe the biokinetics in the NHPs. The proposed structure for Pu biokinetics in the liver are compared with those in the adult human in Fig. 6.1**.**

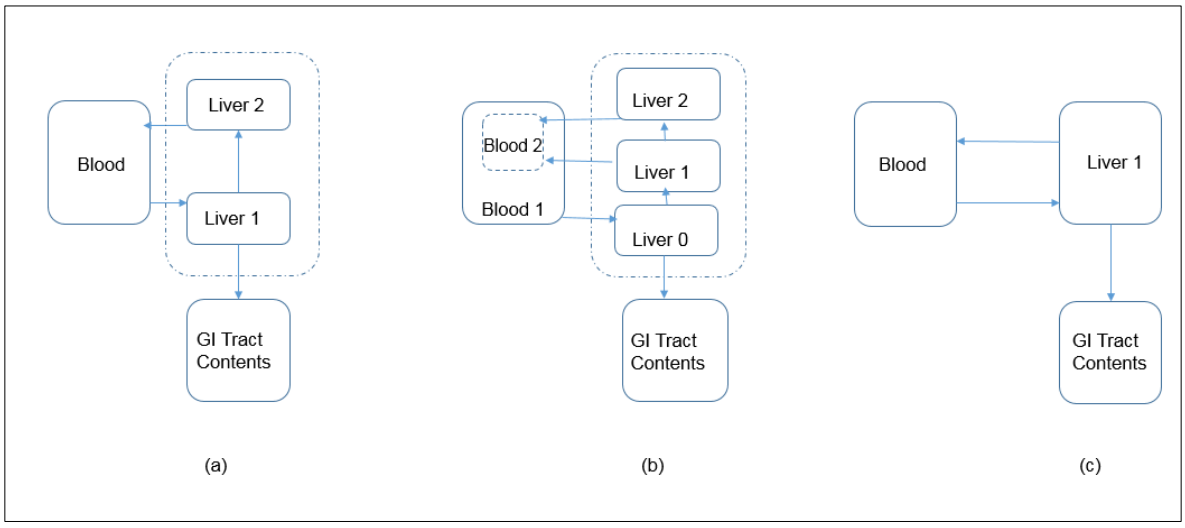

Fig. 6.1. Structure of the liver models a) as described in ICRP 67 (ICRP 1993) and in Luciani and Polig (2000) for adult humans, b) as described in Leggett (2005) for adult humans, and c) proposed by this work for nonhuman primates

The skeletal model proposed for the nonhuman primates is compared with reference human and animal models in Fig. 6.2**.** The structure and the baseline transfer rates between the skeletal compartments are adopted from Leggett et al (2005). This model is different from the one described in ICRP 67 (ICRP 1993) in that the bone volumes receives activity directly from the blood as well as from the bone surface compared to just from the bone surface in ICRP 67. This model is also different from the one described by Polig (1997) and Luciani and Polig (2000) for humans, and by Polig et al. (2000) for beagles in that the bone volume does not receive any activity from the bone surface. Luciani and Polig (2007) indicated that the deposition to bone volume was assumed to describe the rapid burial process of plutonium deposited at sites of formation. The skeletal structure and baseline transfer rates for translocation of activity into, within, and out of skeleton and liver described by Leggett et al. were favored as the starting point compared to ICRP 67 (ICRP 1993) and Luciani and Polig (2000), because of their ability to closely predict the ratio of retention in liver and bone a few days post intake (Poudel et al. 2016a).

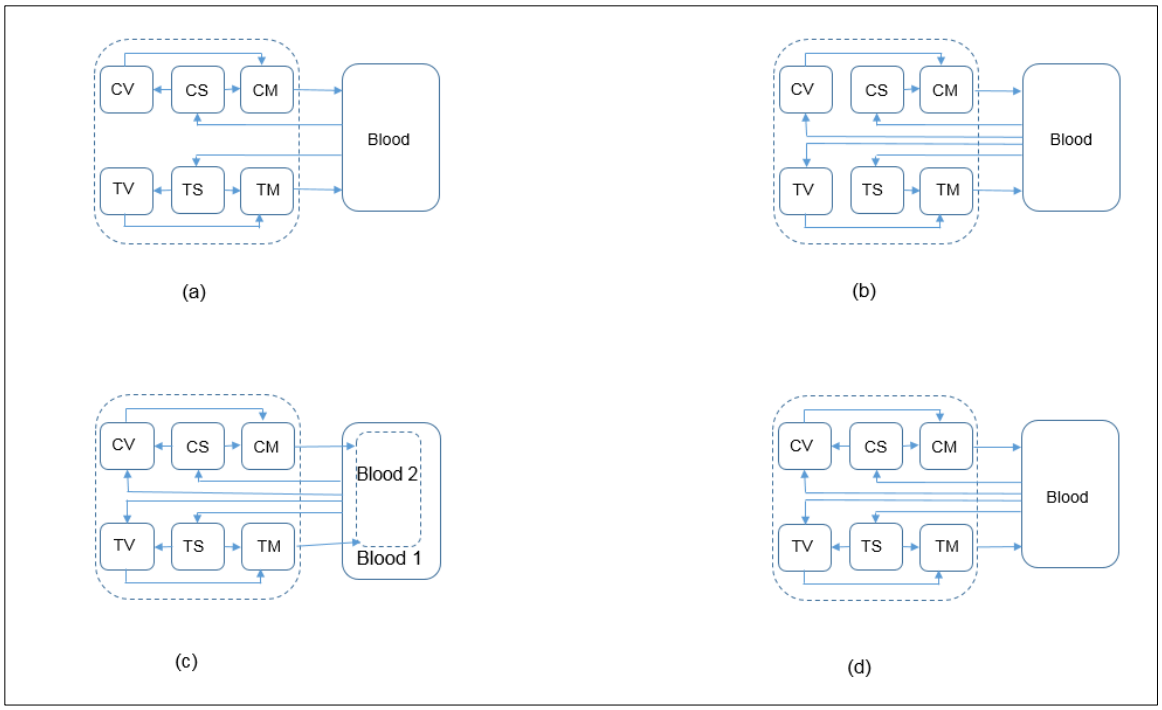

Fig. 6.2. Structure of the skeletal models a) as described in ICRP 67 (ICRP 1993) b) as described by Polig (1997) and Luciani and Polig (2000) for adult humans, and Polig et al (2000) for beagles, and c) as described in Leggett (2005) for adult humans. The skeletal model proposed by this work for nonhuman primates (d) is similar to the Leggett (2005) model, except for the treatment of blood as a uniformly mixed pool.

The ICRP 67 systemic model includes a clearance pathway from ST1 to the urinary bladder that was introduced to account for the increase in clearance of circulating plutonium. In accordance with the recent revisions of the systemic model (Luciani and Polig 2000, Leggett 2005, Konzen et al. 2015), this pathway was eliminated on the basis of a lack of physiology associated with the pathway. Similar to the approach utilized by Luciani and Polig (2000), the transfer of activity from ST1 to the urinary bladder is directed to the blood compartment so that the total clearance from the ST1 compartment stays unchanged (Fig. 6.3).

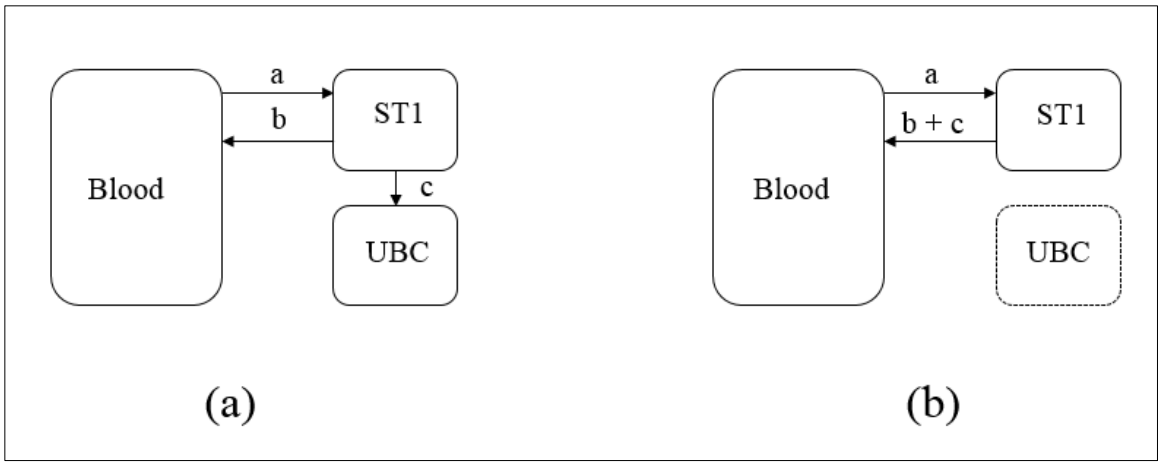

Fig. 6.3. Clearance from ST1 compartment a) in ICRP 67 model, b) as proposed by this paper for NHPs

6.3. Optimization of Transfer Rates

Prior to optimization of the parameters, two of the 17-cases were randomly selected to be withheld from the procedure such that they include one short-term (less than 100-days post intake), and one long-term (more than 100-days post intake) case. These withheld cases were used later to test the validity of the optimized model. A composite dataset of urinary and fecal excretion rates, blood retention, and retention in the skeleton and liver was created using the remainder cases.

The parameters that were selected to be optimized for the NHP population are presented in bold face in Table 6.1. The selection of these parameters was not arbitrary, but based on the pathways that were determined to be significantly different between the NHPs and humans. Actinides are removed from the skeleton only through osteoclast resorption (Durbin and Schmidt 1985). Moreover, most of the plutonium removed during bone remodeling ends up in the excreta, principally the feces (Durbin et al. 1983). Hence, the parameters associated with bone resorption and removal of activity from the bone (i.e., surface to marrow, volume to marrow, marrow to blood) were selected to be optimized.

The parameters associated with the liver (i.e., blood to liver 1, liver 1 to blood) were chosen to be optimized to account for the differences in the activity deposited in liver, and the parameters associated with the alimentary canal (blood to upper large intestine, liver 1 to small intestine) were also optimized to account for the differences in fecal excretion rates in humans and NHPs. Finally, the parameters associated with urinary excretion (i.e., blood to urinary path, blood to bladder, and urinary path to bladder) were chosen to be optimized to make up for the removal of the ST1 to the urinary bladder pathway, and to buffer the differences in the urinary excretion rates caused by changes in the other transfer rates mentioned above.

The optimization of transfer rates was carried out using the Integrated Modules for Bioassay Analysis (IMBA) Uncertainty Analyzer (UA). This software constructs a sample matrix from the user-defined prior distributions of model parameters. The parameters described above were assigned a prior distribution – 0.05 times to 20 times the baseline human parameters. This was based on an assumption that the biokinetic data from the NHPs can be explained, at worst, by changing the parameters for human models by a factor of 20. The prior distributions were divided into 100,000 non-overlapping intervals, the medians of which were selected and randomized in sequence to create 100,000 hypothetical sets of systemic models. The agreement between the predictions of these systemic models with the measured data (urinary and fecal excretion rates, activity in blood, and activities in liver and skeleton at death) was evaluated using the total chi-square statistic. The model parameters that resulted in the minimum chi-square are given in Table 6.1. The predictions of this model are compared against those of human models and the biokinetic data from nonhuman primates in Fig. 6.4 and Fig. 6.5.

Table 6.1. Transfer rates that describe the biokinetics of Pu in NHPs

Pathway	Optimized model transfer rate (d^{-1})	Source
blood to liver 1	0.6442	This paper
blood to cortical surface	0.08778	Leggett
blood to trabecular surface	0.1247	Leggett
blood to cortical volume	0.004620	Leggett
blood to trabecular volume	0.013860	Leggett
blood to urinary bladder content	0.02154	This paper
blood to kidney (urinary path)	0.09998	This paper
blood to other kidney tissue	0.00323	ICRP 67
blood to ULI contents	0.01938	This paper
blood to testes	0.00023	ICRP 67
blood to ovaries	0.000071	ICRP 67
blood to ST0	0.2773	ICRP 67, Luciani
blood to ST1	0.0806	ICRP 67, Luciani
blood to ST2	0.0129	ICRP 67, Luciani
ST0 to blood	0.693	ICRP 67
kidneys (urinary path) to bladder	0.011155	This paper
other kidney tissue to blood	0.00139	ICRP 67
ST1 to blood	0.00095	ICRP 67, Luciani
ST1 to urinary bladder contents		Removed
ST2 to blood	0.000019	ICRP 67, Luciani
trabecular surface to volume	0.000123	Leggett
trabecular surface to marrow	0.004199	This paper
cortical surface to volume	0.000021	Leggett
cortical surface to marrow	0.000266	This paper
trabecular volume to marrow	0.004199	This paper
cortical volume to marrow	0.000266	This paper
cortical marrow to blood	0.03439	This paper
trabecular marrow to blood	0.03439	This paper
liver 1 to liver 2		Removed
liver 1 to small intestine	0.004365	This paper
liver 1 to blood	0.001647	This paper
gonads to blood	0.00019	ICRP 67, Luciani

[a] The parameters have been either adopted from ICRP 67 model (ICRP 1993), Luciani model (Luciani and Polig 2000), Leggett model (Legett 2005), or were the result of optimization for the NHP dataset.

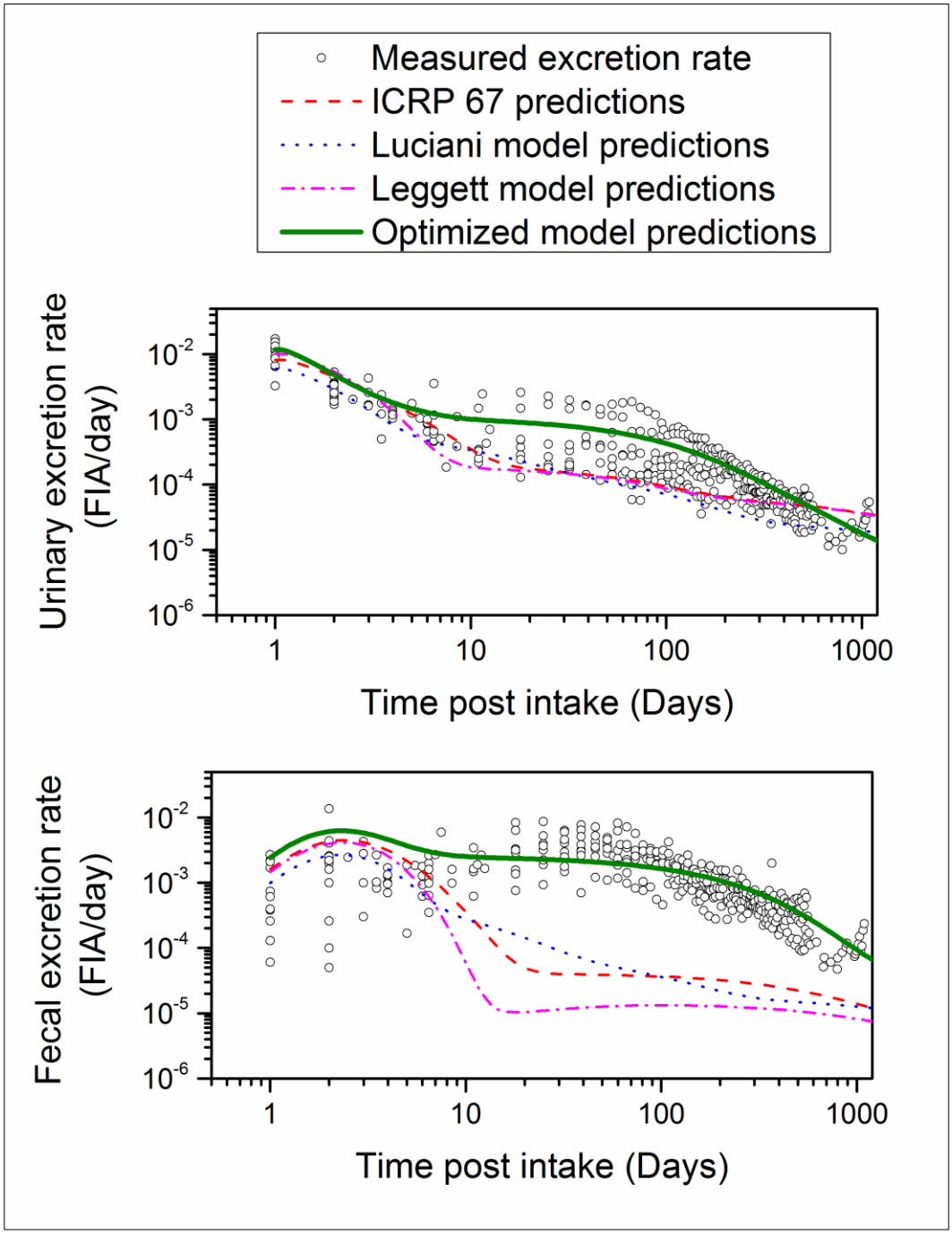

Fig. 6.4. Urinary and fecal excretion rates from the NHPs compared with various reference human models and the optimized model for NHPs

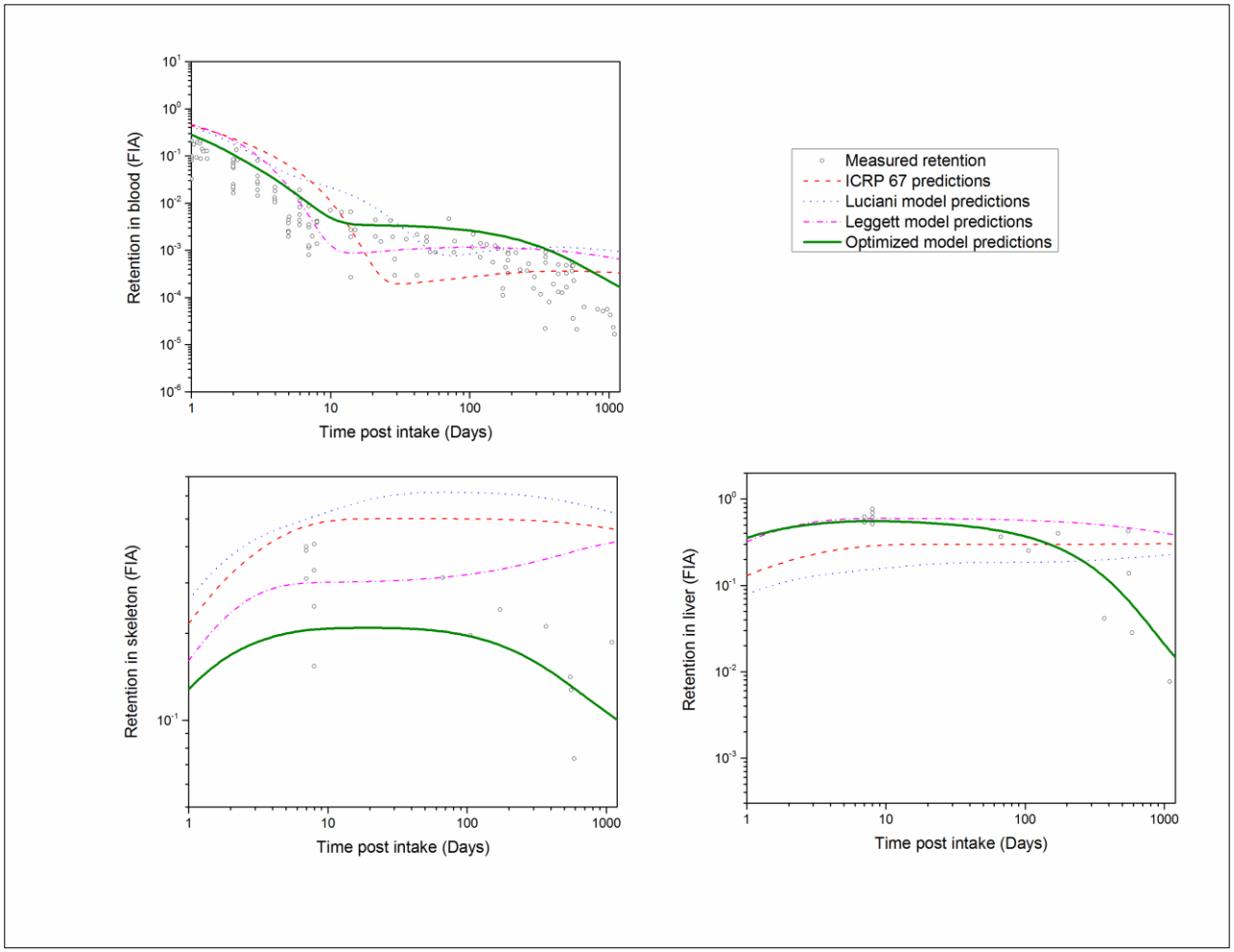

Fig. 6.5. Retention in blood, skeleton and liver in NHPs compared with various reference human models and the optimized model for NHPs

6.4. Model Verification

The model described above was tested with the two animal cases. These two cases were not used in parameterization of the systemic model. Since the actual intake is known, inferences about whether or not the newly developed systemic model fits the actual biokinetic data were made based on comparison of the known intakes with the intakes calculated using the maximum likelihood analysis method, as well as the chi-square values (and the associated p values) which indicate how well the models fit the data.

The internal dosimetry software IMBA Professional Plus was used to calculate intake based on different types of bioassay measurements (urine, feces, and blood data). The software uses the maximum likelihood method to make estimates of intake from a set of multiple bioassay measurements $m_i(t_i)$. The best intake I is calculated such that the product of I and $f(t)$, where $f(t)$ represents an excretion or retention function, best fits the data (James 2005). The input to the IMBA code requires the uncertainty of each bioassay data point and an assumption about the error associated with each data point. According to the IDEAS guidelines (Castellani et al. 2013), the overall uncertainty (scattering factor) on an individual data point can be described by a lognormal distribution. These guidelines suggest a scattering factor of 1.6 for simulated 24-hour urine samples, and 3 for 24-hour fecal samples. The guidelines do not define the scattering factor for blood samples, because blood Pu levels are rarely used for intake predictions or dose assessments. The scattering factor of 2.1 for blood samples as calculated by Konzen et al. (2015) was used for our purpose. A detailed description of the scattering factors as they are used in internal dosimetry calculations was given in section 4.2.2.

The results of the maximum likelihood analysis of the bioassay measurements from two independent test cases using the proposed model were compared with those using the human reference models (Table 6.2). The Leggett and Luciani models are better at predicting the intake from the simultaneous maximum likelihood analysis of urine, feces and blood data for R192M sacrificed 8-days post injection, however the chi-square resulting from such analysis is much lower for the optimized model compared to the reference human models. Considering case C107M, the error in prediction of intake is the lowest using the optimized model compared to that using the reference human models. Moreover, the p value is greater than 0.05 for both cases, which indicated that the biokinetic data from these NHP test cases were fit well by the optimized NHP model.

Since the information on the activities measured in skeleton and liver tissues of the NHPs at death was also available, inferences on whether the optimized model was better than the reference human models could also be made by comparison of measured values against the predictions of the models. The optimized model, overall, was better than the default human models at predicting activities in liver and skeleton at various times post intake (Table 6.2).

Table 6.2. Verification of the optimized model using the test cases

Test cases		Biokinetic model			
		Optimized model	**ICRP 67 model**	**Luciani model**	**Leggett model**
R192M (8 d)	Error in intake prediction[a,e]	44%	52%	26%	31%
	Total chi-square[b], df = 13 (p value)	**12.4 (6.52 x 10^{-1})**	**24.9 (5.13 x 10^{-2})**	29.7 (1.32 x 10^{-2})	**19.7 (1.82 x 10^{-1})**
	Error in prediction of activity in liver[c,e]	27%	62%	80%	22%
	Error in prediction of activity in skeleton[d,e]	-34%	-212%	-231%	-95%
C107M (173 d)	Error in intake prediction[a,e]	63%	-85%	-82%	-103%
	Total chi-square[b], df = 63 (p value)	**72.4 (1.96 x 10^{-1})**	279 (0.00)	320 (0.00)	430 (0.00)
	Error in prediction of activity in liver[c,e]	37%	31%	56%	-27%
	Error in prediction of activity in skeleton[d,e]	12%	-141%	-195%	-61%

[a]The differences between the known intake and the intake estimated using simultaneous maximum likelihood analysis of urinary, fecal and blood data

[a]Total chi-square resulting from the simultaneous maximum likelihood analysis of urine, feces and blood data. Values in bold indicate adequate fits (> 0.05).

[c]The difference between the known activity in liver and the activity predicted by the model in the liver

[d]The difference between the known activity in skeleton and the activity predicted by the model in the skeleton

[e]Positive values indicate underprediction; negative values indicate overprediction.

6.5. Inferences on the Pu-biokinetics in NHPs

The biokinetic data in NHPs can be explained by a structure similar to the ones proposed for humans, however, significant changes to the skeletal and liver parameters were necessary (Table 6.3). The skeletal and liver parameters obtained for the population of NHPs were compared with those for the human reference models in Table 6.3. Compared to the ICRP 67 model for adult humans, plutonium from the skeleton reenters circulation nearly 4.5 times faster in NHPs than in humans. Similarly, the bone volume turnover is 8.52 times faster for trabecular bone and 3.24 times faster for cortical bone in NHPs compared to the ICRP 67 model parameters. The translocation of activity from blood to liver is 3.32 times faster in NHPs while the transfer of activity from liver to blood and liver to the GI tract are 7.81 and 32.8 times faster in NHPs than in adult humans as predicted by the ICRP 67 model.

These changes in the parameters for NHPs were necessarily primarily to explain 1) shorter retention of plutonium in liver and skeleton of NHPs, 2) differences in liver to bone partitioning ratios, and 3) significantly higher excretion of plutonium in feces compared to that in humans. The differences in the partitioning ratio as predicted by various models are shown in Fig. 6.6. According to the optimized model for NHPs, the partitioning ratio of plutonium between liver and bone tissues in NHPs is 2.78 at the beginning, but drops down to 0.17 at 1,100 days post intake. This is somewhat in agreement with the predictions of the Leggett model (2.00 at the beginning, and 0.42 at 1100 days post intake), but is different from those predicted by the ICRP 67 model (nearly time constant partition ratio of 0.60). The maximum uptake in liver was about 55% at 8 days, compared to 30% at nearly 1,000 days post intake as predicted by the ICRP 67 model.

Table 6.3. Skeletal and liver parameters for NHPs compared to those for humans

Compartments	Nonhuman primates	Human reference models		
	This paper	ICRP 67 adult	Luciani and Polig[f]	Leggett
Blood[a] to cortical surface	0.08778	0.1294	0.0952	0.08778
Blood[a] to trabecular surface	0.1247	0.1941	0.226	0.12474
Blood[a] to cortical volume	0.00462	-	0.00448	0.00462
Blood[a] to trabecular volume	0.01386	-	0.0716	0.01386
Cortical surface to marrow	0.000266	0.000082	0.000156	0.000082
Trabecular surface to marrow	0.004199	0.000493	0.00159	0.000493
Cortical surface to volume	0.000021	0.000041	-	0.000021
Trabecular surface to volume	0.000123	0.000247	-	0.000123
Cortical volume to marrow	0.000266	0.000082	0.000082	0.000082
Trabecular volume to marrow	0.004199	0.000493	0.00159	0.000493
Cortical marrow to blood[b]	0.03439	0.0076	0.0076	0.0076
Trabecular marrow to blood[b]	0.03439	0.0076	0.0076	0.0076
Blood to liver[c]	0.6442	0.1941	0.12	0.462
Liver 0 to liver 1	-	-	-	0.045286
Liver 1 to liver 2	-	0.00177	0.01	0.00038
Liver 1 to blood[d]	0.001647	-	-	0.00152
Liver 2 to blood	-	0.000211	0.0004	0.000127
Liver[e] to GI tract content	0.004365	0.000133	0.0004	0.009242

[a]The translocation of plutonium to bone surface and volume occurs through blood 1 compartment in Leggett model.
[b]Plutonium is translocated from bone marrow to blood 2 compartment in the Leggett model.
[c]Plutonium is translocated from blood to Liver through liver 1 compartment in ICRP 67, Luciani and the NHP model, from blood 1 liver 0 compartment in Leggett model.
[d]Plutonium is translocated from liver 1 and liver 2 to blood 2 compartment in Legget model.
[e]Plutonium is translocated to the GI tract through liver 1 in ICRP 67, Luciani and the NHP model; Liver 0 in Leggett model.
[f]Values for humans up to 35 years age.

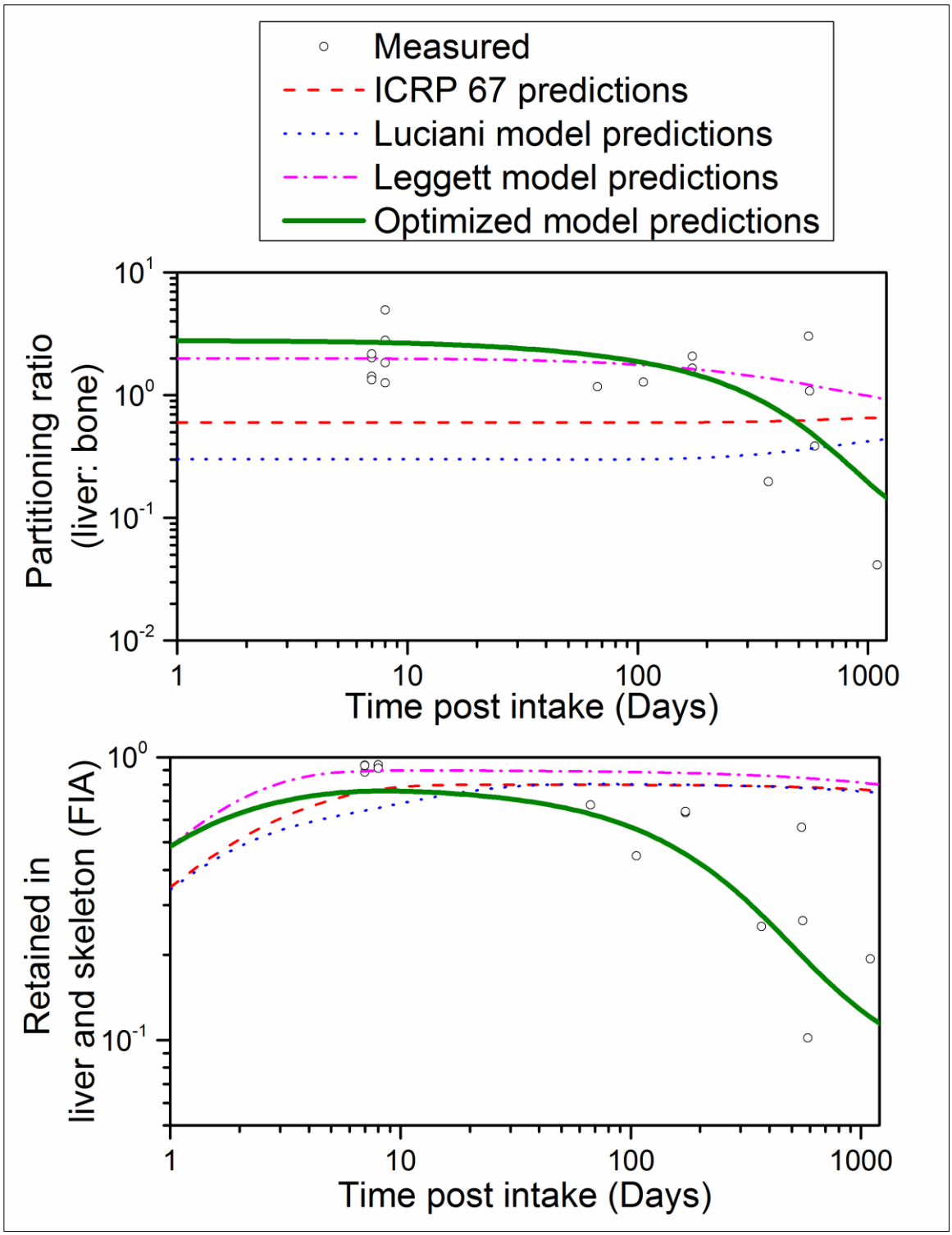

Fig. 6.6. The liver: bone partitioning ratio and total retention in liver and skeleton (FIA) as predicted by reference human models and the optimized model for NHPs

Similarly, the predictions of the optimized model indicated that plutonium in liver and skeleton tissues is retained at a much smaller fraction, and is cleared with a much shorter half-time compared to the predictions of the reference human models (Fig. 6.6).

6.6. Conclusions

Old world monkeys like *Macaca* are one of the closest living relatives to humans (Roos and Zinner 2015). Because of the similarities in the anatomy, physiology, genetics and behavior between the macaques and human, and the ease of handling them in the laboratories, they are frequently used in pharmacokinetic model development and biokinetic model development. However, certain anatomical and physiological differences exist between these NHPs and humans, which need to be taken into account when attempting to scale the parameters of a biokinetic model developed using NHP data to humans. Specific to plutonium, our results indicated that the transfer rates associated with bone and liver tissues need to be scaled appropriately.

Chapter 7 :
Summary and Conclusions

7.1. Systemic Behavior of ^{238}Pu(IV) Citrate in NHPs

The urinary excretion rates of plutonium in the NHPs was explained reasonably well by the ICRP 67, Luciani and Leggett systemic models, but the fecal excretion rates several days post intake could not be explained by any of the three human models. The models were also unable to accurately predict the retention of plutonium in liver and skeleton. Our findings indicated significant differences between the handling of plutonium by humans and NHPs, especially with regards to the pathways involving liver and skeleton. This pointed out the importance of adjustment to the model or the model parameters when using NHP data to extrapolate to humans or *vice-versa*.

The biokinetics of plutonium in NHPs were described by adopting the basic model structure of the human reference models, and adapting the transfer rates described for adult humans. The modification of the model structures and the parameters was carried out based on the understanding of differences between the humans and the NHP physiology as evident in our earlier findings, as well as the early biokinetic studies. These changes were necessary to explain 1) shorter retention of plutonium in NHPs, 2) differences in liver to bone partitioning ratio, and 3) higher fecal excretion rates of plutonium compared to humans. The model thus developed was then tested against the biokinetic data from two independent animal cases, and the optimized model predictions were consistently better than those of the human reference models.

Rhesus monkeys are considered to be one of the closest living relatives to humans, and have been frequently used in pharmacokinetic and biokinetic modeling because of their anatomical, physiological and genetic similarities with humans. However, certain physiological differences must be taken into account when scaling the parameters to humans.

7.2. Wound Behavior of ^{238}Pu(IV) Citrate in NHPs

The urinary and wound retention data from the intramuscularly and subcutaneously injected NHPs were also compared against the predictions of the various NCRP 156 wound models combined with the ICRP 67 systemic model. Although the NCRP 156 wound model categorizes ^{238}Pu(IV) as a strongly retained radionuclide, it was observed that the NCRP 156 wound model parameters for moderately retained radionuclides were better than those for strongly retained radionuclides in predicting the retention of plutonium in wound. Moreover, the parameters for moderately retained radionuclides were adequate to describe the urinary excretion rates in NHPs up to 200-days post intake. The excretion rates after 200-days post intake could not be described well because of the differences in the systemic handling of plutonium by monkeys and humans.

REFERENCES

Allen MB, Brey RR, Gesell T, Derryberry D, Poudel D. Strontium-90 biokinetics from simulated wound intakes in non-human primates compared with combined model predictions from National Council on Radiation Protection and Measurements Report 156 and International Commission on Radiological Protection Publication 67. Health Phys. 100(1):11-28; 2016.

Arnold JS, Jee WSS. Pattern of long term skeletal remodeling revealed by radioautographic distribution of ^{239}Pu in dogs. Health Phys 8:705-707; 1962.

Austin AL, Lord BI. A biokinetic model for alpha-emitting bone surface-seeking radionuclides in the mouse skeleton. Rad Prot Dosim 92(1-3):233-238; 2000.

Baxter DW, Rosental MW, Russell JJ, Moretti E, Chladek D, Lindenbaum A. Comparison of monomeric and polymeric plutonium in the dog and mouse. Radiat Res 54(3): 556-565; 1973.

Bhattacharya MH, Larsen RP, Cohen N, Ralston LG, Moretti ES, Oldham RD, Ayres L. Gastrointestinal absorption of plutonium and uranium in fed and fasted adult baboons and mice: applications to humans. Rad Prot Dosim 26(1-4):159-165; 1989.

Birchall A, Puncher M, Marsh JW, Davis K, Baily MR, Jarvis NS, Peach AD, Dorrian M-D, James AC. IMBA Professional Plus: a flexible approach to internal dosimetry. Radiat Protect Dosim 125:194-197; 2007.

Bunzl K, Kracke W. Fallout 239/240Pu and 238Pu in human tissues from the Federal Republic of Germany. Health Phys 44(Supp.1):441-449; 1983.

Bureau Internation des Poids et Mesures, International Electrotechnical Commission, International Federation of Clinical Chemistry, International Organization for

Standardization, International Union of Pure and Applied Chemistry, International Union of Pure and Applied Physics, International Organization of Legal Metrology. Evaluation of measurements data – guide to the expression of uncertainty in measurement. JCGM 100:2008; 2010.

Cam LL. Maximum likelihood: an introduction. Int Stat Rev 58(2):153-171; 1990.

Castellani CM, Marsh JW, Hurtgen C, Blanchardon E, Berard P, Giussani A, Lopez MA. IDEAS guidelines (Version 2) for the estimation of committed doses from incorporation monitoring data. EURADOS Report 2013-01. 2013. Available at: http://eurados.org/~/media/Files/Eurados/documents/EURADOS%20Report%2013-01%20online%20version.pdf?la=en. Accessed October 10, 2015.

Chipperfield AR, Taylor DM. Binding of plutonium to glycoproteins in vitro. Radiat Res 43:393-402; 1970.

Committee on the Biological Effects of Ionizing Radiation (BEIR). Health risks of radon and other internally deposited alpha-emitters. BEIR IV. National Academy Press, Washington D.C.; 1988.

Cox MG, Harris PM. Best Practice guide No. 6. Uncertainty evaluation. Technical report. National Physical laboratory, Teddington UK; 2004.

Dagle GE, Cannon WC, Stevens DL, McShane JF. Comparative disposition of inhaled ^{238}Pu and ^{239}Pu nitrates in beagles. Health Phys 44:275-277; 1983.

Doerfel H, Andrasi A, Bailey M, Berkovski V, Blanchardon E, Castellani CM, Hurtgen C, LeGuen B, Malatova I, Marsh J, Stather J. Guidelines for the estimation of committed doses from incorporation monitoring data. Project IDEAS-EU Contract No. FIKR-CT-2001-00160. 2006.

Doerfel H, Andrasi A, Bailey M, Berkovski V, Blanchardon E, Castellani CM, Hurtgen C, LeGuen B, Malatova I, Marsh J, Stather J. Internal dosimetry: the science and art of internal dose assessment. 2012. Available at: http://www.irpa.net/members/54302/%7B884C1520-D5CB-4908-94B4-954007C0F734%7D/RC%206%20Internal%20Dosimetry%20-%20The%20Science%20and%20Art%20of%20Internal%20Dose%20Assessment.pdf. Accessed January 1, 2015.

Durbin PW. Plutonium in man: a twenty-five year review. Lawrence Radiation Laboratory, University of California. TID-4500 (58th ed). Berkley, CA. 1971.

Durbin PW, Horovitz MW and Close ER. Plutonium deposition kinetics in the rat. Health Phys 22(6):731-741; 1972

Durbin PW. Plutonium in mammals: influence of plutonium chemistry, route of administration, and physiological status of the animal on initial distribution and long-term metabolism. Health Phys. 29: 495-510; 1975.

Durbin PW, Jeung N, and Schmidt CT. Distribution and retention of ^{238}Pu in macaque monkeys. In: Biology and Medicine Division annual Report 1982-1983. Lawrence Berkeley Laboratory, Berkley, CA. 1983.

Durbin PW, and Schmidt CT. The US Tranuranium Registry report on the ^{241}Am content of a whole body. Part V: Implications for metabolic modelling. Health Phys 49(4): 623-661; 1985.

Durbin PW, Jeung N, Schmidt CT. ^{238}Pu(IV) in monkeys. U.S. Nuclear Regulatory Commission Report No. NUREG/CR-4355 (NRC, Washington, D.C.); 1985.

Durbin PW, Jeung N. Collected original data on distribution of ^{238}Plutonium in soft tissues and bones of monkeys. Division of Research Medicine and Radiation Biophysics, Lawrence Berkeley Laboratory. LBL-28648. 1990a.

Durbin PW, Jeung N. Collected original data on distribution of ^{238}Plutonium in plasma and excreta of monkeys. Division of Research Medicine and Radiation Biophysics, Lawrence Berkeley Laboratory. LBL-28651. 1990b.

Durbin PW. Plutonium in man: a new look at the old data. In: Radiobiology of plutoium. (Stover BJ and Jee WSS, eds.). The JW Press, Dept. of Anatomy, University of Utah, Salt Lake.

Ellender M, Haines JW, Harrison JD. The distribution and retention of plutonium, americium and uranium in CBA/H mice. Hum Exp Toxicol 14(1):38-48; 1995.

Etherington G, Stradling GN, Hodgson A., Fifield LK. Anomalously high excretion of Pu in urine following inhalation of plutonium nitrate. Radiat Prot Dosim 105(1-4): 321-324; 2003.

Fox T, Tietjen GL, McInroy JF. Statistical analysis of a Los Alamos scientific laboratory study of plutonium in U.S. autopsy tissue. Health Phys 39:877-892; 1980.

Gregersen, MI, Sear H, Rawson RA, Chien S, Saiger Gl. Cell volume, plasma volume, total blood volume and F_{cells} factor in the rhesus monkey. Am. J. Physiol. 196, 184-187; 1959.

Guilmette RA, Cohen N, Wrenn ME. Distribution and retention of ^{241}Am in the baboon. Radiat. Res. 81, 100-119; 1980.

Guilmette RA, Durbin PW, Toohey RE, Bertelli L. The NCRP wound model: Development and application. Radiat Protect Dosim, 127(1-4):103-107; 2007.

Ham GJ, Harrison JD. The gastrointestinal absorption and urinary excretion of plutonium in male volunteers. Radiat Prot Dosim 87(4): 267-272; 2000.

Hodgson, A, Shutt, AL, Etherington, G., Hodgson, SA, Rance, E, Stradling, GN, Youngman, MJ, Ziesenis, A, Kreyling, WG. Comparison of predicted with observed biokinetics of inhaled plutonium nitrate and gadolinium oxide in humans. Radiat. Protect. Dosim. 105(1-4): 91-94, 2003.

Hoffman DC, Lawrence FO, Mewherter JL, Rourke FM. Detection of plutonium-244 in nature. Nature 234(5325): 132-134; 1971.

Hurtgen C, Cossonnet C. A survey on uncertainties in bioassay measurements carried out with the ominex project. Radiat Prot Dosim: 105:375-378; 2003.

International Agency for Research on Cancer (IARC). Ionizing radiation, part 2: some internally deposited radionuclides. IARC Monographs on the Evaluation of Carcinogenic Risks to Humans, Volume 78. IARC Press, Lyon, France; 2001.

International Atomic Energy Agency (IAEA). Assessment of occupational exposure due to intakes of radionuclides. Safety Standard Series, No. RS-G-1.2. Vienna, 1999.

International Atomic Energy Agency (IAEA). Assessment of occupational exposure due to intakes of radionuclides: lecture notes. 2003.

International Atomic Energy Agency (IAEA). Methods for assessing occupational radiation doses due to intakes of radionuclides. Safety Series No. 37. Vienna, 2004.

International Commission on Radiological Protection (ICRP). Permissible dose for internal radiation. ICRP Publication No. 2. Pergamon Press, Oxford, England; 1959.

International Commission on Radiological Protection (ICRP). The metabolism of compounds of plutonium and other actinides. ICRP Publication No. 19. Pergamon Press, Oxford, England; 1972.

International Commission on Radiological Protection (ICRP). Report of the task group on reference man. ICRP Publication No. 23. Pergamon Press, Oxford, England; 1974.

International Commission on Radiological Protection (ICRP). Limit for intakes of radionuclides by workers. ICRP Publication No. 30 (Part 1). Pergamon Press, Oxford, England; 1979.

International Commission on Radiological Protection (ICRP). Radionuclide transformations – energy and intensity of emissions. ICRP Publication No. 38. Ann. ICRP 11-13. Pergamon Press, Oxford, England; 1983.

International Commission on Radiological Protection (ICRP). The metabolism of plutonium and related elements. ICRP Publication No. 48. Pergamon Press, Oxford, England; 1986.

International Commission on Radiological Protection (ICRP). Age-dependent doses to members of the public from intake of radionuclides – Part 1. ICRP Publication No. 56. Ann. ICRP 20(2). Pergamon Press, Oxford, England; 1990.

International Commission on Radiological Protection (ICRP). Age dependent dose to members of the public from Intake of radionuclides. Oxford: Pergamon Press; ICRP Publication 67; Ann. ICRP; 23(3/4): 1993a.

International Commission on Radiological Protection. Age dependent doses to members of the public from intake of radionuclides: part 2, ingestion dose coefficients. Oxford: Pergamon Press; ICRP Publication 67; Ann ICRP 23(3/4); 1993b.

International Commission on Radiological Protection. Human respiratory tract model for radiological protection. Oxford: Pergamon Press; ICRP Publication 66; Ann ICRP 24(1-3); 1994.

International Commission on Radiological Protection (ICRP). Age-dependent doses to members of the public from intake of radionuclides: part 3 ingestion dose coefficients. Oxford: Pergamon Press; ICRP Publication 69; Ann ICRP 25(1); 1995a.

International Commission on Radiological Protection (ICRP). Age-dependent doses to members of the public from intake of radionuclides: part 4 inhalation dose coefficients. Oxford: Pergamon Press; ICRP Publication 71; Ann ICRP 25(3-4); 1995b.

International Commission on Radiological Protection (ICRP). Individual monitoring for internal exposure of workers. Oxford: Pergamon Press; ICRP Publication 78; Ann ICRP 27(3-4); 1997.

International Commission on Radiological Protection (ICRP). Doses to the embryo and fetus from intakes of radionuclides by the mother. ICRP Publication No. 88. Pergamon, Oxford, England. 2001.

International Commission on Radiological Protection. Human alimentary tract model for radiological protection. Oxford: Pergamon Press; ICRP Publication 100; Ann ICRP 36(1-2); 2006

James AC. User manual for IMBA Professional Plus (Version 4.0), ACJ & Associates, Inc. 2005.

James AC, Brooks BG. The United States Transuranium and Uranium Registries (USTUR): learning from plutonium and uranium workers. Available at: http://www.ustur.wsu.edu/publications/Files_Pubs/Publications06/USTUR-0225-06_paper.pdf. Accessed January 1, 2015.

Jensen MP, Gorman-Lewis D, Aryal B, Paunesku T, Vogt S, Rickert PG, Seifert S, Lai B, Woloschak GE, Soderholm L. An iron-dependent and transferrin-mediated cellular uptake pathway for plutonium. Nat Chem Biol 7(8): 560-565; 2012.

Jones JE. Process for producing ultra-pure plutonium-238. US Patent 6896716. 2005.

Khursheed A, Fell TP, Kendall GM, Phipps AW. Simplified organ retention functions for physiologically based recycling biokinetic models. Health Phys. 70(5):656-664; 1996.

Konzen K. Development of a plutonium-DTPA biokinetic model with suggested modification to the plutonium systemic model. Dissertation. Idaho State University, Pocatello, ID. 2014.

Konzen K, Brey R and Guilmette R. Early blood plutonium retention in nonhuman primates compared to the NCRP 156 wound biokinetic model. Health Phys. 108(3):383–387; 2015.

Konzen K, Miller S Brey R. Proposed modification to the plutonium systemic model. Health Phys 109(4): 307-318; 2015.

Langham, WH, Bassett SH, Hams, PS, Carter RE. Distribution and excretion of plutonium administered intraveneously to man. Los Alamos, NM: Los Alamos Scientific Laboratory; LASL Report LA 1151; 20 September 1950. Reprinted in Health Phys. 38: 103 1-1060; 1980.

Larsen RP, Bhattacharya MH, Oldham RD, Moretti ES, Cohen N. Gastrointestinal absorption and retention of plutonium and uranium in the baboon. Argonne National Laboratory. ANL-83-100: 51-60; 1983.

Leggett RW. A retention-excretion model for americium in humans. Health Phys 62(4):228-310: 1992.

Leggett RW, Eckerman KF. Evolution of the ICRP's biokinetic models. Radiat Prot Dosim 53(1-4):147-155; 1994.

Leggett RW. Reliability of the ICRP's dose coefficients for members of the public. III. Plutonium as a case study of uncertainties in the systemic biokinetics of radionuclides. Rad Prot Dosim 106(2): 103-120; 2003.

Leggett RW, Eckerman KF, Khokhryakov VF, Suslova KG, Krahenbuhl MP, Miller SC. Mayak worker study: An improved biokinetic model for reconstructing doses from internally deposited plutonium. Radiat. Res 164:111-122; 2005.

Lloyd RD, McFarland SS, Atherton DR and Mays CW. Plutonium retention, excretion and distribution in juvenile beagles soon after injection. Rad Res 75(3):663-641; 1978.

Lloyd RD, Mays CW, Jones CW, Atherton DR, Bruenger FW, Shabestari LR, Wrenn ME. Retention and dosimetry of injected ^{241}Am in beagles. Radiat Res 100: 564-575; 1984.

Lloyd RD, Miller SC, Taylor GN, Bruenger FW, Angus W and Jee WSS. Comparison of internal emitter radiobiology in animals and humans. Health Phys 72(1): 100-110; 1997.

Luciani A and Polig E. Verification and modification of the ICRP-67 model for plutonium dose calculation. Health Phys. 78(3):303-310; 2000.

Luciani A, and Polig E. Surface-seeking radionuclides in the skeleton: Current approach and recent developments in biokinetic modelling for humans and beagles. Rad Prot Dosim 127(1-4): 140-143; 2007.

Luciani A. Plutonium biokinetics in human body. PhD Dissertation, FZKA 6748, Forschungszentrum Karlsruhe GmbH, Karlsruhe; 2002. Available at http://bibliothek.fzk.de/zb/berichte/FZKA6748.pdf

Markley JF, Rosenthal MW, Lindenbaum A. Distribution and removal of polymeric plutonium in rats and mice. Int J Rad Biol 8(3):271-278; 1964.

Marsh JW, Blanchardon E, Castellani CM, Desai AD, Dorrian MD, Hurtgen C, Koukouliou V, Lopez MA, Luciani A, Puncher M, Andrasi A, Bailey MR, Berkovski V, Birchall A, Bonchug Y, Doerfel H, Malatova I, Molokanov A, Ratia H. Evaluation of scattering factor values for internal dose assessment following the ideas guidelines: preliminary results. Radiation Protection Dosimetry 127(1-4): 339-342; 2007.

Morin M, Nenot JC, Lafuma J. Metabolic and therapeutic study following administration to rats of ^{238}Pu Nitrate – a comparison with ^{239}Pu. Health Phys 23(4):475-480; 1972.

Mussalo H, Jakkola T, Miettinen JK, Laiho K. Wrenn ME (Ed.) Fallout plutonium in bone samples of southern Finns. RD Press, Salt Lake City, UT. 1981.

National Council on Radiation Protection and Measurements (NCRP). Some aspects of strontium radiobiology. NCRP Report No. 110. NCRP, Bethesda, MD; 1991.

National Council on Radiation Protection and Measurements (NCRP). Research needs for radiation protection. NCRP Report No. 117. NCRP, Bethesda, MD; 1993.

National Council on Radiation Protection and Measurements (NCRP). Radionuclide exposure of the embryo/fetus. NCRP Report No. 128. NCRP, Bethesda, MD; 1998.

National Council on Radiation Protection and Measurements (NCRP). Liver cancer risk from internally-deposited radionuclides. NCRP Report No. 135. NCRP, Bethesda, MD; 2001.

National Council on Radiation Protection and Measurements. Development of a biokinetic model for radionuclide contaminated wounds and procedures for their assessment, dosimetry and treatment. Bethesda, MD: NCRP; Report No. 156; 2006.

Newton D, Talbot RJ, Kang C and Warner AJ. Uptake of plutonium by human liver. Rad Prot Dosim. 80(4): 385-395; 1998.

Polig E. Kinetic model of the distribution of ^{239}Pu in the beagle skeleton. Health Phys 57(3):449-460; 1989.

Polig E. Labels of surface-seeking radionuclides in the human skeleton. Health Phys 72(1): 19-33; 1997.

Polig E, Bruenger FW, Lloyd RD, Miller SC. Biokinetic and dosimetric model of plutonium in the dog. Health Phys 78(2): 182-190; 2000.

Potter CA. Internal dosimetry: a review. Health Phys 87(5): 455-468; 2004.

Poudel D. Biokinetics of intravenously injected plutonium in macaques. Thesis. Idaho State University, Pocatello, ID; 2012.

Poudel D, Krage ES, Brey RR and Guilmette RA. Comparison of ICRP 67 and other plutonium systemic model predictions with the biokinetic data from nonhuman primates. Health Phys 110(4):361-369; 2016a.

Poudel D, Guilmette RA, Konzen K, Krage ES, Brey RR. Application of NCRP 156 wound model and ICRP 67 systemic plutonium model for analysis of urine data from simulated wounds in nonhuman primates. Health Phys *In Press*; 2016b.

Poudel D, Guilmette RA, Gesell TF, Harris JT, Brey RR. Biokinetics of plutonium in nonhuman primates. Health Phys. *In press;* 2016c.

Priest ND, Haines JW, Humphreys AM, Metivier H, Kathren RL. The bone volume effect on the dosimetry of plutonium-239 and americium-241 in the skeleton of man and baboon. J Radioanal Nucl Chem 156(1):33-53; 1992.

Roos C, and Zinner D. Diversity and evolutionary history of macaques with special focus on *Macaca mulatta* and *Macaca fascicularis*. In: Bluemel J, Korte S, Schenck E, Weinbauer GF, eds. The nonhuman primate in nonclinical drug development and safety assessment. New York, NY: Elsevier; 2015: 3-16.

Rosenthal MW, Lindenbaum A, Russel JJ, Moretti E, and Chladek D. Metabolism of monomeric and polymeric plutonium in the rabbit: Comparison with the mouse. Health Phys 23: 231-238; 1972.

Schubert J, Fried JF, Rosenthal MW, Lidenbaum A. Tissue distribution of monomeric and polymeric plutonium as modified by a chelating agent. Radia Res 15:220-226; 1961.

Seaborg GT, McMillan EM, Kennedy JW, Wahl AC. Radioactive element 94 from deuterons. Phys Rev 69:366-367; 1946.

Skrable KW, Chabot GE, French CS, LaBone TR. Intake retention functions and their applications to bioassay and the estimation of internal radiation doses. Health Phys 55(6):933-950; 1988.

Sontag W. Microdistribution of ^{239}Pu in the rat skeleton. Int J Radiat Biol 60(4):677-694; 1991.

Stanley JA, Edison AF, Mewhinney JA. Distribution, retention and dosimetry of plutonium and americium in the rat, dog and monkey after inhalation of an industrial-mixed uranium and plutonium oxide aerosol. Health Phys 43(4):521-530; 1982.

Talbot RJ, Knight DA, Morgan A. Biokinetics of Pu-237 citrate and nitrate in the rat: Implications for Pu studies in man. Health Phys 59(2):183-187; 1990.

Talbot RJ, Newton D, Warner AJ. Metabolism of injected plutonium in two healthy men. Health Phys 65(1):41-46; 1993

Talbot RJ, Newton D, Dmitriev SN. Sex-related differences in the human metabolism of plutonium. Rad Prot Dosim 71(2): 107-121; 1997.

Taylor DM. Some aspects of the comparative metabolism of plutonium and americium in rats. Health Phys 8(6):673-677; 1962.

Taylor DM. Interactions between transuranium elements and the components of cells and tissues. Health Phys 22: 575-581; 1972.

Taylor DM. Chemical and physical properties of plutonium. In Uranium, Plutonium, Transuranic elements. Eds: Hodge HC, Stannard JN, Hursch JB. Springer – Verlag, Heidelberh: 323-347; 1973.

Taylor DM. The bioinorganic chemistry of actinides in blood. Journal of Alloys and Compounds 6-10:271-273; 1998.

United States Nuclear Regulatory Commission (USNRC). Interpretation of bioassay measurements. NUREG/CR-4884; BNL-NUREG-52063. New York, NY; 1987. Available at: http://pbadupws.nrc.gov/docs/ML1128/ML11285A018.pdf. Accessed 1 January 2015.

Vasilenko EK, Khokhryakov VF, Miller SC, Fix JJ, Eckerman K, Choe DO, Gorelov M, Khokhryakov VV, Knyasev V, Kahrenbuhl MP, Schrepelz RI, Smetanin M, Suslova K, Vostrotin V. Mayak worker dosimetry study: an overview. Health Phys 93(3):190-206; 2007.

Watts L. Clearance rates of insoluble plutonium-239 compounds from the lung. Health Phys 29: 53-59; 1975.